



THE HONG KONG  
POLYTECHNIC UNIVERSITY

香港理工大學

Pao Yue-kong Library

包玉剛圖書館

---

## Copyright Undertaking

This thesis is protected by copyright, with all rights reserved.

**By reading and using the thesis, the reader understands and agrees to the following terms:**

1. The reader will abide by the rules and legal ordinances governing copyright regarding the use of the thesis.
2. The reader will use the thesis for the purpose of research or private study only and not for distribution or further reproduction or any other purpose.
3. The reader agrees to indemnify and hold the University harmless from and against any loss, damage, cost, liability or expenses arising from copyright infringement or unauthorized usage.

### IMPORTANT

If you have reasons to believe that any materials in this thesis are deemed not suitable to be distributed in this form, or a copyright owner having difficulty with the material being included in our database, please contact [lbsys@polyu.edu.hk](mailto:lbsys@polyu.edu.hk) providing details. The Library will look into your claim and consider taking remedial action upon receipt of the written requests.

**DEVELOPMENT OF HYDROPHOBIC FILMS,  
SUPER-HYDROPHOBIC NANOFIBROUS NETWORKS,  
AND DRUG ENCAPSULATION SYSTEMS FROM ZEIN  
WITH ENHANCED PROPERTIES FOR APPLICATIONS  
IN BIOMEDICAL ENGINEERING**

**DONG FANGYUAN**

M.Phil

The Hong Kong Polytechnic University

2016

The Hong Kong Polytechnic University  
Department of Applied Biology and Chemical Technology

**Development of Hydrophobic Films, Super-hydrophobic  
Nanofibrous Networks, and Drug Encapsulation Systems  
from Zein with Enhanced Properties for Applications in  
Biomedical Engineering**

**DONG Fangyuan**

A Thesis Submitted in Partial Fulfilment of Requirements for the  
Degree of Master of Philosophy

February 2015

## **Certificate of originality**

I hereby declare that this thesis is my own work and that, to the best of my knowledge and belief, it reproduces no material previously published or written, nor material that has been accepted for the award of any other degree or diploma, except where due acknowledgement has been made in the text.

---

Fangyuan DONG

February, 2015

## **Abstract**

Zein, a major protein extracted from corn, is an abundant and reproducible biopolymer which has excellent mechanical properties and biocompatibility. It has been widely applied in food and pharmaceutical industrials. In this study, the hydrophobic films, super-hydrophobic nanofibrous networks, and drug encapsulation systems were developed from zein to obtain enhanced properties for applications in biomedical engineering.

In chapter 2, zein was used to form surfaces with high hydrophobicity through self-assembly monolayer (SAM) assisted EISA. The present method is facile and inexpensive. Scanning electron microscope (SEM) and energy dispersive X-ray spectroscopy (EDS) were applied to characterize the morphology and the elements of the formed zein surfaces, respectively. Water contact angle (WCA) values of the formed zein surfaces were also measured to study the hydrophobicity of formed zein surfaces. The effects of both the concentrations of zein solutions and solvent on the WCA values of the formed zein surface were investigated. A zein surface with a high WCA value ( $126^\circ$ ) was also formed through size controlled SAM assisted EISA.

In chapter 3, zein super-hydrophobic/hydrophobic nanofibrous networks were formed by electrospinning. The formed zein networks showed high hydrophobicity with the WCAs ranging from  $130.5^\circ$  to  $153.6^\circ$ . The cell attachment and growth on the zein networks were studied. It was observed that the amount of the cells attaching and growing in the zein nanofibrous networks were higher than the ones on the conventional zein casting films. The results indicated that the electrospun zein

nanofibrous network had great potential as scaffolds in tissue engineering to support cell growth and tissue regeneration.

In chapter 4, super-hydrophobic/hydrophobic surfaces were formed from zein by electrospinning. WCA and SEM were used to characterize the hydrophobicity and surface morphology. The highest WCA of the zein electrospun surfaces could reach 155.5°. A formation mechanism was proposed based on the orientation of the amphiphiles during the solvent evaporation of different fabrication methods. The droplet-based or jet-based evaporation during electrospinning and spray drying led to the formation of the super-hydrophobic/hydrophobic surface by the accumulation of the hydrophobic groups of the amphiphiles on the surface, while the surface-based evaporation during cast drying led to the formation of the hydrophilic surface by the accumulation of the hydrophilic groups of the amphiphiles on the surface.

In chapter 5, a double-layer zein/CS structure was utilized to encapsulate vitamin C (VC). VC was first encapsulated by chitosan (CS) with sodium tripolyphosphate (STPP). Then zein was added to coat the formed VC-loaded CS nanoparticles (NPs). The formed VC-loaded zein/CS microspheres (MPs) had a good sphericity with particle size ranging from 720 to 1100 nm. VC was greatly protected from degradation by the double-layer coating and only 5% of VC was oxidized after 10-day storage at room temperature. The double-layer structure also had a better performance on retarding the release of VC in simulated gastric fluid (SGF) and achieving controlled release in simulated intestinal fluid (SIF), which provided a method for further utilization of nutrients in human body.

## Publication list

1. **Dong, F. Y.;** Zhang, M.; Huang, W. Y.; Zhou, L. P.; Wong, M. S.; Wang, Y., Superhydrophobic/hydrophobic nanofibrous network with tunable cell adhesion: Fabrication, characterization and cellular activities. *Colloid Surface A* 2015, 482, 718-723.
2. **Dong, F. Y.;** Zhang, M.; Tang, W. W.; Wang, Y., Formation and Mechanism of Superhydrophobic/Hydrophobic Surfaces Made from Amphiphiles through Droplet-Mediated Evaporation-Induced Self-Assembly. *J Phys Chem B* 2015, 119 (16), 5321-5327.
3. **Dong, F. Y.;** Padua, G. W.; Wang, Y., Controlled formation of hydrophobic surfaces by self-assembly of an amphiphilic natural protein from aqueous solutions. *Soft Matter* 2013, 9 (25), 5933-5941.
4. **Dong, F. Y.;** Dong, X. L.; Zhang, M.; So, P. K.; Xiao, H. H.; Wang, Y., Encapsulation of vitamin C by a double-layer zein/chitosan structure with improved stability and controlled release. *Submitted*.

## **Acknowledgements**

First of all, I would like to express my deepest gratitude to my chief supervisor, Dr. Yi Wang for his professional guidance and kind encouragement during my MPhil study period. He gave me many great ideas and inspired my interest in the area of nanomaterial science.

I am very grateful to the help from my colleagues Miss Wai-Wa Tang, Miss Huan Zhang, Miss Xiaoli Dong and Miss Liping Zhou. They taught me a lot in the practical work and shared plenty of experiment experience with me. I also want to thank the FYP students Mr. Man-him Ching, Mr. Long-tsz Poon, Miss Mi Zhang, Miss Wenyu Huang, Miss Qiongyu Li, Mr. Ewan Chiang and Miss Yan-san Lam in our research group for their valuable assistance in my experiments.

In addition, I would like to thank Dr. Mo Yang from Department of Biomedical Engineering and Dr. Zijian Zheng from Institute of Textiles & Clothing for allowing me to use their lab equipment. I also appreciate the help from Dr. Wei Lu and Dr. Hardy H. F. Lui from the Material Research Center of the Hong Kong Polytechnic University.

Moreover, I want to give my great thanks to all academic and technical staff members of the Department of Applied Biology and Chemical Technology for their technical guidance and support. Especially I want to thank Mr. Chor-hing Cheng for the daily technical guidance, Dr. Pui-Kin So for his guidance in MS spectra, and Miss Sara Yeung for her training for freeze dryer and ultra-speed centrifuge.

Last but not least, I would like to express my sincere appreciation to my family and friends for their support and care throughout my MPhil study.

# Contents

Certificate of originality .....	I
Abstract.....	II
Publication list.....	IV
Acknowledgements .....	V
Contents .....	VI
List of tables.....	XI
List of figures.....	XII
Abbreviations .....	XVI
Chapter 1: Literature Review .....	1
1.1 Introduction of zein.....	1
1.2 Introduction of hydrophobic surfaces.....	5
1.3 Tissue engineering.....	6
1.3.1 Biomaterials for tissue engineering .....	6
1.3.2 Applications of hydrophobic surfaces in vascular stents engineering	12
1.4 Nano-encapsulation technology .....	15
1.5 Drug delivery system .....	17
1.5.1 Background .....	17
1.5.2 Introduction of endocytosis .....	18
1.5.3 Methods used to study endocytosis of NPs .....	20

1.5.4 <i>Modifications of NPs for targeted drug delivery</i> .....	23
<b>1.6 Project aims and significance</b> .....	25
<b>Chapter 2: Hydrophobic surfaces formed from zein in aqueous solutions by self-assembly</b> .....	27
<b>2.1 Introduction</b> .....	27
<b>2.2 Materials and Method</b> .....	30
2.2.1 <i>Materials</i> .....	30
2.2.2 <i>Preparation of OT SAMs on gold coated substrates</i> .....	31
2.2.3 <i>Preparation of zein films with hydrophobic surfaces</i> .....	31
2.2.4 <i>WCA</i> .....	31
2.2.5 <i>SEM</i> .....	32
<b>2.3 Results and Discussion</b> .....	32
2.3.1 <i>Hydrophobic zein film</i> .....	32
2.3.2 <i>Mechanism of hydrophobic zein film formation</i> .....	35
2.3.3 <i>Effect of zein concentrations on surface hydrophobicity</i> .....	37
2.3.4 <i>Effect of ethanol concentrations on surface hydrophobicity</i> .....	40
2.3.5 <i>Surface wetting models</i> .....	43
2.3.6 <i>Improvement of surface hydrophobicity of zein film by size control EISA</i> .....	45
<b>2.4 Conclusions</b> .....	49
<b>Chapter 3: Super-hydrophobic/Hydrophobic Nanofibrous Network with Tunable Cell Adhesion: Fabrication, Characterization and Cellular Activities</b> .....	51

<b>3.1 Introduction</b> .....	51
<b>3.2 Materials and methods</b> .....	53
3.2.1 <i>Materials</i> .....	53
3.2.2 <i>Electrospinning</i> .....	53
3.2.3 <i>WCA</i> .....	54
3.2.4 <i>SEM</i> .....	54
3.2.5 <i>Oxygen plasma treatment</i> .....	54
3.2.6 <i>Cell culture</i> .....	55
3.2.7 <i>Cell adhesion assay</i> .....	55
<b>3.3 Results and discussion</b> .....	56
3.3.1 <i>Effects of the zein concentration on the surface hydrophobicity of ZENN</i> .....	56
3.3.2 <i>Effects of the electrospinning voltage on the surface hydrophobicity of ZENN</i> .....	59
3.3.3 <i>Cell attachment behaviors</i> .....	61
3.3.4 <i>Effects of plasma treatment induced tunable wettability on cell attachment</i> .....	62
<b>3.4 Conclusions</b> .....	64
<b>Chapter 4: Formation and mechanism of super-hydrophobic/hydrophobic surfaces made from amphiphiles through droplet-mediated evaporation-induced self-assembly</b> .....	66
<b>4.1 Introduction</b> .....	66

<b>4.2 Materials and methods</b> .....	69
4.2.1 <i>Materials</i> .....	69
4.2.2 <i>Sample solution preparation</i> .....	69
4.2.3 <i>Electrospinning</i> .....	70
4.2.4 <i>Spray drying</i> .....	70
4.2.5 <i>WCA</i> .....	71
4.2.6 <i>SEM</i> .....	71
4.2.7 <i>ATR-FTIR</i> .....	71
<b>4.3 Results and discussion</b> .....	72
4.3.1 <i>Super-hydrophobic/hydrophobic surfaces made from amphiphiles using electrospinning</i> .....	72
4.3.2 <i>Hydrophobic surfaces made by spray drying</i> .....	75
4.3.3 <i>The <math>\alpha</math> helix-<math>\beta</math> sheet transformation during evaporation-induced self-assembly</i> .....	77
4.3.4 <i>Formation mechanism of super-hydrophobic/hydrophobic surfaces</i> ..	79
<b>4.4 Conclusions</b> .....	82
<b>Chapter 5: Encapsulation of vitamin C using a double-layer zein/CS structure with improved stability and controlled release</b> .....	84
<b>5.1 Introduction</b> .....	84
<b>5.2 Materials and methods</b> .....	87
5.2.1 <i>Materials</i> .....	87
5.2.2 <i>Preparation of VC-loaded CS NPs</i> .....	88

5.2.3 Preparation of VC-loaded zein/CS MPs .....	88
5.2.4 Particle size evaluation and morphological observation .....	89
5.2.5 Encapsulation efficiency of VC-loaded CS NPs .....	89
5.2.6 ESI-MS analysis .....	90
5.2.7 Release test in simulated gastrointestinal fluids .....	90
<b>5.3 Results and discussion .....</b>	<b>91</b>
5.3.1 Particle size and morphology .....	91
5.3.2 Stability of VC-loaded in zein/CS MPs .....	94
5.3.3 Effect of different formations on in vitro release of VC .....	96
5.3.4 Release of VC from zein/CS MPs in different simulated fluids .....	98
<b>5.4 Conclusions .....</b>	<b>99</b>
<b>Future research perspectives .....</b>	<b>101</b>
<b>References .....</b>	<b>103</b>

## List of tables

<b>Table 1.1</b> The commonly used pharmacological inhibitors for identifying the endocytic pathways of uptake of NPs .....	22
<b>Table 1.2</b> The commonly used markers for identifying the intracellular colocalization of uptake of NPs .....	23
<b>Table 2.1</b> The percentage of different elements on the surface of zein film made on the microscope slide with OT SAM from 0.05 wt% zein solution.....	35
<b>Table 2.2</b> The WCA values of zein films made on the microscope slides with OT SAM from 0.025, 0.05, 0.1, 0.3, and 0.5 wt% zein solution, respectively.....	39
<b>Table 2.3</b> The WCA values of zein films made on the microscope slides with OT SAMs from 0.05 wt% zein dissolved in 40, 50, 60, 80, and 95% ethanol, respective .....	42
<b>Table 2.4</b> The WCA values of the zein films made on microscopy slides coated with OT SAM from 0.5, 1, and 2 wt% zein solutions transferred after 0, 15, 30, and 45 min evaporation, respectively .....	47
<b>Table 3.1</b> The WCAs of ZENNs obtained from zein solutions with the concentration of 5, 10, 15, 20, 25, and 30 wt%, respectively .....	58
<b>Table 3.2</b> The WCAs of ZENN made by electrospinning at applied voltages of 10, 18, 21, and 24 kV from zein solution with a concentration of 10 wt%, respectively .....	60
<b>Table 5.1</b> The average particle sizes of different particles .....	92

## List of figures

<b>Figure 1.1</b> The location of major components in the corn kernel .....	1
<b>Figure 1.2</b> Diagram of zein tertiary structure.....	2
<b>Figure 1.3</b> (a) SEM image of VD3, (b) SEM image of oregano oil, and (c) citral encapsulated zein NPs, respectively .....	4
<b>Figure 1.4</b> SEM images of electrospun networks from (a) concentrated zein solution of 50 wt%; (b) zein solutions with a tip-to-collector distance of 15 cm; (c) diluted zein solution of 12 wt%; (d) acidified zein solution .....	5
<b>Figure 1.5</b> A Schematic basic setup of electrospinning .....	8
<b>Figure 1.6</b> Optical microscope image (left) and fluorescence microscope image (right, actin filaments red, nuclei blue) of human dermal fibroblasts after 24 h in cell culture on nanofiber scaffold .....	10
<b>Figure 1.7</b> SEM images of the hybrid scaffolds containing (a) CS/PLA and (b) collagen/PLA, and (c) bi-layer scaffold.....	12
<b>Figure 1.8</b> The hypothetical cellular endocytic pathways.....	20
<b>Figure 2.1</b> The WCA of (a) a microscope slide without OT SAM, (b) a microscope slide with OT SAM, (c) zein film made on the untreated microscope slide from 10 wt% zein solution, and (d) zein film made on the microscope slide with SAM from 0.05 wt% zein solution .....	33
<b>Figure 2.2</b> SEM (a) SEM image and (b) the corresponding EDS spectrum of zein film made on the microscope slide with OT SAM from 0.05 wt% zein solution.....	35
<b>Figure 2.3</b> The formation process of zein hydrophobic surface by SAM assisted EISA	

.....	37
<b>Figure 2.4</b> SEM images of the surfaces of zein films made on the microscope slides with OT SAMs from 0.025, 0.05, 0.1, 0.3 and 0.5 wt% zein solution, respectively .....	40
<b>Figure 2.5</b> SEM images of the surfaces of zein films made on the microscope slides with OT SAMs from 0.05 wt% zein dissolved in 40, 50, 60, 80, and 95% ethanol, respectively .....	43
<b>Figure 2.6</b> Different behaviors of a droplets on a hydrophobic surface under (a) Cassie-Baxter state and (b) Wenzel state .....	44
<b>Figure 2.7</b> The WCA values of zein films made on the microscope slides with OT SAMs from 0.05 wt% zein solution measured at (a) 0 s and (b) 13 s after the water droplet was placed.....	45
<b>Figure 2.8</b> SEM image of zein film made on microscopy slide coated with OT SAM from 1 wt% zein solution transferred after 45 min of solvent evaporation. The inset showed the WCA of the surface .....	48
<b>Figure 2.9</b> A Graphic illustration of zein hydrophobic films made on microscope slides coated with OT SAM from the transferred zein solution after various evaporation time .....	49
<b>Figure 3.1</b> SEM and WCA images of ZENN obtained by electrospinning from zein solutions with the concentration of (a) 5, (b) 10, (c) 15, (d) 20, (e) 25, and (f) 30 wt%, respectively.....	58
<b>Figure 3.2</b> SEM and WCA images of the ZENN made by electrospinning at (a) 10, (b)	

18, (c) 21kV, and (d) 24kV from zein solution with the concentration of 10 wt%, respectively .....	60
<b>Figure 3.3</b> (a) SEM image and (b) Fluorescence image of HepG2 cell growth on the ZENN.....	61
<b>Figure 3.4</b> Fluorescence images of HepG2 cell attachment on (a) ZENN and (b) ZC .....	62
<b>Figure 3.5</b> Fluorescence images of HepG2 cell attachment on the ZENNs treated with oxygen plasma for (a) 0 min, (b) 5 min, and (c) 10 min, respectively. Fluorescence images of UMR106 cell attachment on the ZENNs treated with oxygen plasma for (d) 0 min, (e) 5 min, and (f) 10 min, respectively.....	64
<b>Figure 4.1</b> WCA images of ZEF made from a solution containing (a) 10 and (b) 30 wt% of zein in 80% ethanol, respectively .....	73
<b>Figure 4.2</b> WCA images of ZCF made from a solution containing (a) 10 and (b) 30 wt% of zein in 80% ethanol, respectively .....	73
<b>Figure 4.3</b> SEM images of ZEF made from a solution containing (a) 10 and (b) 30 wt% of zein in 80% ethanol, respectively .....	74
<b>Figure 4.4</b> WCA images of surface obtained from a solution containing 5 wt% of PEG-PLA in chloroform by (a) electrospinning and (b) cast drying, respectively .....	75
<b>Figure 4.5</b> (a) WCA and (b) SEM image of SDZP prepared from 10 wt% of zein in 80% ethanol.....	76
<b>Figure 4.6</b> FTIR spectra (blue dotted line) at Amide I region and the corresponding	

secondary derivatives (red solid line) of (a) ZCF, (b) ZEF prepared from 10 wt% zein solution, (c) ZEF prepared from 30 wt% zein solution, and (d) SDZP, respectively .....	78
<b>Figure 4.7</b> Schematic illustration of zein super-hydrophobic/hydrophobic surface formation during electrospinning and spray drying.....	80
<b>Figure 5.1</b> SEM images of VC-loaded zein/CS MPs with various zein/CS mass ratio of (a) 0.5:1, (b) 1.0:1, (c) 1.5:1, (d) 2:1, (e) 2.5:1, and (f) 3.0:1 .....	93
<b>Figure 5.2</b> Negative ion ESI-MS spectrum for the VC-loaded zein/CS MPs.....	95
<b>Figure 5.3</b> Negative ion ESI-MS/MS spectrum for the m/z 173 ion .....	96
<b>Figure 5.4</b> The <i>in vitro</i> release curves of VC from VC-loaded CS NPs and VC-loaded zein/CS MPs in SGF, respectively .....	98
<b>Figure 5.5</b> The <i>in vitro</i> release curves of VC from VC-loaded zein/CS MPs in SGF and SIF, respectively.....	99

## **Abbreviations**

**EISA:** evaporation-induced self-assembly

**NP:** nanoparticle

**MP:** microspheres

**SAM:** self-assembly monolayer

**SAXS:** X-ray scattering

**SPR:** surface plasmon resonance

**WCA:** water contact angles

**ECM:** extra cellular matrix

**PLGA:** Poly (lactic-co-glycolic acid)

**PLA:** polylactide

**PLLA:** poly-L-lactide

**BMS:** bare metal stents

**DES:** drug-eluting stent

**PEG:** polyethylene glycol

**SEM:** scanning electron microscope

**TEM:** transmission electron microscope

**EDS:** X-ray spectroscopy

**CD:** circular dichroic spectrum

**AFM:** atomic force microscopy

**OT:** 1-octanethiol

**ZENN:** zein electrospun nanofibrous network

**DMEM:** Dulbecco's Modified Eagle Medium

**FBS:** fetal bovine serum

**PBS:** phosphate buffer saline

**OZENN:** oxygen plasma treated ZENN

**ZCF:** zein casting film

**DAPI:** 4',6-diamidino-2-phenylindole

**ZEF:** zein electrospun film

**ATR-FTIR:** attenuated total reflection-Fourier transform infrared spectroscopy

**PS:** polystyrene

**SDZP:** spray dried zein powder

**EPPE:** electrospun PEG-PLA film

**CDPP:** cast-drying of the PEG-PLA

**VC:** vitamin C

**Chitosan:** CS

**STPP:** sodium tripolyphosphate

**EE:** encapsulation efficiency

**LE:** loading efficiency

**ESI-MS:** electrospray ionization mass spectrometry

**SGF:** simulated gastric fluid

**SIF:** simulated intestinal fluid

# Chapter 1: Literature Review

## 1.1 Introduction of zein

Corn, which is also called maize, is a very important food and industrial crop in the world. In the endosperm and the germ of corn kernel, the most of the starch and oil are stored (Figure 1.1) [1]. Endosperm tissue is also where most of the protein content (about 75%) is contained. The remaining protein is distributed between the bran and germ [1]. There are mainly four processing methods for corn: alkaline processing, wet milling, drying milling and the dry grind process for ethanol production. Corn contains four primary classes of protein, which are classified by their solubility in certain solvents. Among the four classes of protein (albumins, zein, globulins and glutelin), zein and glutelin constitute most of the protein in the whole kernel. Their protein fractions are about 30% and 40% (dry basis), respectively [1].

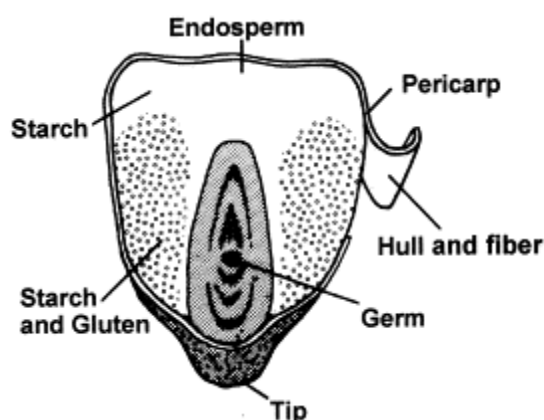


**Figure 1.1** The location of major components in the corn kernel.

Zein is a kind of protamine with an average molecular weight of 44000 Da [2, 3]. Different from the majority of natural materials, zein cannot be dissolved in either

ethanol or water alone; however it is soluble in 70-80% aqueous ethanol. Its specific solubility behavior can be attributed to the high percentage of nonpolar amino acid residues in the zein molecular [1]. It has been reported that more than 50% of its amino acids constituents are hydrophobic [4]. X-ray scattering (SAXS), CD spectra and surface plasmon resonance (SPR) are three common methods used to investigate the molecular structure of zein. Argos et al. have [5] studied the molecular structure of zein in 70% methanol using CD spectra. They proposed a structural model of a ribbon-type structure of size  $13 \times 1.2 \times 3 \text{ nm}^3$ , in which 9-10 helical segments were aligned in an antiparallel style and the segments were linked together by glutamine-rich turns. Later, Matsushima et al. investigated the structure of zein in 70% ethanol solution using SAXS and a rectangular prism model, similar to the one given by Argos et al., was proposed (Figure 1.2) [6]. In both arrangements, the top and bottom of the zein molecule, which were made by the glutamine-rich bridges, were hydrophilic, while the sides of the zein molecule, which were the zein  $\alpha$ -helices, were hydrophobic. Recently, Wang et al. have proved that there were sharply defined hydrophobic and hydrophilic domains at the surface of zein molecule by SPR [7].

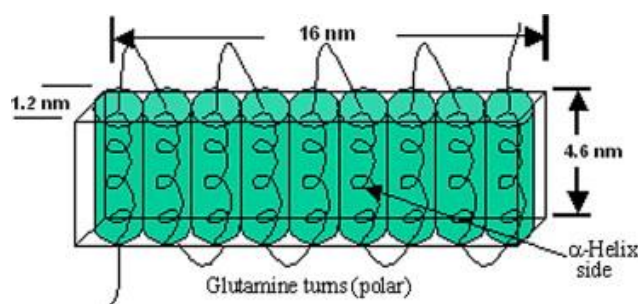


**Figure 1.2** Diagram of zein tertiary structure.

Zein is an abundant, inexpensive, and reproducible biopolymer having excellent mechanical properties and biocompatibility. It has been widely used in food and pharmaceutical industrials because of its good biocompatibility and degradability. Self-assembly is one of its important characteristics which makes zein have high potential applications in nano-encapsulation. It is a process that is induced by a polarity change in 70% ethanol solution with the preferential evaporation of one solvent (ethanol). The process is called evaporation-induced self-assembly (EISA). It is a spontaneous process which only depends on weak molecular interactions, such as capillary, van der Waals, hydrogen bonds, and  $\pi$ - $\pi$  [8].

Because of its self-assembly property, zein has been used to encapsulate many bioactive compounds. For example, Parris et al. have successfully encapsulated three essential oils (oregano, red thyme, and cassia) into zein nanoparticles (NPs) by phase separation (Figure 1.3a) [9]. It has also been reported that vitamin D3 could be encapsulated by zein NPs coated with carboxymethyl chitosan (CS) (Figure 1.3b) [10] and that citral and lime encapsulated by zein core-shell structure after EISA (Figure 1.3c) [11]. The diameters of these formed particles differed from less than 100nm to several micrometers, which were determined by the methodology, core-shell interaction and other environmental variables. In most occasions, the nano-scale drug-encapsulated particles were fabricated by phase separation, which meant the sudden addition of poor solvent (water) and desolvation of the zein [12]. Applications in plasmid DNA and 5-fluorouracil showed that drug-encapsulated zein NPs had eminent drug delivery efficiency [13, 14]. Improved drug stability, sustained release

and high therapeutic index could be possibly achieved by this technique.

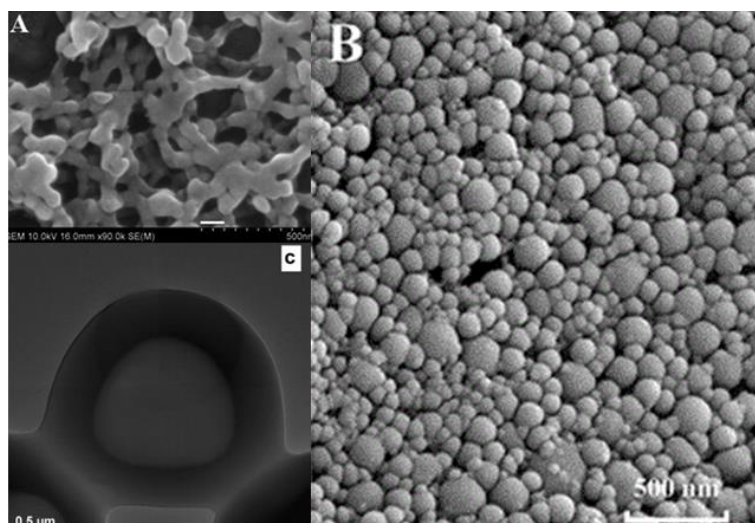


**Figure 1.3** (a) SEM image of VD3, (b) SEM image of oregano oil, and (c) citral encapsulated zein NPs, respectively.

Moreover, zein can also be used to fabricate fibers or ultrathin fibrous networks by electrospinning technique. At early times, Croston et al. spined alkaline zein solutions, coagulated them with acids and salts, and finally cured them with formaldehyde to fabricate fibers [15]. The formed zein fibers possessed good properties, such as comfort and warmth. Later the cross-linked zein fibers were fabricated using a drying spinning method [16, 17]. Recently, Lagaron et al. have successfully electrospun different zein solutions using various electrospinning conditions (Figure 1.4) [18]. They investigated in detail the effects of zein solution concentration, applied voltage, ethanol content, the distance of tip-to-collector, and flow rate on the morphologies of zein fibers.

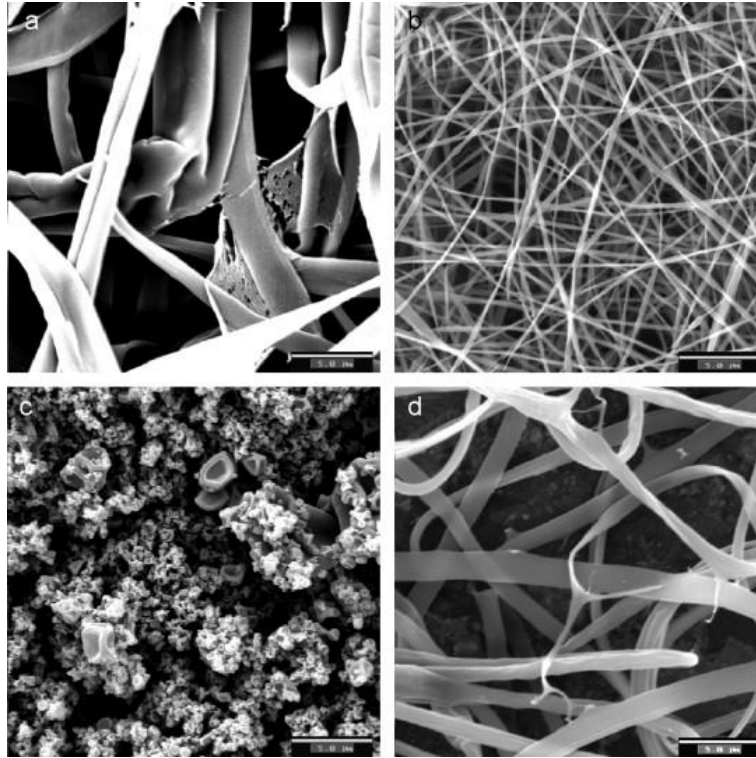


**Figure 1.4** SEM images of electrospun networks from (a) concentrated zein solution of 50 wt%; (b) zein solutions with a tip-to-collector distance of 15 cm; (c) diluted zein solution of 12 wt%; (d) acidified zein solution.

## 1.2 Introduction of hydrophobic surfaces

Water contact angle (WCA), also wetting angle is a measure of the wettability of a solid surface. When the WCA of a solid surface  $0^\circ$ , the surface the solid is defined as completely hydrophilic; when the WCA is between  $0^\circ$  and  $90^\circ$ , the surface is hydrophilic; and when the WCA is larger than  $90^\circ$ , the surface is hydrophobic [19]. Hydrophobic surfaces show very low water wettability. There is an equation called Young equation which explains the relationship of contact angle  $\theta$ , the surface tension of the liquid  $\sigma_l$ , the interfacial tension  $\sigma_{sl}$  between liquid and solid, and the surface

free energy  $\sigma_s$ :

$$\sigma_s = \sigma_{sl} + \sigma_l \cdot \cos \theta$$

Moreover, super-hydrophobic surface is a special hydrophobic surface with a WCA more than 150 °. It has been widely studied due to their self-cleaning and wetting properties [20]. Self-cleaning property, also called the “Lotus-Effect”, refers to the high water repellence. A Surface with self-cleaning property can hardly hold water droplets and thus water droplets will roll off the surface very quickly even at slight inclinations. This phenomenon can be attributed to the specific micro- or nanostructures on the surface, which leads to the minimization of droplet’s adhesion on the surface. Hydrophobic surfaces can be successfully fabricated on various materials, such as metals, synthetic polymers, glass slides, and Si wafers [21-23]. Hydrophobic surfaces have attracted much attention because of their broad applications in drug delivery, packaging, coating industry, electronic devices, textile industry, and bioengineering [24-26].

### **1.3 Tissue engineering**

#### ***1.3.1 Biomaterials for tissue engineering***

Tissue engineering is a technique aimed to find biological replacements which can help human body recover the bio-functions or substitute some human tissues. It involves various applications that repair or replace portions of or whole tissues, such as blood vessels, bones, cartilages et al. [27]. In tissue engineering, an artificial structure

called scaffold is often required for the incorporation of living cells. Scaffolds will help cells to adhere, grow, differentiate, and form three-dimension tissue. Considering its biological applications, scaffolds place high demands on materials properties including mechanical strength, biocompatibility, degradability and the activation of specific cell-material interactions [28].

Generally, porous materials, fibrous materials and hydrogel are the three kinds of scaffolds [29]. And there have been many processing methods for preparing these kinds of structures to be employed as scaffolds, such as solvent casting & particulate leaching (SCPL), electrospinning, textile technologies, and emulsification/freeze-drying [27]. Among them, electrospinning is a popular method used to fabricate continuous nanofibers which can be applied for tissue engineering scaffolds. In electrospinning, the solution is positively charged and the charged liquid jets in it are ejected by a syringe pump. And after flying cross the high electric field the jets are deposited on a collector to form a highly porous network consisting of nanofibers (Figure 1.5) [30]. By adjusting the conditions of electrospinning including solution concentration, voltage and liquid jet speed, the tensile strength and porosity of the formed nanofibers can be controlled. The formed electrospun nanofibrous scaffold has a high surface to volume ratio and interconnectivity which would simulate the extra cellular matrix (ECM) and offer a good environment for cells to grow, thus are feasible for vascular, bone and tendon impairments [30]. Moreover, it has been reported that the cell adhesion is regulated by the cell transmembrane receptor, called integrin. Usually the cell-adhesion-regulating molecules (e.g.

fibronectin, vitronectin) are physically absorbed or covalently attached onto the surface of nanofibers to improve the accessibility to the cell transmembrane receptor, thus promoting the cell adhesion. The electrospun scaffold itself should also be highly biocompatible after implantation and completely degraded after a while when the scaffold finishes its functions. Therefore the material selection of the scaffolds is crucial. There have been lots of natural and synthetic materials being electrospun to fabricate scaffolds in the tissue engineering. These materials include collagen, gelatin, polystyrene, and polyethylene oxide. And to improve the biocompatibility, various surface modifications were conducted onto the formed scaffolds, such as oxygen plasma treatment, surface chemistry combining molecules and so on.

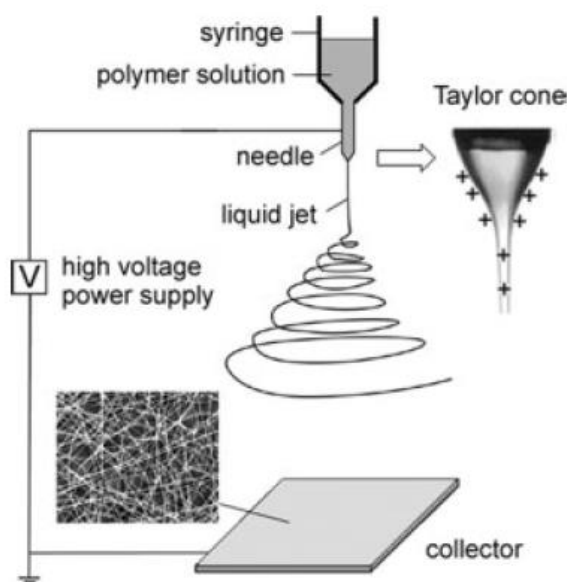


**Figure 1.5** A Schematic basic setup of electrospinning.

### Synthetic polymers

Synthetic polymers are always the materials of choice for tissue engineering scaffolds due to its easy production, ready availability and versatility of manipulation, and controlled polymer properties [31]. Baker et al. have reported a well-characterized polystyrene scaffold fabricated by electrospinning technique. Further three-dimensional *in vitro* cell experiments were also conducted on the argon plasma treated scaffolds and good cell attachment was observed. Poly (lactic-co-glycolic acid) (PLGA) is also a commonly used synthetic polymer for tissue engineering scaffolds due to its good biodegradability and biocompatibility. It has been electrospun to fabricate the protein-resistant, functionalized nanofibers with the addition of a six-armed star shaped poly (ethylene oxide-stat-propylene oxide) which was used to alter the wettability of nanofiber scaffold surface, and cell-adhesion-mediating peptides (Gly-Arg-Gly-Asp-Ser) which could enhance the cell attachment [32]. The subsequent human dermal fibroblast cells experiments were conducted and the formed scaffold demonstrated good cell proliferation in the meshes (Figure 1.6) [33].

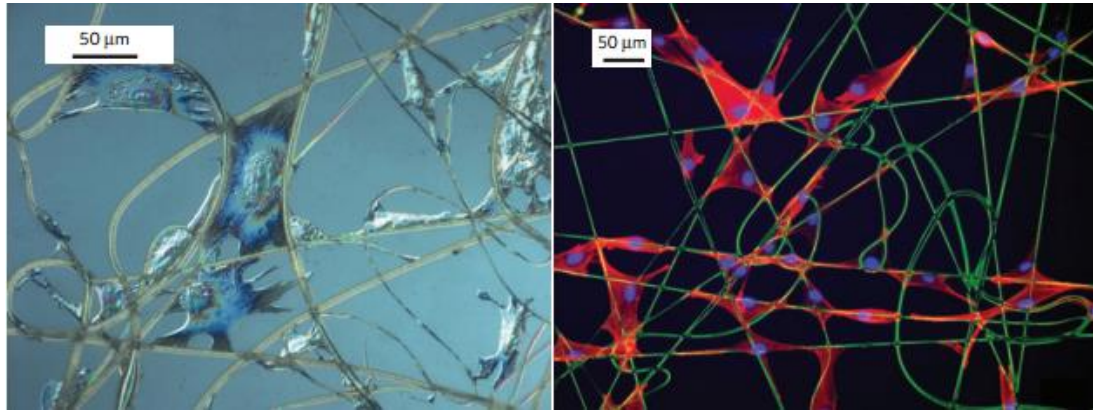


**Figure 1.6** Optical microscope image (left) and fluorescence microscope image (right, actin filaments red, nuclei blue) of human dermal fibroblasts after 24 h cell culture on nanofiber scaffold [33].

Another example of electrospun nanofibrous PLGA scaffolds was reported by Thomopoulos et al. [34]. They presented a novel scaffold combined with a hydrogel delivery system and applied it for the tendon repair. The formed scaffold could be biodegradable in an aqueous environment but was resistant to enzymatic degradation. Moreover, the degradation rate and mechanical properties of the scaffold could be controlled by altering the ratio of lactic to glycolic monomers. Besides *in vitro* cell viability experiment, the *in vivo* implantation was also investigated using a canine animal model. The results showed controlled growth factors release from the scaffold and successful implantation at a flexor tendon repair site *in vivo*.

### Natural polymers

Compared with synthetic materials, natural biopolymers are inexpensive, biocompatible, soft, biodegradable, with low/no toxicity, sustainable, and sustainable.

They are the ideal materials for scaffolds and constructs in tissue engineering because of their good cytocompatibility [35]. They have similar molecular structures and functions to the ECM, and the environment of human body is willing to recognize and deal with them. Due to their similarity with the ECM, compared with synthetic polymers, there is not stimulation of chronic inflammation or immunological reactions after the implantation of natural biopolymers into human body [36]. Collagen is one of the widely used natural polymers for tissue engineering scaffolds because it is a primary structural element of ECM in native tissues [37]. Both Matthews et al. [38] and Boland et al. [39] have described the fabrication of collagen nanofibrous scaffolds for preliminary tissue engineering tests. And both their *in vitro* cell experiments demonstrated the promising applications of electrospun collagen scaffolds in tissue engineering. Nevertheless, the commonly used natural materials, like cellulose [40, 41], have their weak points. They are hydrophilic and can be easily dissolved in water, which limits their applications in biomedical engineering [42, 43].

#### *Synthetic and natural polymer hybrids*

In spite of the favorable properties the natural polymers possess, general natural materials have their own weak points. Their hydrophobicity and water-absorbing quality make them present a main drawback of a rapid solubilization in aqueous environments, which limits their applications in biomedical engineering [42, 44]. Moreover, the low mechanical strength is also a limitation for most natural materials, such as CS and collagen. In order to utilize the respective advantages of different

polymers, synthetic/natural polymer hybrid scaffolds have been developed in recent years. In hybrid scaffolds, the synthetic polymers can give mechanical strength while the nature polymers can offer a more natural tissue environment for cell proliferation. There has been a study to investigate the electrospun hybrid scaffolds made of collagen/polylactide (PLA), CS/PLA, and collagen/CS/PLA, respectively, for employing in cartilage tissue engineering (Figure 1.7) [45]. Their results showed that compared with the plain scaffolds fabricated with only collagen or CS, the hybrid scaffolds showed better mechanical properties and penetration of chondrocytes into the scaffolds. Recently Lou et al. [46] also reported a similar bi-layer scaffold containing a superficial CS/PCL nanofibrous mat and an underlying poly-L-lactide (PLLA) microporous disc to mimic the two-layered structure of native skin. (Figure 1.7)

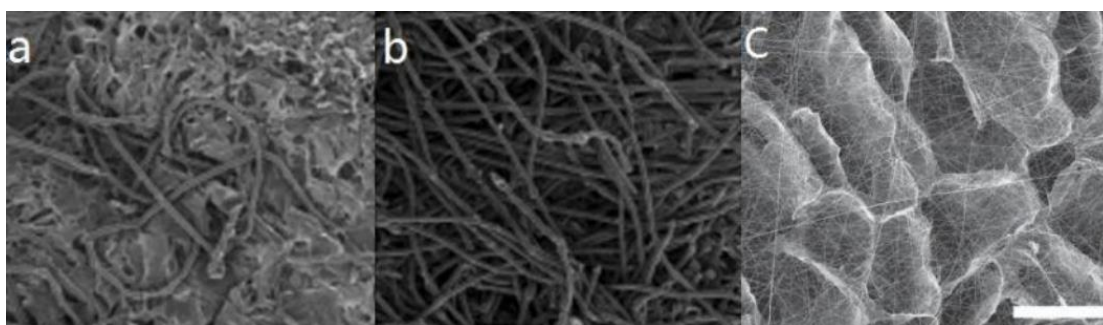


**Figure 1.7** SEM images of the hybrid scaffolds containing (a) CS/PLA and (b) collagen/PLA, and (c) bi-layer scaffold.

### ***1.3.2 Applications of hydrophobic surfaces in vascular stents engineering***

Vascular stents were introduced in 1990s to treat coronary vessel narrowing and clotting caused by atherosclerosis and coronary [47]. In 2009, it was reported that more

than 250,000 stents are implanted in human bodies every year in Germany. Cobalt-chromium alloys, nickel-titanium and stainless steel are three primary kinds of materials used to fabricate the bare metal stents (BMS) [48]. BMS, which is a better choice over the traditional bypass graft surgery, avoids vessel recoil during the treatment of coronary artery disease. However, BMS implantation raised the risks of restenosis and thrombosis, which was mainly caused by vascular injury during the stent implantation surgery. It has been reported that in about 15-20% of all these cases, patients need re-intervention with 6-12 months after the BMS implantation [49]. To avoid thrombosis, anti-coagulant is usually used. However, because of its side effect on the prevention of blood platelet aggregation, anti-coagulant can lead to an increase in the risk of major bleeding. Restenosis is recurrence of stenosis, which is the narrowing of a blood vessel. Restenosis will lead to the restricted blood flow. Restenosis happens when a stent is used. The stent, as a foreign body, can react with artery and the immune system will respond and result in further narrowing near or inside the stent. To prevent restenosis, anti-platelet drugs are used immediately after surgery. Again, similar to the effect of anti-coagulant, anti-platelet may result in an increase in the risk of major bleeding.

Reducing thrombosis and restenosis is an important objective in scientific research and development of new endovascular technologies. The occurrence of thrombosis and restenosis can be attributed to the agglomeration of blood platelets. Generally using anti-restenosis drugs, surface modification, and applying biocompatible materials are the primary ways to reduce the aggregation of blood platelets. Then the response of the

immune system, which is because of the implanted stent as a foreign body, is reduced and therefore the restenosis will be reduced.

Drug eluting-stent (DES) is the stent that can contain anti-restenosis drugs. A DES usually consists of a permanent BMS platform and a permanent non-absorbable, non-degradable coating which contains an active pharmaceutical drug, such as sirolimus and paclitaxel [50]. The controlled release of the drugs from the coating directly to the site of vascular injury dramatically inhibits the in-stent restenosis [51]. It is reported that by adding a drug-eluting coating, the rate of restenosis has been reduced to 5% or less [52]. Although DES is very effective and promising regarding the inhibition of in-stent restenosis, it still has many disadvantages such as local drug toxicity and even death [53, 54].

Stent surface modification is another method used to avoid thrombosis and restenosis. Super-hydrophobic surface stent is a stent that has special surface properties, which can reduce the surface aggregation of proteins and cells. Super-hydrophobic surface stent is better than DES because no drug is involved and thus there is no drug toxicity problem. Super-hydrophobic surface is a special kind of hydrophobic surface that has a WCA higher than  $150^\circ$ . Super-hydrophobic surface has very low water wettability and special adsorption behaviors of different kinds of materials. Super-hydrophobic surface has wide applications in drug delivery, packaging, textiles, electronic devices, coatings, and bioengineering [24-26]. Super-hydrophobic surfaces have been broadly investigated and applied because of their self-cleaning properties, which means the water droplet can flow down and clean the surface when the surface is

not flat [20]. Therefore, the self-cleaning property of super-hydrophobic surface can reduce the adhesion of protein, blood platelets, and smooth muscle cells, thus reducing the risk of thrombosis and restenosis and making super-hydrophobic surface a desired coating material for vascular stents.

The possibility of restenosis can also be reduced using materials with high biocompatibility for stent formation. In biomedical engineering, a foreign synthetic material, which may have low biocompatibility or even have toxicity, in the living tissue of human body will cause many unwanted reactions [55]. The materials with the best biocompatibility could be the natural materials derived from edible plants.

#### **1.4 Nano-encapsulation technology**

Cancer, caused by uncontrolled cellular proliferation, is a leading cause of death in the 21st century [56]. Various anticancer drugs, including traditional Chinese medicine that can effectively kill cancer cells, were developed in the last decade. However, the problem is still about the low therapeutic index of the drugs, which means the effective dose of drugs will cause cytotoxicity to normal cells.

Nano-technology is expected to play an important role in the fast developing area of nano-medicine. It provides new solutions for currently untreated disease and tools for drug delivery, gene therapy and so on [57-59]. Nano-encapsulation is one of the hottest applications of nanotechnology in recent years. It is defined as loading drugs into ultrafine vesicles or colloidal capsules. The particles fabricated should be on the nanoscale (with all three Cartesian dimensions less than 100nm). Nano-encapsulation

is a superior method in drug delivery system with many advantages. The cell membrane is hard for complexes larger than 1 kDa to permeate, however, drugs with large macromolecules as their delivery vehicles can entry cells due to the specific active internalization mechanism of cell membrane. In nano-encapsulation, drugs are loaded into ultrafine vehicles or capsules that are in the size of nanomaterial level. Nano-encapsulation, because of its small size, large surface area, and high mobility, could dramatically improve the bioavailability of insoluble drugs. Nano-encapsulation is also found effective in some cancer treatments because NPs can easily pass through the leaky tumor capillary fenestrations and accumulate within the tumors because of the enhanced permeability and retention (EPR) effect [13]. Besides, the core-shell structure of nano-encapsulation increases the stability of the drug and realizes sustained release [60]. It also allows increased intracellular accumulation of the therapeutic agent and limits the uptake by healthy tissues. Nano-encapsulation is also being studied as a method to stop metastasis of tumor cells by preventing the adhesion of polymorphonuclear cells to the endothelial cells [61].

A variety of drugs have been encapsulated using different techniques, such as nano-suspension and liposomes, to improve its solubility and cellular uptake. However, for nano-suspension, the high-pressure homogenization used in fabrication may lead to the loss of the bioactivity of the active compounds. And for liposome, the low encapsulation efficiency, short circulation time and poor stability for lipid vehicles are the problems [62]. Moreover, surfactant and chemical linkers are constantly used in these methods, such as sucrose monolaurate [63] and polyethylene glycol (PEG) [64].

These materials could significantly increase the final size of the particles formed or may have inferior biocompatibility. To improve the nano-encapsulation of drugs, natural materials, such as protein, with self-assembly properties are considered as a better option because of the good biodegradability, high nutritional value, renewable sources, and large binding capacity of drugs.

## **1.5 Drug delivery system**

### ***1.5.1 Background***

Cancer counts for one in four deaths in the US. Currently, tons of anti-cancer drugs have been developed. However, the general problem of these drugs is that they lack efficient selectivity toward tumor cells. They kill both normal and cancer cells and result in toxicity to normal tissues. Because of the weak selectivity, the drug reaches the target site in concentrations much less than effective [65]. In this case, the drug dose has to be further increased to make it effective, and thus, more toxicity will be given to the normal tissues. Severe side effects decrease the life quality of the patients and can be fatal at times. Site-specific delivery, which protects the drug from release until the target site is reached, should be applied to increase the drug concentration at the target site, and thus a lower dose with reduced incidence of the side effects will be applied.

Novel pharmaceutical agents with tumor selectivity and specificity and limited side effects could be of great therapeutic value. The material selection for the drug delivery agents is important and it will determine the selectivity and specificity as well as the toxicity of the agent. So far, the site-specific delivery is still a problem because of

the selection of the carrier materials, and a balance between the biocompatibility and functionality of the carrier materials is difficult to achieve. A drug delivery system is often associated with particulate carriers, such as polymeric micelles, emulsions, liposomes [66], nanotubes, dendrimers [67], and NPs [68-72], which are designed to localize drugs at the target sites [73].

Selecting and using the biomaterials with special interactions to the targeted cells or tissues, it can improve the drug efficacy and lower the toxicity [74]. The better material choices for biomedical applications are natural materials derived from plants, because of their biocompatibility, biodegradability, non-toxicity, and even edibility. However, general natural materials may have their own weak points and are not the best and direct choices, because most of the natural biomaterials are hydrophilic, water absorbing, and they have a main disadvantage of a fast solubilization in water [42, 43].

### ***1.5.2 Introduction of endocytosis***

The mechanism of cellular uptake and intracellular trafficking of NPs have been well investigated by scientists. It is found that endocytosis is the mechanism most relative to the cellular uptake of NPs [75]. Endocytosis (Figure 1.8) is known as a process that the cell membrane invaginates to engulf molecules and the intracellular membrane-bound endosome containing the molecules subsequently traffic through the cells. There are mainly four subtypes of endocytic pathways for NPs to enter the cells. They are phagocytosis (“cell eating”), macropinocytosis (“cell drinking”), clathrin-mediated endocytosis (CME) and lipid raft/caveolae-mediated endocytosis.

Phagocytosis is used for large particles, such as bacterial, to enter the cells. It is the first step of cellular uptake and degradation of particles large than 500 nm. Macropinocytosis is used to internalize fluid surrounding the cell to take up the substances in the fluid phase simultaneously. CME is a process that the protein, clathrin, recruits cargo into developing clathrin-coated pits (CCPs), and subsequently forms clathrin-coated vesicles (CCVs) [76-78]. These endocytic vesicles later mature into late endosomes and fuse with lysosomes [78]. Caveolae-mediated endocytosis is a process involving formation of so called caveolae on the plasma membrane by the clustering of lipid raft components. The formed caveolae is a result of the interactions of different proteins, mainly caveolin, with the cellular membrane.

It was found that nanostructured calcium phosphate particles entered cells via clathrin-mediated and caveolae-mediated endocytosis [79], and that highly fluorescent conjugated polymers and siRNA-loaded lipid NPs entered cells through micropinocytosis [80, 81]. There are also studies showed that one kind of NPs can enter the cell using two or more kinds of endocytic pathways, such as hydrophobically modified glycol CS NPs could enter cells through micropinocytosis, caveolae-mediated endocytosis, and clathrin-mediated endocytosis [82].

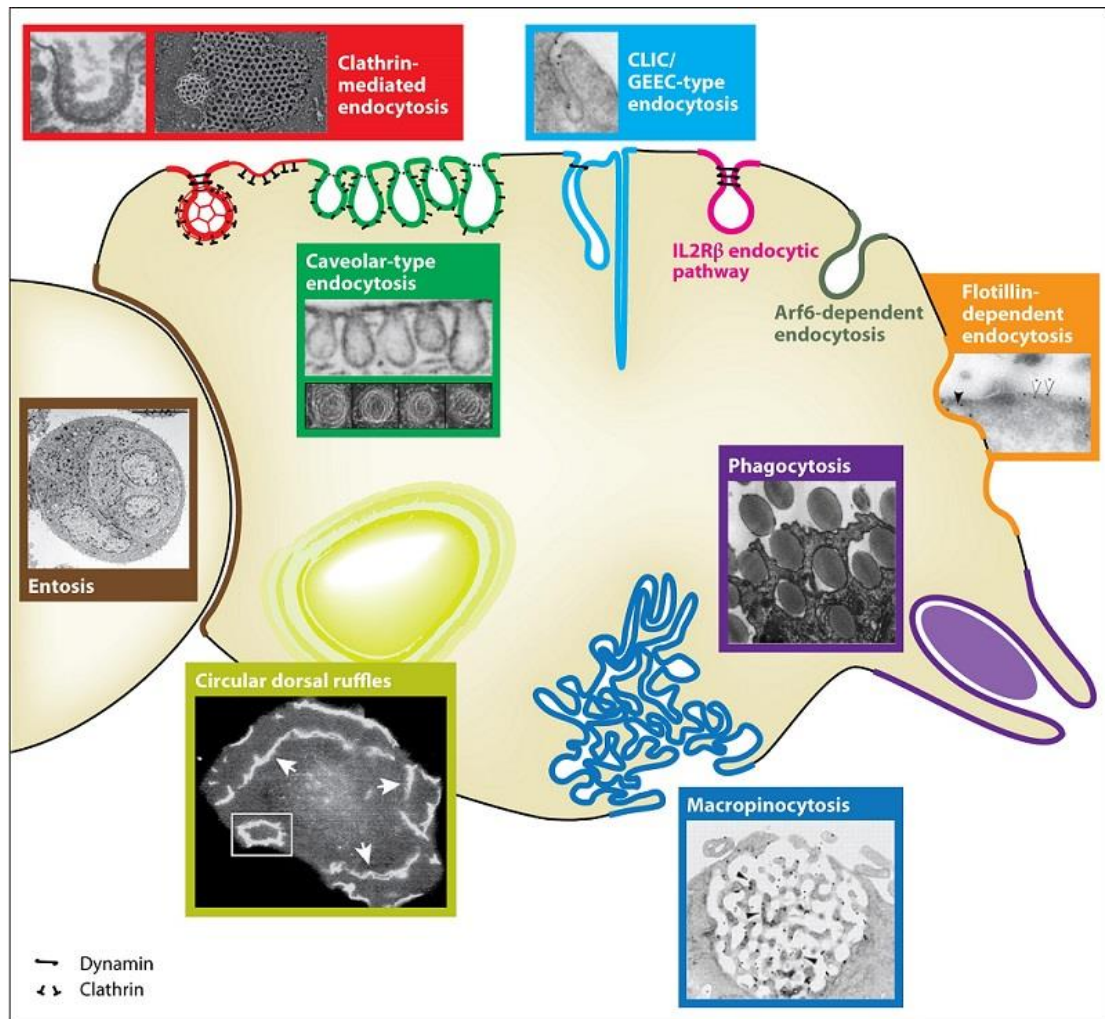


**Figure 1.8** The hypothetical cellular endocytic pathways. Figures are modified based on the following sources: Clathrin-mediated endocytosis [83], caveolae-mediated endocytosis [84], CLIC/GEEC-type endocytosis [85, 86], the putative flotillin-associated endocytic structures [87], phagocytosis, macropinocytosis [88], circular dorsal ruffles [89], and entosis [90].

### 1.5.3 Methods used to study endocytosis of NPs

The mechanisms of cellular uptake of NPs have been studied by adding inhibitors, mutated proteins, and localization of NP with markers and fluorescent dyes.

### Pharmacological inhibitors

Pharmacological inhibitors are usually employed to study which endocytotic pathway is account for NPs entering cells and various inhibitors have been used for studies of different kinds of endocytotic pathways (Table 1.1). For example, the uptake of the fluorescent NPs was systematically measured in the presence and absence of a variety of pharmacological inhibitors. And the efficacy of the inhibition of NP uptake in different cell lines was evaluated by quantifying the fluorescence intensity of different experiment groups using flow cytometry [78].

However, the approach using inhibitors for identifying different endocytotic pathways is not that reliable because these inhibitors do not have specific effects on one endocytotic mechanism. For instance, the most popular inhibitors used for studying endocytotic mechanisms of cellular uptake of NPs are methyl- $\beta$ -cyclodextrin (m $\beta$ CD, for cholesterol depletion), filipin or nystatin (cholesterol-binding drugs for perturbation of the chlesterol function). However, cholesterol is not only responsible for the caveolae-meditated uptake, but also for macropinocytosis. [91-93] Moreover, m $\beta$ CD treatment also inhibits clathrin-meditated uptake. [94] Therefore, depletion of cholesterol cannot be used to identify one endocytosis mechanism. Another example is potassium depletion of cells for removing clathrin from the membrane, which was used to block clathrin-meditated endocytosis. [95]. It is also an unspecific method with side-effects on cellular physiology.

**Table 1.1** The commonly used pharmacological inhibitors for identifying the endocytic pathways of uptake of NPs.

	<b>Pathway</b>	<b>Inhibitors</b>
	Phagocytosis	Sodium azide, cytochalasin B
	Macropinocytosis	EIPA, wortmannin, cytochalasin D
<b>Endocytosis</b>	Clathrin-mediated endocytosis	m $\beta$ CD, nystatin, genistein, filipin, cytochalasin D
	Lipid raft/caveolae-mediated endocytosis	PAO, phnylarsine oxide, cytochalasin D

### Expression of mutated proteins

Expression of mutated proteins using siRNA is another method with advantages used to study the endocytotic pathways. Compared with the old method with pharmacological inhibitors, the latter one has less side-effects and more specific. However, expression of a mutated protein may lead to lower-affinity interactions and siRNA treatment may give rise to unwanted cellular changes and interfere with the determination of the target protein [96, 97].

### Cell imaging

After entering the cell, the NPs could be transported from apical early endosome (AEE) to late endosome (LE) and further to lysosome (AEE/LE/lysosome route). The alternative pathway was from AEE to recycling endosome compartment (REC) or endoplasmic reticulum (ER). Both of these two routes are involved in the polymer NP trafficking [98]. The intracellular pathway of NPs has been investigated by fluorescently labelled NPs, and electron and confocal microscopy. Compared with

confocal microscopy, which has low resolution, the direct electron microscopy observation can make it sure that whether the NPs are taken up into the cells or just attached to cell surface. Furthermore, the use of different markers of intracellular organelles is much of helpfulness for identifying the colocalization of NPs. The markers used for the intracellular mechanism study are listed in Table 1.2.

To sum up, it is desired to combine different methods, such as different inhibitors, mutated proteins and microscopy to elucidate the mechanism of endocytosis when one is not specific enough to figure out the endocytic pathways.

**Table 1.2** The commonly used markers for identifying the intracellular colocalization of uptake of NPs.

	<b>Compartments</b>	<b>Markers</b>
<b>Intracellular trafficking</b>	Early endosomes	Rab5, EEA1, TfR
	Late endosomes	Rab7, ESCRTs
	Lysosomes	LAMP-1, LAMP-2
	Recycling compartment	Rab11
	Trans-Golgi	TGN46
	Cis-Golgi cisternae	GM130, giantin

#### ***1.5.4 Modifications of NPs for targeted drug delivery***

NPs containing drugs can offer improved drug delivery by entering cells due to the specific active internalization mechanism of cell membrane. They can be absorbed through the vesicles formed by cell membrane engulfing, subsequently transported to early endosomes where they can be recycled and exocytosed [99] or trafficked to organelles such as golgi, mitochondria and lysosomes. It is reported that the

intracellular trafficking pathway is controlled by the initial pathway of endocytosis [100]. For example, those NPs taken up by clathrin-mediated endocytosis will be typically degraded by lysosomes, such as virus, lipids, nucleic acid, carbohydrates, and nucleic acids. However, in the case of clathrin-independent endocytosis, the formed endosomal vesicles accumulate and proceed through a nondegradable path. Therefore, the selective incorporation of material as drug carriers is depended on the required type of cellular uptake endocytosis for different therapies.

Lots of natural and synthetic materials are being applied as drug carriers. For instance, Zein, a prolamine protein, is considered as one of the superior candidate carrier in particulate delivery. As a natural polymer derived from plants, zein has good biocompatibility and degradability, which makes it a suitable material for food and pharmaceutical industries. In addition, zein is especially valued in drug encapsulation in both macro- and nano-scales due to its unique self-assemble behavior. A lot of bioactive compounds have been successfully encapsulated by zein. The diameters of the product particulates differ from less than 100nm to several micrometers.

However, the natural materials used for carries do not always satisfy the requirements of therapies. Therefore, the modification of the formed NPs for targeted drug delivery is necessary. The fundamental aim of targeted delivery is to avoid the lysosomal trafficking, thus protecting the drugs from enzymatic degradation. In order to direct the formed NPs containing drugs to the endolysosomal system of particle cell populations, many ligands have been incorporated on the NPs, such as folic acid [101], riboflavin [102], and nicotinic acid [103].

To sum up, the types of endocytosis of cellular uptake depend on different types of cells and NPs. There are mainly four types of endocytosis involved in uptake of NPs, namely phagocytosis, macropinocytosis, clathrin-mediated endocytosis and caveolae-mediated endocytosis. To clarify the specific type of cellular uptake of NPs, there are currently three different methods, including pharmacological inhibitors, mutated protein expression and microscopic observation. Due to the complexity of NPs, the combination of different methods should be used to avoid misunderstanding the mechanisms of cellular uptake of NPs. Moreover, recently scientists have devoted themselves to modifying the NPs with particle ligands in order to get the specific cellular organelle targeting and the desired drug delivery.

## **1.6 Project aims and significance**

The project present in the thesis explores several potential applications of zein in biomedical engineering. There are mainly two aims in this thesis: (1) fabrication of zein structures with hydrophobic surfaces in facile methods; (2) examination of the formed zein hydrophobic structures for their application in tissue engineering; (3) investigation of the formation mechanism of the formed zein hydrophobic structures; (4) encapsulation of vitamin C using zein to obtain controlled release in gastrointestinal fluids. For hydrophobic surface formation, the work in the thesis is trying to find out other approaches beyond the traditional processing methods and supplement the current research about zein with more knowledge about its EISA property, thus providing a potential model for amphiphilic molecules like zein to form

various structures with different surface wettability. Moreover, the work extends the application of another natural polymer zein in biomedical engineering. For encapsulation, the work proposes another route to encapsulate polar and sensitive compounds using zein through EISA process. In addition, its pharmacokinetic release in intestinal fluids suggests a potential use in oral administration of medical drugs to improve their absorption efficiency in the intestine.

## **Chapter 2: Hydrophobic surfaces formed from zein in aqueous solutions by self-assembly**

### **2.1 Introduction**

Hydrophobic surface is a kind of surface with low wettability and special adsorption of different materials, like cells and proteins. It has a WCA larger than  $90^\circ$ . Because of its special properties, hydrophobic surface has been widely used in packaging, coating industry, electronic devices, textile industry, bioengineering, and drug delivery [24-26]. When the WCA value of a hydrophobic surface is larger than  $150^\circ$ , it is called super-hydrophobic surface. It has been broadly investigated and applied due to its special self-cleaning property [20]. It is reported that the primary materials used for the formation of hydrophobic surfaces so far are: glass slides, synthetic polymers, metals, and Si wafers [21-23]. However, the rigid substrates used in the fabrication limits the applications of these materials [104]. Their hydrophobicity is very likely to be damaged as these substrates deform. Moreover, in biomedical engineering, the inherent flexibility of the substrate used is required to match the mechanical and physical properties of different tissues and organs in human body [105]. Further, good transparency is also required for these soft materials [106, 107]. Finally, considering about the toxicity and biocompatibility of the materials, the implantation of such materials into human body is likely to cause lots of undesired immunoreaction, such as blood clotting [55].

Natural polymers are usually low/now toxic, biocompatible, biodegradable, possibly transparent, and sustainable. They have a high potential to be used constructs

or scaffolds in the tissue engineering [35]. Natural biomaterials are very similar to the ECM, and therefore the human body environment is willing to recognize and deal with them, which will avoid unwanted immunological reactions after implantation. Nevertheless, the commonly used natural polymers, like cellulose [40, 41], have many disadvantages when they are formed the hydrophobic surfaces. Cellulose is hydrophilic and water absorbing and it can solubilize rapidly in aqueous environments, which is the main drawback of most natural biomaterials [42, 43].

In general, to increase the roughness of a surface and to decrease the energy of a surface are the two primary methods to increase the hydrophobicity of a surface [108]. Surface roughness refers to the component of surface texture. The roughness of a surface can be determined by the deviations in the direction of the normal vector of a real surface from its ideal form [109]. The larger the deviations are, the rougher the surface. It is reported that to obtain the nano/micrometer-scale roughness on a surface, there are various ways, like controlled crystallization, chemical etching, lithography, templating, graft polymerization, phase separation, electrospinning, deposition, and colloidal self-assembly [106, 110-113]. Nevertheless, there are the two main drawbacks involved in the above methods: size limitation and costly equipment [22, 114]. Moreover, in most reported fabrication methods for hydrophobic/super-hydrophobic surfaces, fluorine-containing materials were used to achieve the low surface energy, which are not only costly but also harmful to the environment [115].

In this chapter, a facile and economical method is presented to fabricate the hydrophobic surfaces: SAM assisted EISA. SAM refers to a monolayer which is

formed through the active chemicals adsorbing spontaneously onto the substrates of a surface. SAM can be used to change surface wetting properties [106, 116]. EISA is a process that the solute in a solution can self-assemble into particles with the evaporation of the solvent. There are usually two or three solvents involving in the process of EISA. The faster evaporation of one solvent in the solution causes the change of the solution polarity. The changing polarity then serves as the force to drive the self-assembly of solutes. Compared with the expensive, easily contaminated and time-consuming methods, the self-motivated process method can dramatically save the cost and energy.

Zein, as an amphiphilic protein, can self-assemble into different structures. Wang et al. [117] have studied in detail the mechanism involved in the formation of zein microspheres (MPs), sponges, and films under different conditions. In their study, the effects of different zein and ethanol concentrations on the formation behaviors of different structures were investigated. When the concentration of zein was increased, zein would like to form in an order of MPs, sponges and films. They also investigated the kinetics of zein MP formation and size control [118]. Zein has good film forming property. It is also reported that Lai et al. [119] have successfully fabricated films through EISA from zein and plasticizers. Based on the interactions of the plasticizer and hydrophilic regions in zein molecule, they proposed a model of zein film formation.

It has been reported that zein molecules showed different adsorption behaviors on hydrophobic and hydrophilic materials, although they can interact with these two

kinds of surfaces because of the amphiphilicity of zein molecules. The different adsorption behaviors were observed by AFM and SPR on the surfaces covered with carboxyl or methyl monolayers, respectively [7]. They concluded that zein could self-assemble and adsorb onto both kinds of surfaces. They also concluded that, zein was more inclined to adsorb onto the hydrophilic surface than the hydrophobic one, which could be attributed to the specific structure of zein molecules.

In this chapter, zein was used to form a hydrophobic surface by a facile method: SAM assisted EISA. It was for the first time that the hydrophobic surface was made from natural materials, no surface coating or molecular modification. The material used was biodegradable and inexpensive. Comparing to rigid materials used in electronic devices, the flexible zein hydrophobic surfaces have much more advantages. Furthermore, with its biocompatibility, non-toxicity, and even edibility, the hydrophobic zein surface can well applied in tissue engineering. We believe this novel kind of surface can encourage a further development of zein-coated electronic devices and zein-based biomaterials.

## **2.2 Materials and Method**

### **2.2.1 Materials**

Zein was purchased from Wako Pure Chemical Industries, Ltd. (Tokyo, Japan). Ethanol (96% v/v) was purchased from Guangdong Guanghua Sci-Tech Co., Ltd (Guangzhou, China). 1-octanethiol (OT, C<sub>8</sub>H<sub>18</sub>S, ≥98.5%) was purchased from Sigma-Aldrich (St. Louis, MO, USA).

### ***2.2.2 Preparation of OT SAMs on gold coated substrates***

Microscope slides were first washed by 80% ethanol to remove any residual stains on them. After the slides were dried, they were coated with a 3 nm adhesive layer of Cr, followed with 15 nm Au layer. 2 mM OT was first dissolved in 80% ethanol. Then the gold coated slides were put into the OT solution for 30 min, during which OT molecules would spontaneously adsorb onto the gold coated slides [7]. Afterwards, the gold coated slides were washed by 80% ethanol-water to make sure there were not any residual OT molecules on the surface besides one OT monolayer.

### ***2.2.3 Preparation of zein films with hydrophobic surfaces***

Zein was dissolved in 80% ethanol, and the mixture was sonicated by an ultrasound generator (Sonics and Materials, Inc., Newton, CT, USA) at 300 W for 2 min. 0.5 mL of zein solution was then dropped on the prepared microscope slides coated with OT SAMs. After drying, zein films were formed and then removed off the slides. The zein film for control group was made on microscope slides without OT SAM from 10 wt% zein solution.

### ***2.2.4 WCA***

The hydrophobicity of the formed surface was determined by WCA value. The WCA of a hydrophobic surface is larger than 90°. The higher the hydrophobicity of a surface is, the larger its WCA value. For each zein film sample, triplicate were

measured to get an average. A standard goniometer (Kruss GmbH DSA 100, Hamburg, Germany) was used to measure the WCA value. The water droplets were deposited on three various areas of the surface, and each area was measured for 3 times. The whole process was recorded using a camera system. The WCA value was then calculated by the computer.

### **2.2.5 SEM**

SEM was used to examine the surface morphology of the formed zein films. The samples were gold coated (300Å) using the Edwards S150B sputter coater, which could increase the electrical conductivity. SEM images were captured using a JEOL JSM-6490 SEM (Tokyo, Japan).

## **2.3 Results and Discussion**

### **2.3.1 Hydrophobic zein film**

OT ( $\text{CH}_3(\text{CH}_2)_6\text{CH}_2\text{SH}$ ) is a linear-chained molecule. There are a  $\text{CH}_3$ - group and a  $\text{SH}$ - group at each end of the chain. It is broadly used to form hydrophobic SAMs. It is reported that  $\text{SH}$ - group of OT had a strong interaction with Au. Therefore after the microscope slides were immersed into the OT solution, OT could be attached on to the gold coated microscope slides to form OT SAMs after the slides were washed by the ethanol solution.  $\text{CH}_3$ - group is non polar and they constituted the surface of the formed monolayers, therefore, the surface of the finally prepared slides were hydrophobic. Figure 2.1a and Figure 2.1 b showed the WCAs of surfaces of two kinds of slides: one

without OT SAM and the other with OT SAM, respectively.

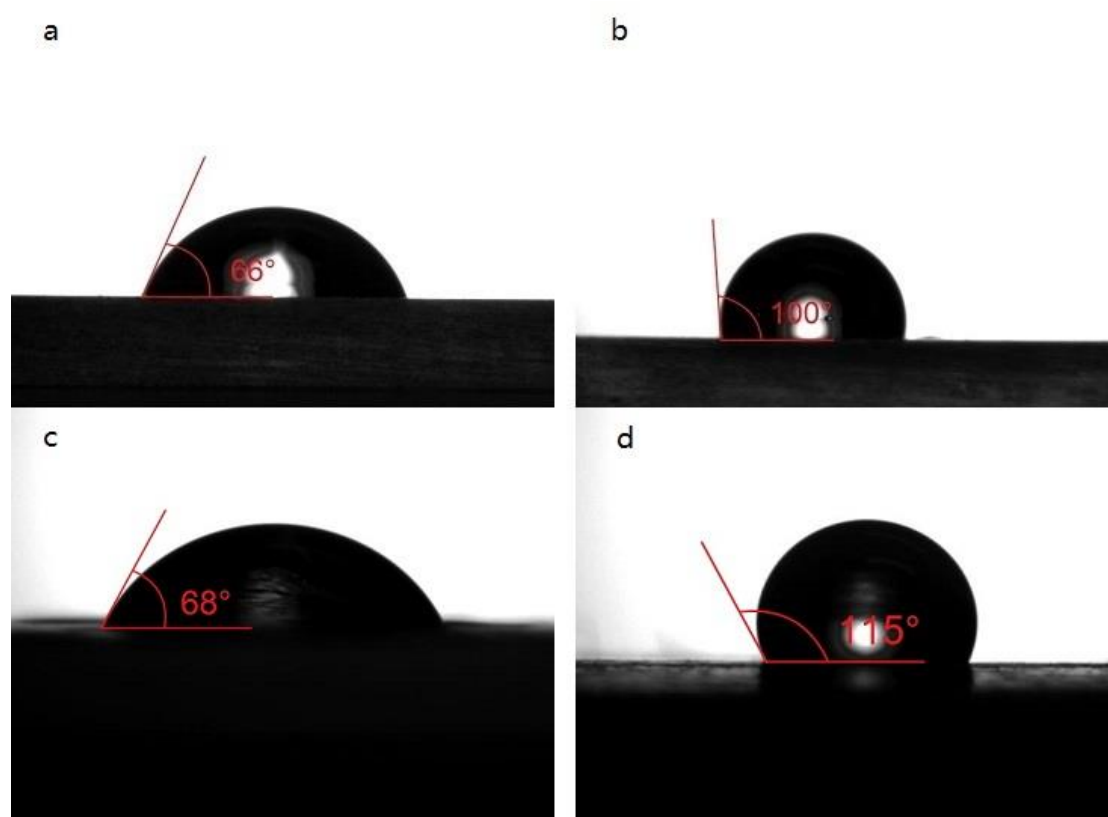


**Figure 2.1** The WCA of (a) a microscope slide without OT SAM, (b) a microscope slide with OT SAM, (c) zein film made on the untreated microscope slide from 10 wt% zein solution, and (d) zein film made on the microscope slide with SAM from 0.05 wt% zein solution.

The normal zein film was prepared by pouring 0.5 mL of 10 wt% zein solution onto an untreated microscopy slide. After drying, the formed zein film was removed off the slide and the WCA of the formed zein film was measured. Figure 2.1c showed that the surface of the formed zein film had a WCA of 68°, which indicated that it was

hydrophilic. Then an equal volume of 0.05 wt% zein solution was poured onto a microscope slide with OT SAM on it to form a film. After drying, the formed film was removed off the slide and the WCA of it was measured. Figure 2.1d showed the WCA of the surface, which faced to the OT layer. The WCA value was 115°, which was higher than 90, indicating the formed zein film had a hydrophobic surface.

To further ensure the increase of surface hydrophobicity of the formed zein film was not because of the remained OT left on the film when it was split from the microscope slide, EDS was then applied to characterize the element composition on the film surface. When the film was prepared, there were probably Cr, O, C, and Au involving in the process, therefore those elements were input the computer for analysis.

Figure 2.2 showed the EDS spectrum of a selected field from a film made on the microscope slide with OT SAM from 0.05 wt% zein solution. Table 2.1 showed the percentage of different elements on the surface of this field. The presence of 5.11% Au could be attributed to the gold coating during treatment for better SEM sample. Moreover, as shown in table 2.1, there were only 2.27% S, which was much lower than the percentage of C (78.18%) and O (14.44%). The surface of slide was covered with OT SAM with CH<sub>3</sub>- groups facing outside, and SH- groups connecting with Au on the other side. If OT SAM was taken away with the formed zein film by splitting, the percentage of S would have been higher than the current one. Furthermore, the formed zein film had a WCA of 115°, which was quite different from that of the surface made by CH<sub>3</sub>- groups of OT SAM (100°).

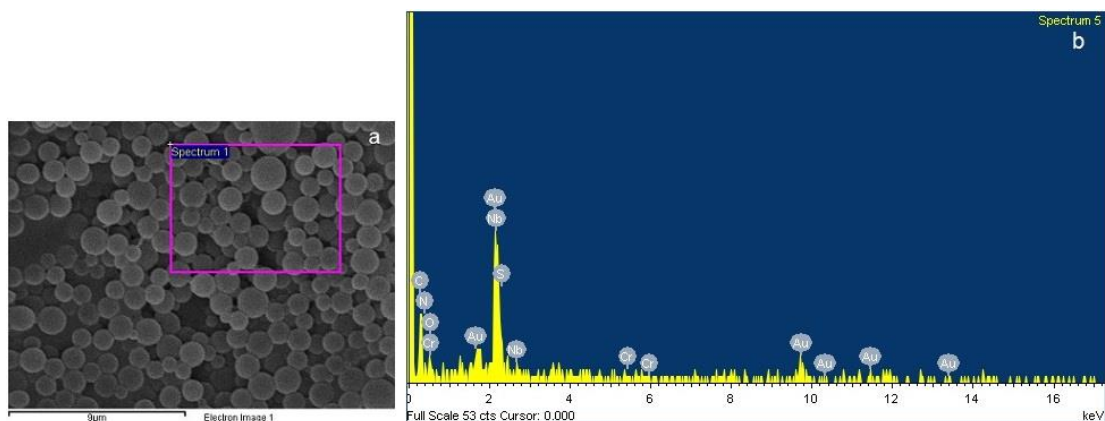


**Figure 2.2** (a) SEM image and (b) the corresponding EDS spectrum of zein film made on the microscope slide with OT SAM from 0.05 wt% zein solution.

**Table 2.1** The percentage of different elements on the surface of zein film made on the microscope slide with OT SAM from 0.05 wt% zein solution.

Element	C	O	S	Cr	Au	Total
Atomic %	78.18	14.44	2.27	0.00	5.11	100

### 2.3.2 Mechanism of hydrophobic zein film formation

To explain the mechanism involved in the formation of the hydrophobic zein film, a process was shown in Figure 2.3. The formation of hydrophobic surface can be attributed to the specific structure of zein molecule and its self-assembly property. There are defined hydrophobic and hydrophilic regions in the zein molecule. In the EISA process, water could not evaporate as fast as ethanol, which resulted in increased solvent polarity. And the solvent becomes more and more hydrophilic. The self-assembly of zein molecules was driven by the increasing solvent polarity. In order to decrease contact areas to the increasing hydrophilic solvent, there was a tendency for zein molecules to connect their hydrophobic regions together, resulting in the hydrophobic

regions attached to each other and staying inside. As a result, the formed aggregates by zein molecules had a hydrophilic surface. The aggregates then settled down on the bottom to form zein film, which caused the surface of the finally formed zein film to be hydrophilic after EISA.

However, when the zein solution was poured onto a microscope with OT SAM, during EISA process, the zein aggregates were affected by the hydrophobic surface of OT SAM. In the solution, the zein molecules first formed the same aggregates as discussed above. But when the formed aggregates reached the surface of the monolayer, its hydrophobic regions inside the formed aggregates were forced to face outside because of the interactions between the hydrophobic regions and  $\text{CH}_3^-$  groups. After EISA, the hydrophobic regions of zein aggregates constituted bottom surface of the formed film, the one faced to OT SAM. Therefore, the WCA, measured after splitting, was more than  $90^\circ$ . Wang et al. also reported the similar behavior of zein molecules when they performed on OT SAMs [7].

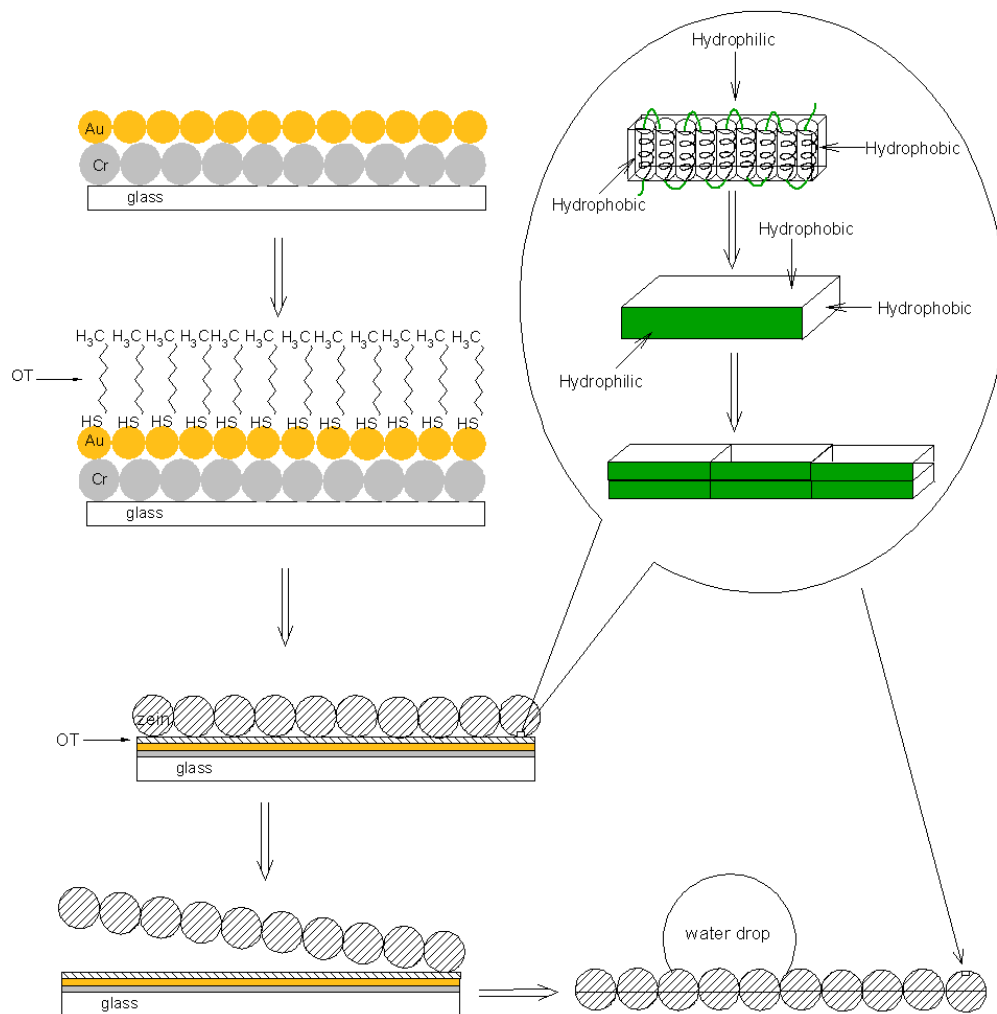


**Figure 2.3** The formation process of zein hydrophobic surface by SAM assisted EISA.

### ***2.3.3 Effect of zein concentrations on surface hydrophobicity***

0.5 ml of 0.025, 0.05, 0.1, 0.3, 0.5 wt% zein solutions were poured onto the microscope slides coated with OT SAM, respectively. After drying, the zein films were removed off the slides. Table 2.2 showed the WCA values of the film surfaces, which faced down to the OT monolayer. As shown in Tables 2.2, the WCA values of the surfaces of the formed zein films made from 0.025, 0.05, 0.1, 0.3, 0.5 wt% zein solutions were 93 °, 115 °, 76 °, 76 °, and 73 °, respectively. WCA results showed that the

films made from 0.1, 0.3 and 0.5 wt% zein solutions were hydrophilic, but those made from 0.025 and 0.05 wt% were hydrophobic. Among these formed zein films, the one made from 0.05 wt% zein solution had the most hydrophobic surface with a WCA of 115 °. Moreover, as the concentration of zein solution was decreased or increased from 0.05 wt%, the surface hydrophobicity decreased, with a smaller WCA value. In general, the hydrophobicity of a surface can be improved by two ways: increasing the roughness of the surface or decreasing the energy of the surface. The reason for different surface hydrophobicity of these formed zein films was that their surfaces had different roughness, which exhibited different surface morphologies. The surface morphologies of the formed zein films from various zein solutions were shown in Figure 2.4. Zein film formed a flat surface with spheres on it at the concentration of 0.025 wt%, shown in Figure 2.4a. The zein surface was fully covered with spheres at the concentration of 0.05 wt%, as shown in Figure 2.4b. And figure 2.4c showed zein spheres embedded in the flat zein film matrix when zein concentration reached 1 mg/ml. Nevertheless, when the concentration of zein solution was increased to above 0.1 wt%, the solid zein films formed with smooth and flat surfaces, as shown in Figure 2.4d and Figure 2.4e. Spheres give a higher roughness than flat surface. So the film formed from 0.05 wt% zein solutions had the highest surface roughness. And at the concentration of 0.025 wt%, the surface of the formed zein film was covered by smaller spheres than that on the surface formed by 0.05 wt% zein solution, which resulted in lower roughness. At higher concentrations larger than 0.05 wt%, the formed zein films had flat surface. Therefore, they showed less roughness than the other two.

The different morphologies on zein films could be attributed to the mechanism of EISA [117]. In the process of EISA, zein molecules aggregated to form small spheres, and the size of formed small spheres would grow and fused together as the concentration of zein was increased. As shown in Figure 2.4a, at low concentration of 0.025 wt%, zein molecules were not adequate to form the spheres covering the whole surface, which lead to the low roughness. When the concentration of zein solution was increased to 0.05 wt%, the size of the spheres was larger than that formed at lower concentration and the surface of the formed zein film was fully covered, which lead to increased roughness. However, when the concentration of zein solution was increased to above 0.1 wt%, the formed spheres would melt into each other, which would cause the reduced roughness.

**Table 2.2** The WCA values of zein films made on the microscope slides with OT SAM from 0.025, 0.05, 0.1, 0.3, and 0.5 wt% zein solution, respectively.

<b>Zein concentration (wt%)</b>	<b>0.025</b>	<b>0.05</b>	<b>0.1</b>	<b>0.3</b>	<b>0.5</b>
<b>WCA (°)</b>	93	115	76	76	73

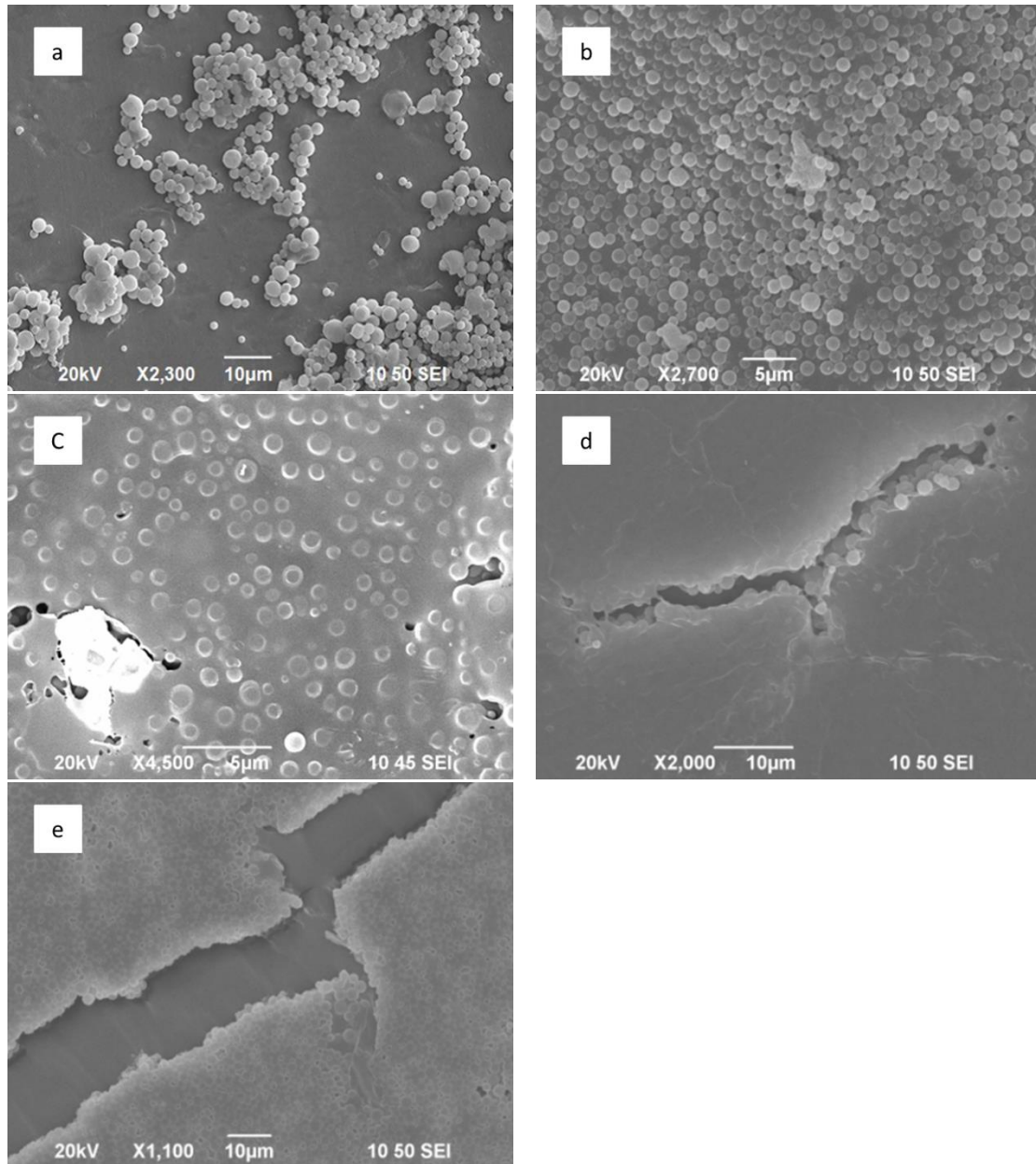


**Figure 2.4** SEM images of the surfaces of zein films made on the microscope slides with OT SAMs from 0.025, 0.05, 0.1, 0.3 and 0.5 wt% zein solutions, respectively.

### ***2.3.4 Effect of ethanol concentrations on surface hydrophobicity***

To investigate the effects of solvent concentrations on the hydrophobicity of the surface of zein films made on microscope slide with OT SAM, zein (0.05 wt%) was dissolved in the ethanol solutions of different concentrations: 40%, 50%, 60%, 80%,

and 95%, respectively. Different zein films were prepared according to section 2.3.3. Table 2.3 showed the WCA values of surfaces of the formed zein films. As shown in table 2.3, when films were made from zein dissolved in 40%, 50%, 60%, 80%, and 95% ethanol solutions, the corresponding WCA values were 105 °, 108 °, 114 °, 119 °, and 110 °. WCA results showed that all the films were hydrophobic. Compared with the concentration of zein solution, which could largely affect the surface hydrophobicity of the formed film, the concentration of ethanol had fewer effects on hydrophobicity, which exhibited the smaller changes of WCA values. The reason for different surface hydrophobicity of these formed zein films was that their surfaces had different roughness, which exhibited different surface morphologies. Figure 2.5 shows the surface morphologies characterized by SEM. In figure 2.5a, the formed zein spheres on the flat surface had both small and large sizes. In Figure 2.5b and Figure 2.5c, different from Figure 2.5a, the sizes of the formed zein spheres were much more uniform and there are more spheres covering on the surface. In Figure 2.5d, the surface was fully covered with spheres with the similar size. Figure 2.5e showed that the surface was partially covered and the spheres were not even in size. With the change of ethanol concentration, the solubility of zein changed. It is reported that the optimal ethanol concentration for zein to dissolve in is 70% [120]. And below or above this concentration, zein cannot be dissolved in the solvent very well. Among those concentrations of ethanol solution, the optimal one for zein to be dissolved in was 80%. And at other concentrations, the poor solubility caused zein to aggregate and form larger spheres in the solution. But since sonication was applied at the same time, small

zein spheres were also formed in the solution. Therefore, with the decrease of solubility, the size distribution of zein spheres enlarged. Figure 2.5 showed that, the formed zein spheres were smaller and more homogeneous when the concentration of ethanol was increased from 40% to 80%. Moreover, because these zein films were made from zein solutions of the same concentration, and under poor solubility condition, more larger spheres were formed, so there were fewer and fewer zein spheres when the concentration of ethanol was decreased from 80% to 40%. As a result, the surfaces of the formed zein films were partially covered at low ethanol concentrations, which decreased the surface roughness as a whole. In contrast, in the surface of the zein film made from zein dissolved in the 80% ethanol solution, the homogenous size distribution made the surface most hydrophobic. Finally, when zein was dissolved in 95% ethanol, compared with 80%, the size distribution of formed zein spheres became larger due to the poorer solubility and thus the surface hydrophobicity decreased.

**Table 2.3** The WCA values of zein films made on the microscope slides with OT SAMs from 0.05 wt% zein dissolved in 40, 50, 60, 80, and 95% ethanol, respectively.

<b>Ethanol concentration (v/v)</b>	<b>40%</b>	<b>50%</b>	<b>60%</b>	<b>80%</b>	<b>95%</b>
<b>WCA (°)</b>	105	108	114	119	110

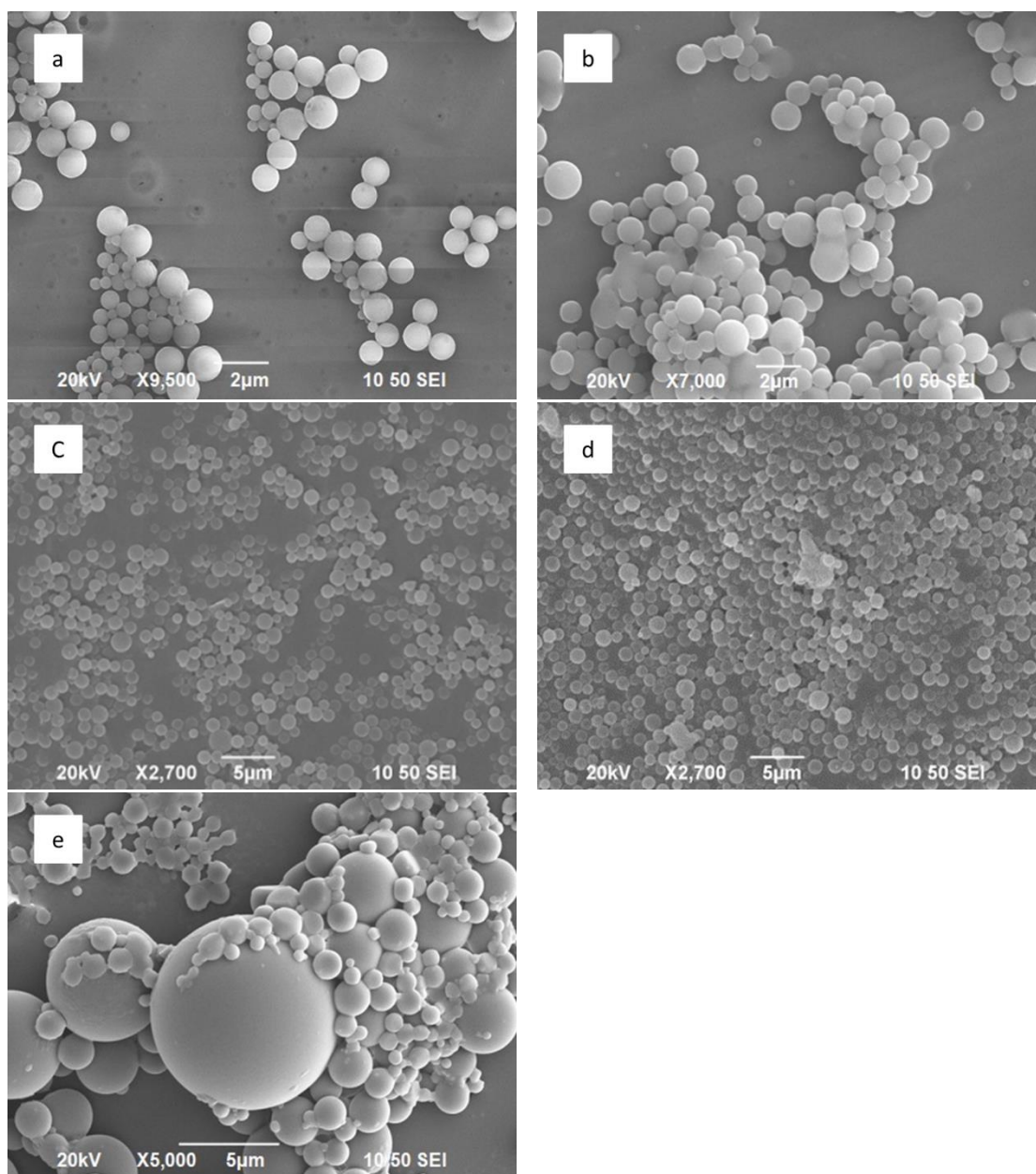


**Figure 2.5** SEM images of the surfaces of zein films made on the microscope slides with OT SAMs from 0.05 wt% zein dissolved in 40, 50, 60, 80, and 95% ethanol, respectively.

### **2.3.5 Surface wetting models**

There are two surface wetting models describing the wetting state of the surface and its WCA value. One is Cassie-Baxter model, as shown in Figure 2.6a, in which air

is trapped in the gap of the solid surface and the water droplet. The other one is Wenzel model, as shown in Figure 2.6b, in which the water droplet penetrates small cavities on rough surface and contacts the groove. Compared with Wenzel model, in the Cassie-Baxter one, the water droplet had less contact with the solid surface. To investigate the wetting state of the water droplet on the surface of the formed zein film by SAM assist EISA, a zein film was made on the microscope slide with OT SAM from 0.05 wt% zein solution, and its WCAs were measured after a water droplet was put onto the surface for 0 and 13 s, respectively. Figure 2.7 showed that, the WCA value measured at 13 s was 103 °, which was smaller than that measured at 0 s (115 °). The decrease of WCA was attributed to the change of the wetting state from Cassie-Baxter state to Wenzel state. It has been reported that there is a relationship between surface roughness ( $r$ ) and the WCA value [121]. When the  $r$  value of a surface was between 1 and 1.1, its WCA value was between 114 ° and 138 °, and the wetting model of the surface was Wenzel. While when  $r$  was larger than  $r > 1.23$ , the WCA value would be higher than 150 °, and the wetting model of the surface was Cassie-Baxter.

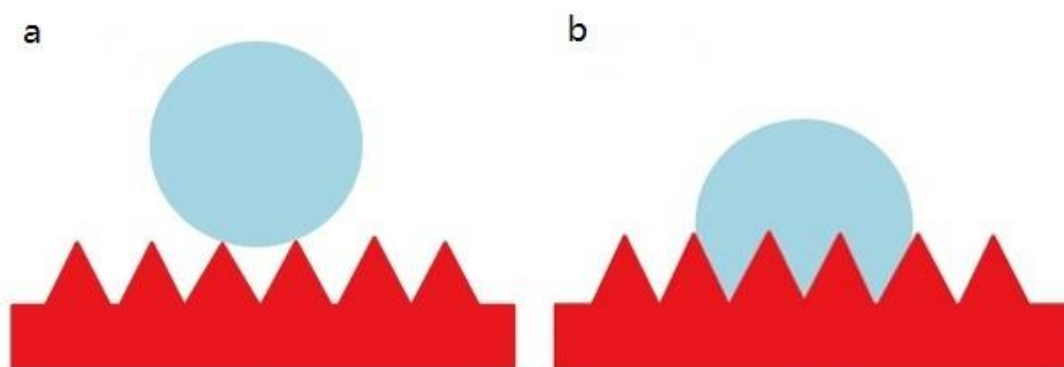


**Figure 2.6** Different behaviors of a droplet on a hydrophobic surface under (a) Cassie-Baxter state and (b) Wenzel state.

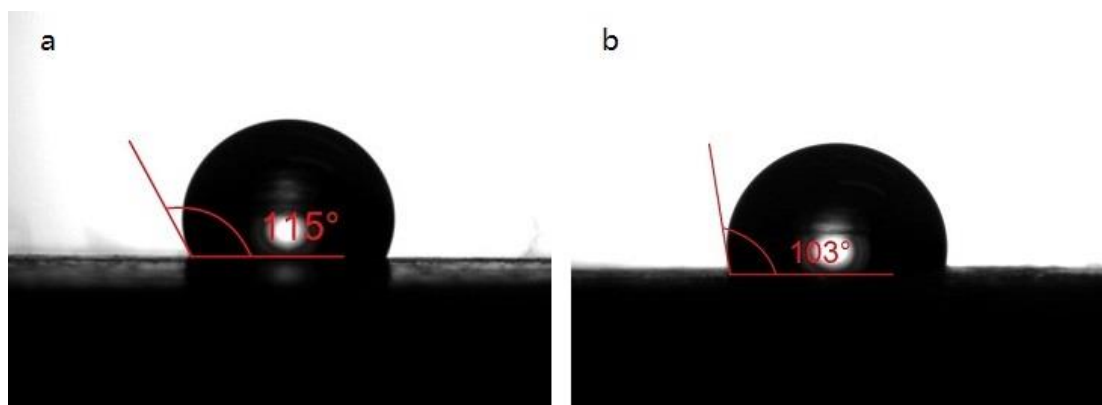


**Figure 2.7** The WCA values of zein films made on the microscope slides with OT SAMs from 0.05 wt% zein solution measured at (a) 0 s and (b) 13 s after the water droplet was placed.

### ***2.3.6 Improvement of surface hydrophobicity of zein film by size control EISA***

In order to increase the surface hydrophobicity of zein films, modifications were made to increase the roughness of the surface. 0.5 wt% zein dissolved in 80% ethanol was first put into a dish for the solvent to evaporate. Then 0.5 ml of liquid sample was collected at selected time intervals: 0, 15, 30, and 45 min. And these samples were then poured onto the microscope slides coated with OT SAM to make zein films, respectively. After the drying process, zein films were split off the microscope slides and the WCAs of the zein surfaces were measured. The WCA values of different zein films were demonstrated in Table 2.4. For the zein films made from the solution samples collected at 0, 15, 30, and 45 min, their surface WCA values were 73 °, 77 °, 109 °, and 124 °, respectively. Similar to 0.5 wt%, the WCA values of zein films made

from 1 wt% zein solution collected in the selected time intervals were 75 °, 84 °, 105 ° and 126 °, respectively. These results indicated that as the evaporation time was longer, the surface hydrophobicity of formed zein film was improved. Figure 2.8 showed the SEM images of the surface of zein film made from 1 wt% zein solution collected at 45 min.

A formation mechanism was proposed to explain the improvement of surface hydrophobicity and a schematic diagram was shown in Figure 2.9. In general, as the process of EISA continued, the formed zein aggregates tended to settle down toward to the bottom to form the final structure of zein. Wang et al. have [117, 118] studied the formation of zein MPs and their growing process as the process of EISA continued. A conclusion was made that zein MPs became larger when the evaporation continued. Thus, at initial period of EISA, small-sized zein aggregates formed and settled down to constitute the bottom layer of zein structure. As the process of EISA went on, the formed zein aggregates became larger and made up the upper layer of the zein structure.

When zein solutions were transferred from evaporation dishes onto the microscopy slides coated with OT SAM for further evaporation, demonstrated in Figure 2.9, the zein aggregates formed in the transferred solution would constitute the bottom layer of the finally formed zein structure. Before the solutions were transferred, the later the collection time, the larger the formed zein aggregates in the solution. Therefore, the larger-sized zein aggregates resulted in the improved roughness of the formed zein film and thus increased its surface hydrophobicity.

Nevertheless, Table 2.4 also showed that the WCA values for the films made from

2 wt% zein solutions collected at the same time intervals were 76 °, 74 °, 85 ° and 73 °, respectively. Wang et al. [117] concluded that as zein concentration was increased, the formed zein microstructures after EISA process changed from MPs to sponges and then to films. During EISA process, when the concentration of zein solution was low, zein aggregated into MPs and the size of them increased. Nevertheless, at high concentration, the size of the MPs first increased and then fused into a sponge or even a film as time went on. Therefore at different collection times, there are MPs, sponges or films in the solution. Among MPs, sponges and films, the roughness of MPs was the highest, whereas that of the film lowest. Therefore, at zein concentration of 2 wt%, in the initial, there were mainly MPs in the collected solution. As the collected time was longer, the size of the formed MPs increased, which resulted in the increased surface roughness. However, when the collection time was further extended, there appeared sponges in the solution, leading to the decreased surface roughness.

**Table 2.4** The WCA values of the zein films made on microscopy slides coated with OT SAM from 0.5, 1, and 2 wt% zein solutions transferred after 0, 15, 30, and 45 min evaporation, respectively.

<b>Zein concentration (mg/ml)</b>	<b>Evaporation time (min)</b>			
	<b>0</b>	<b>15</b>	<b>30</b>	<b>45</b>
<b>5</b>	73	77	109	124
<b>10</b>	75	84	105	126
<b>20</b>	76	74	85	73

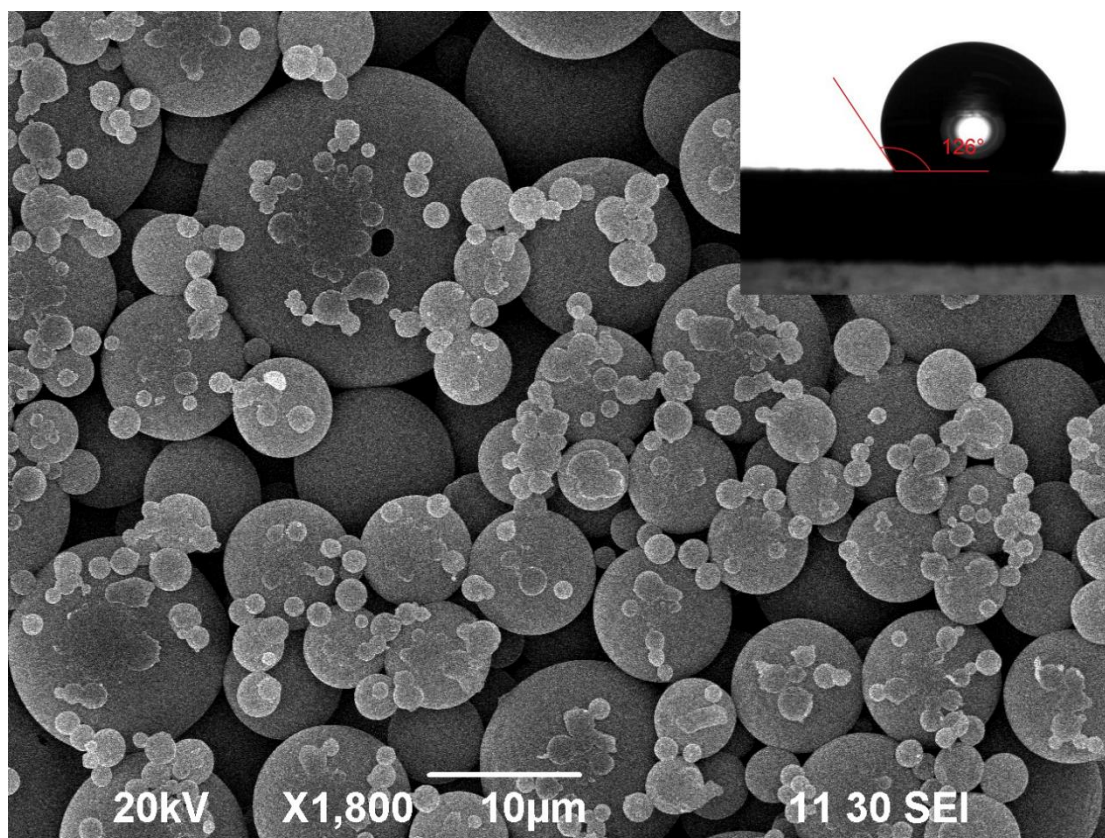


**Figure 2.8** SEM image of zein film made on microscopy slide coated with OT SAM from 1 wt% zein solution transferred after 45 min of solvent evaporation. The inset showed the WCA of the surface.

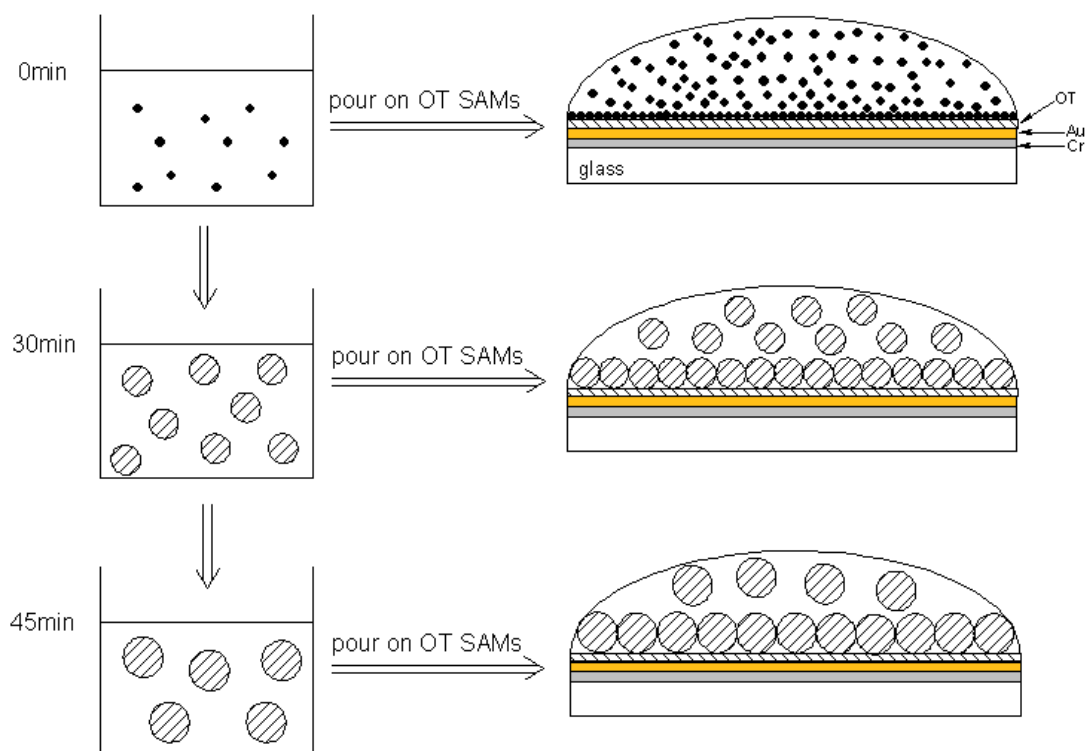


**Figure 2.9** A graphic illustration of zein hydrophobic films made on microscope slides coated with OT SAM from the transferred zein solution after various evaporation time.

## 2.4 Conclusions

In this chapter, OT SAMs were used as substrates to fabricate zein films with hydrophobic surfaces through EISA. Both the concentration of zein solution and ethanol solution had effects on the surface hydrophobicity of the formed zein films. When the concentration of zein solution was increased from 0.025 wt% to 0.05 wt%, the formed zein aggregates became larger, leading to the increase of the surface roughness. However, when the concentration of zein solution was further increased from 0.05 wt% to 0.5 wt%, the formed zein aggregates melt and fused, which decrease the surface roughness of the finally formed zein film. When the concentration of

ethanol was increased or decreased from 80%, the surface roughness of the formed zein film decrease. This was attributed to the different solubility of zein in ethanol solutions with different concentrations. In addition, zein film with further increased surface hydrophobicity was made on the microscope slide with OT SAM by a size controlled EISA. The size of zein aggregates deposited onto the slides was controlled by the evaporation time of zein solution before transferring to the slides. By size control, the surface roughness of formed zein film was largely improved and its WCA can achieve 126°.

# **Chapter 3: Super-hydrophobic/Hydrophobic Nanofibrous Network with Tunable Cell Adhesion: Fabrication, Characterization and Cellular Activities**

## **3.1 Introduction**

Hydrophobic surfaces have attracted much attention because of their potential applications in tissue engineering such as textile, coating, electronic devices, packaging, and biomedical engineering [122-124]. It is a kind of surface with a WCA of larger than  $90^\circ$ . Super-hydrophobic surface is a special hydrophobic surface with a WCA of more than  $150^\circ$ . Super-hydrophobic surface has attracted much attention over the past decades for its applications in many areas including microfluidics [125] and self-cleaning surfaces [126]. Hydrophobic surfaces play an important role in biomedical engineering, especially tissue engineering. Tissue engineering is aiming to create biochemical and physico-chemical substitutes to improve or replace the biological functions of portions or the whole tissue of human body. In tissue engineering, scaffolds are necessary for supporting cells to adhere, grow, and differentiate. The hydrophobicity and roughness of the surface as well as the microenvironment in the scaffold affect the cell attachment and growth [127]. For example, Valamehr et al. [128] had confirmed that hydrophobic surfaces promoted the proliferation and differentiation of the stem cells.

Generally, to increase the roughness of the surface and to decrease the energy of the surface are two primary methods that can improve the hydrophobicity of the surface [129]. There are many ways to improve the roughness of a surface at nano- or

micrometer scale, including phase separation, chemical etching, lithography, sol-gel, templating, and controlled crystallization [110]. Various substrates are used to fabricate the hydrophobic surfaces. The commonly used substrates are metal, Si wafers, synthetic polymers, and glass slides [22, 130]. But these substrates are usually too rigid to be used in biomedical engineering [131]. Moreover, the hydrophobicity may decrease rapidly as the substrates deform [132]. For biomedical applications, high biocompatibility and low toxicity are required. Therefore, foreign synthetic materials are extremely limited for such uses. Natural plant-based biomaterials are biocompatible, low/non-toxic, inexpensive, sustainable, and biodegradable [133]. However, most of the natural biomaterials are hydrophilic and water absorbing, and they also have a main disadvantage of a fast solubilization in water, which is not good for tissue engineering applications [134].

Zein is a primary protein from maize. It can be easily dissolved in 75% ethanol [117]. It can also self-assemble into different structures, such as MPs, bicontinuous sponges, films, and fibers [135]. Zein has more than 60% of hydrophobic amino acids, which makes it amphiphilic and highly potential for hydrophobic surface formation. Zein, as a natural biopolymer, has advantages over manufactured synthetic polymers, such as good biodegradability, low toxicity, and high biocompatibility, and those are especially important for applications in biomedical engineering areas. In addition, different from other natural biopolymers, zein is not water-absorbing.

In this chapter, the fabrication of zein super-hydrophobic/hydrophobic nanofibrous network using electrospinning is reported. The effects of different zein

concentrations and applied electrospinning voltages on the surface hydrophobicity of the zein electrospun nanofibrous network (ZENN) were investigated. WCA and SEM were used for characterizations. The results indicated that the ZENN could mimic the ECM to support the cell growing and were highly potential for tissue engineering applications.

## **3.2 Materials and methods**

### **3.2.1 Materials**

Zein was obtained from Wako Pure Chemical Industries, Ltd. (Tokyo, Japan). Ethanol (96%, v/v) was purchased from Guangdong Guanghua Sci-Tech Co., Ltd. (Guangzhou, China).

### **3.2.2 Electrospinning**

Zein solutions of various concentrations (5, 10, 15, 20, 25, and 30 wt%) were prepared by dissolving zein in 80% (v/v) aqueous ethanol solution followed by 10-minute sonication. A nanofiber electrospinning unit (Kato Tech Co., Ltd, Tokyo, Japan) with an adjustable high voltage power supply of 0-40 kV was used. The positive electrode was adhered to a metal needle with an internal diameter of 0.9 mm connected to a 10-ml syringe filled with zein solution [18]. The syringe was placed horizontally on a controlled syringe pump and the flow rate was kept at 0.5 ml/h. And the needle was horizontally directed towards the collector, which is rotating at 1200 rpm. Under the applied voltage of 10-24 kV and with the tip-to-collector distance of

15 cm, zein solution was positively charged and pulled forwards to form a Taylor cone by electronic force. When the electronic force overcame the surface tension, the positively charged jets formed, ejected out, and deposited on the collector.

### **3.2.3 WCA**

The hydrophobicity of the formed surface was determined by WCA value. The WCA of a hydrophobic surface is larger than 90 ° and that of a super-hydrophobic surface is larger than 150 °. A standard goniometer (Kruss GmbH DSA 100, Hamburg, Germany) was used to measure the WCA value. The water droplets were deposited on three various areas of the surface, and each area was measured for 3 times. The whole process was recorded using a camera system. The WCA value was then calculated by the computer.

### **3.2.4 SEM**

SEM was used to examine the surface morphology of the ZENN. The ZENN were gold coated using the Edwards S150B sputter coater, which could increase the electrical conductivity. SEM images were captured using a JEOL JSM-6490 SEM (Tokyo, Japan).

### **3.2.5 Oxygen plasma treatment**

Oxygen plasma was used to introduce the oxidation of the hydroxyl groups on

ZENN surfaces to increase the surface wettability [136]. A PDC-32G plasma cleaner (Harrick Plasma, USA) with low-pressure mercury vapor lamp was used to treat the ZENN. The ZENN was placed in a vacuum chamber, the pressure in which is 110-115 mTorr, and exposed to oxygen plasma for 5-10 min.

### ***3.2.6 Cell culture***

Human liver hepatocellular carcinoma cells (HepG2) and rat osteoblastic UMR106 cells were incubated in Dulbecco's Modified Eagle Medium (DMEM), which contained 100 mg/ml penicillin and 100 mg/ml streptomycin. The cells were supplemented with 10% fetal bovine serum (FBS), and maintained in a humidified incubator at 37°C in an atmosphere of 5% CO<sub>2</sub>. Then, the cells were trypsinized using a 0.25% trypsin solution in PBS buffer for 5 min and re-suspended in the complete culture medium.

### ***3.2.7 Cell adhesion assay***

The cell attachment assays of HepG2 and UMR106 were conducted on three samples, the ZENNs, the oxygen plasma treated ZENNs (OZENNs), and the zein casting films (ZCFs), respectively. The ZENN was made from the zein solution (30 wt%). It was cut into pieces in the size of 10×10 mm<sup>2</sup>. Each ZENN sample was then attached on a microscope cover glass and hold in a 6-cell plate. The ZCF sample was prepared by cast drying of the 30 wt% zein solution. All the samples were sterilized using UV light for 30 min before the cell experiments. SEM was used for the cell

adhesion study. For sample preparation of SEM, cells were seeded on the 6-well plate at a density of  $2 \times 10^5$  cells/ml and allowed for cell attachment for 24 h [32]. After incubation, the samples were washed three times by PBS and fixed by the 4% paraformaldehyde solution. The samples were freeze-dried overnight before the SEM observation. The behaviors of cell attachment were also investigated by fluorescence-based assay. Before cells were seeded onto those samples, the cells were first stained by 4',6-diamidino-2-phenylindole (DAPI) [137]. For staining, the attached cells in the culture dish were immersed in 5 ml of 10  $\mu$ g/ml DAPI solution, and it was performed at 37°C for 30 min without light. After staining, PBS was then used to wash the cells for 3 times to remove any residual DAPI on cell surface. After wash, cells were trypsinized and centrifuged for collection. The DAPI stained cells were then re-dispersed in the DMEM and seeded on the ZENN, OZENN, and ZCF samples, respectively, at a density of  $2 \times 10^5$  cells/ml. After 24 h of incubation, cells were fixed with the 4% paraformaldehyde solution.

### **3.3 Results and discussion**

#### ***3.3.1 Effects of the zein concentration on the surface hydrophobicity of ZENN***

Zein solutions of various concentrations (5, 10, 15, 20, 25, and 30 wt%) were electrospun to prepare ZENNs. All the other parameters of the electrospinning were kept constant in this study. Table 3.1 showed the WCA values of the ZENNs prepared from different zein concentrations. All the ZENNs were highly hydrophobic as they all had a WCA larger than 130°. The WCA of ZCF was also measured, and it was 76.5°

(Figure not shown) and the ZCF was hydrophilic. The electrospinning made the zein structure changed from hydrophilic to hydrophobic. Among the ZENN samples, the ones made from 10 and 15 wt% zein solutions were super-hydrophobic with the WCAs of 153.6° and 150.4°, respectively. The surface morphology of the ZENNs was studied using SEM, and the images were shown in Figure 3.1. It showed that there were two kinds of zein structures on the surface of ZENNs: beads and fibers. It was considered that the beads were formed when the concentration (5 and 10 wt%) as well as the viscosity of the zein solution was low [138]. When the zein concentration was 30 wt%, the morphology of the ZENN were fibers. And 15 wt% of zein concentration was a transition state between the beads and fibers. It was also observed that there were two kinds of beads: solid beads and collapsed beads. As the concentration of zein solution was increased from 5 to 15 wt%, the size of the formed beads increased as well as the amount of collapsed beads. Because the collapsed beads had rough surface while the solid beads had smooth surface, the roughness of the collapsed beads was higher. So the roughness of the ZENN surfaces increased when the zein concentration was increased from 5 to 15 wt%, and the WCA also increased. It was also observed that there were two kinds of fibers on ZENN: solid fibers and collapsed fibers. When the zein concentration was increased from 15 to 30 wt%, the diameter of the fibers increased and the amount of collapsed fibers decreased. Because the roughness of the collapsed fibers was higher than that of the solid fibers, so the roughness decreased when the zein concentration was increased from 15 to 30 wt%. So the WCAs of the ZENN samples decreased.

**Table 3.1** The WCAs of ZENNs obtained from zein solutions with the concentration of 5, 10, 15, 20, 25, and 30 wt%, respectively.

Zein (wt%)	5	10	15	20	25	30
Morphology	bead	bead	bead-fiber	bead-fiber	fiber	fiber
WCA (°)	138.2	153.6	150.4	143.8	141.0	136.4

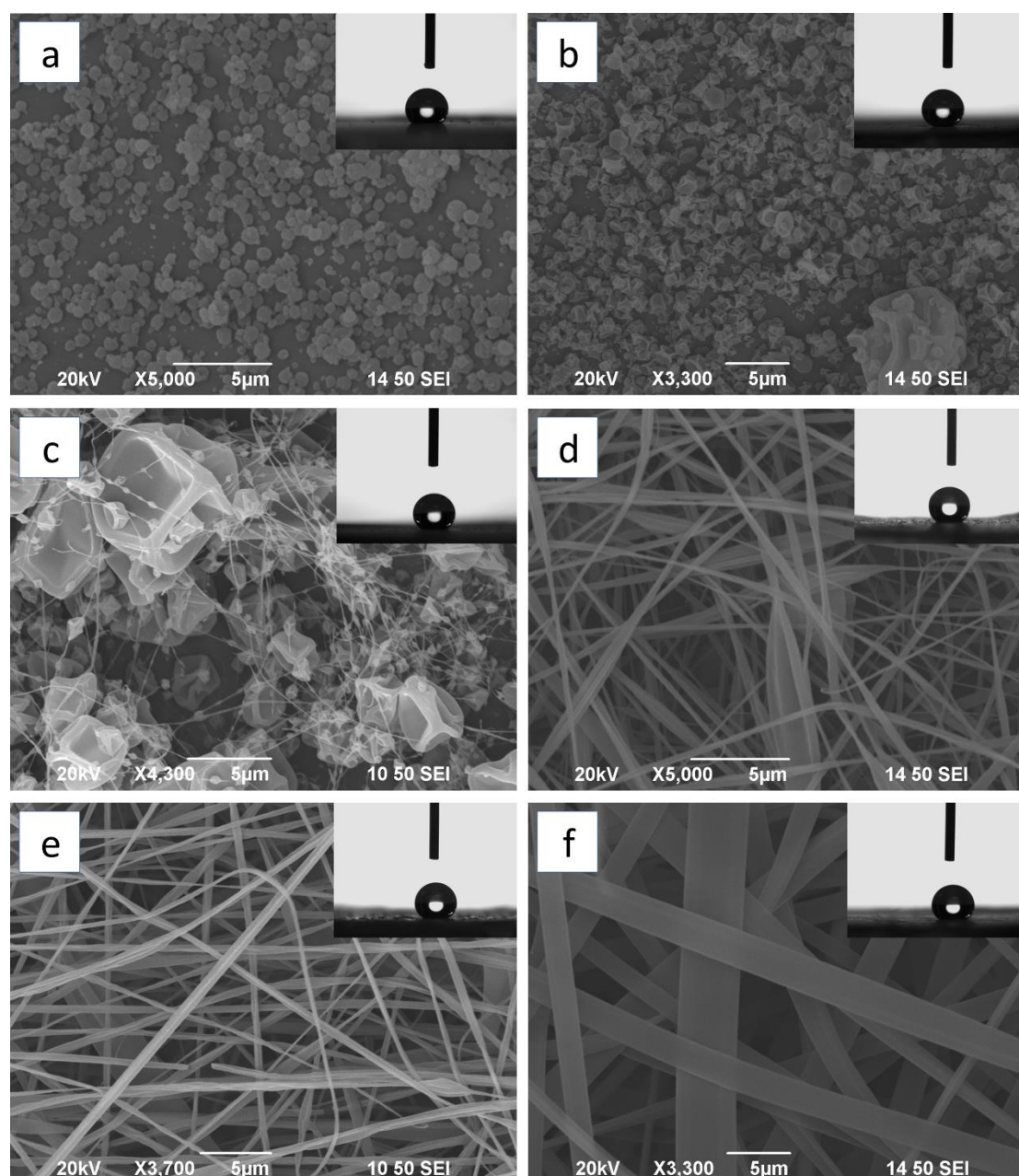


**Figure 3.1** SEM and WCA images of ZENN obtained by electrospinning from zein

solutions with the concentration of (a) 5, (b) 10, (c) 15, (d) 20, (e) 25, and (f) 30 wt%, respectively.

### ***3.3.2 Effects of the electrospinning voltage on the surface hydrophobicity of ZENN***

The effects of the electrospinning voltage on the surface hydrophobicity of the ZENN samples were also investigated. Samples were prepared under various voltages: 10, 18, 21, and 24 kV, and the WCA values of the ZENN samples were shown in Table 3.2. The WCA of the ZENN samples increased from 130.5 ° to 153.6 ° as the voltage increased from 10 kV to 18 kV, but decreased from 153.6 ° to 135.5 ° as the voltage further increased from 18 kV to 24 kV. The morphology of the ZENN samples was investigated by SEM, and the images were shown in Figure 3.2. There was a linear relationship between the voltage and the solution flow rate [18, 139]. As the voltage was increased from 10 to 18 kV, the solution flow rate was increased, which resulted in the increase of the amount of the beads, leading to increased roughness. And the beads were almost collapsed beads. Further, when the voltage was increased from 18 to 21 kV, out of the total amount of beads, the amount of solid beads increased. When the voltage was 24 kV, fibers started to appear. The increase of the amount of solid beads and fibers decreased the roughness, which resulted in the decreased WCAs.

**Table 3.2** The WCAs of ZENN made by electrospinning at applied voltages of 10, 18, 21, and 24 kV from zein solution with a concentration of 10 wt%, respectively.

Voltage (kV)	10	18	21	24
Morphology	bead	bead	bead	bead-fiber
WCA (°)	130.5	153.6	139.4	135.5

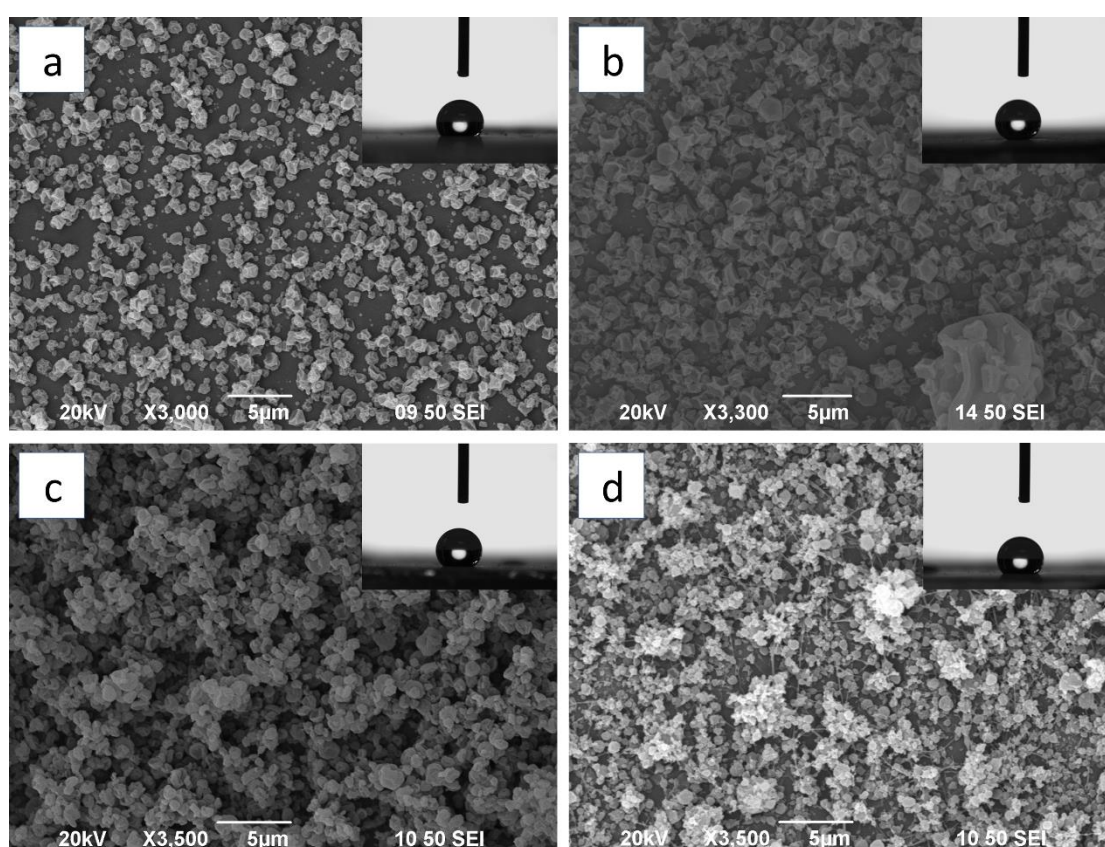


**Figure 3.2** SEM and WCA images of the ZENN made by electrospinning at (a) 10, (b) 18, (c) 21kV, and (d) 24kV from zein solution with the concentration of 10 wt%, respectively.

### 3.3.3 Cell attachment behaviors

To further evaluate whether the ZENN was suitable for tissue engineering applications, a series of in vitro cell attachment experiments were conducted. The ZENN sample made from 30 wt% zein solution was chosen for the cell attachment study [140]. The cell growth behavior of the ZENN samples was investigated using Human liver hepatocellular carcinoma cells (HepG2). The cells were seeded on the sample surfaces and incubated for 24 hours. SEM was used to study the cell adhesion (Figure 3.3a). Figure 3.3a showed that the cells adhered and grew between the electrospun zein fibers. The cell attachment behaviors on ZENN can also be visualized through fluorescence microscopy images (Figure 3.3b). The DAPI stained cell nuclei showed blue color under laser excitation. Figure 3.3b showed that the cells grew not only on the surface but also into the fibrous network, which indicated that the porous ZENN successfully mimicked the in vivo extracellular environment.

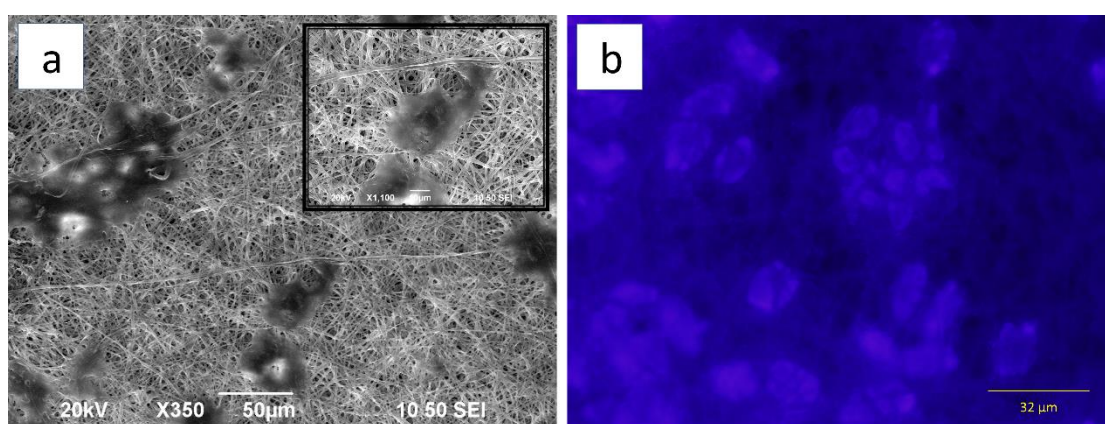


**Figure 3.3** (a) SEM image and (b) Fluorescence image of HepG2 cell growth on the ZENN.

The cell attachments of HepG-2 on 3D ZENN and 2D ZCF were compared and the result showed that 3D ZENN had structural advantages over 2D ZCF on cell adhesion. Figure 3.4 showed that, compared to ZCF, much more cells were attached to the ZENN. The better cell adhesion behaviors on ZENN could be attributed to both the surface morphology and the 3D structure. Compared to the flat and solid surface of ZCF, ZENN had a fibrous and porous 3D structure. The 3D structure of ZENN resulted in a large superficial area with a high surface to volume ratio and a large interconnectivity, which favored cell adhesion.

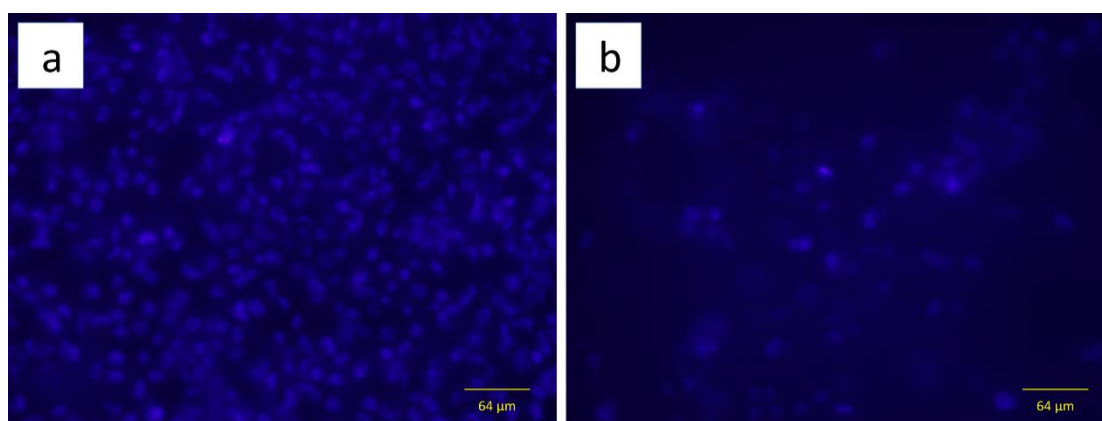


**Figure 3.4** Fluorescence images of HepG2 cell attachment on (a) ZENN and (b) ZCF.

### ***3.3.4 Effects of plasma treatment induced tunable wettability on cell attachment***

There is a broadly applied technique to adjust the surface hydrophobicity of various materials: the oxygen plasma treatment. The oxygen plasma treatment introduces specific functional groups to the surfaces of the materials by oxidation. For example, this technique can increase the wettability and hydrophilicity of the material surfaces by the formation of oxidized chemical groups, such as carbonyl, ester groups

and carbonyl [141]. To better understand the relation between surface wettability and cell adhesion, the oxygen plasma treatment was applied to change the surface hydrophobicity and the attachments of HepG2 and UMR106 cells on the treated samples were studied. ZENN samples (made from 30 wt% zein) were treated with oxygen plasma for various time lengths. It was found that the longer the treatment time, the higher the surface hydrophilicity. From the SEM images, it was observed that a considerable amount of cells were attached to the highly hydrophobic ZENN (Figure 3.5a and 3.5d). The amount of attached cell decreased after ZENN treated by oxygen plasma for 5 min (Figure 3.5b and 3.5e). The amount of the attached cells was further decreased when the ZENN was treated with oxygen plasma for 10 min (Figure 3.5c and 3.5f). The decreased cell attachment on ZENN after oxygen plasma treatment can be attributed to the decrease of the amount of the cell adhesion-mediating proteins adsorbed to the treated ZENN surface. It has been reported that the amount of the absorption of cell adhesion-mediating protein, fibronectin, decreased in the following order of the chemical groups:  $\text{NH}_2 > \text{CH}_3 > \text{COOH} > \text{OH}$  [142]. The carboxyl groups on the ZENN created by the oxygen plasma, compared to the original  $\text{CH}_3$  and  $\text{NH}_2$  groups on the ZENN surface, led to less adsorbed proteins, thus less cell adhesion.

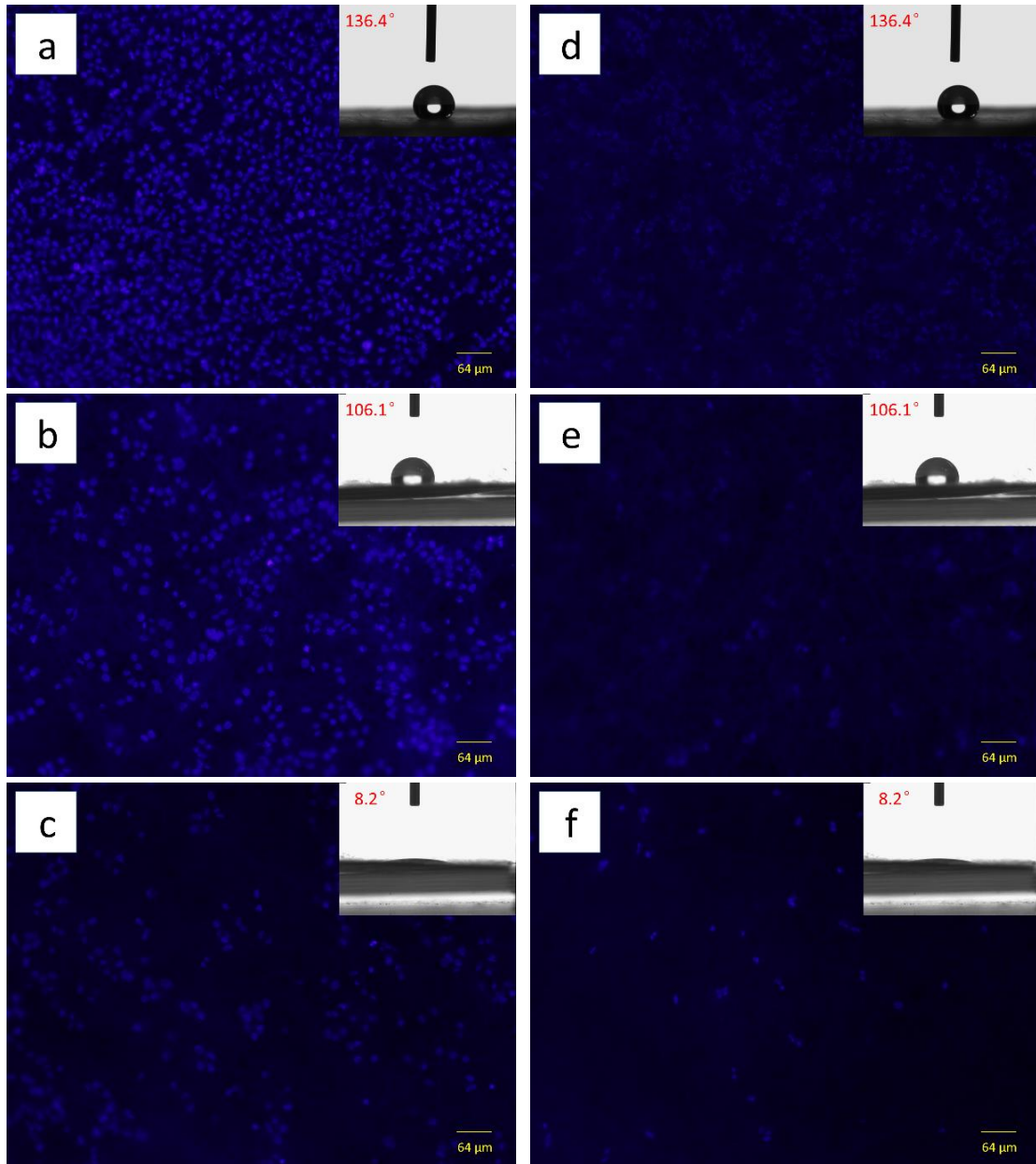


**Figure 3.5** Fluorescence images of HepG2 cell attachment on the ZENNs treated with oxygen plasma for (a) 0 min, (b) 5 min, and (c) 10 min, respectively. Fluorescence images of UMR106 cell attachment on the ZENNs treated with oxygen plasma for (d) 0 min, (e) 5 min, and (f) 10 min, respectively.

### 3.4 Conclusions

This research work provides a facile method to fabricate

super-hydrophobic/hydrophobic surfaces. Zein super-hydrophobic/hydrophobic nanofibrous networks were successfully fabricated using electropinning, and the highest WCA of the prepared ZENNs could reach 153.6°. The effects of zein concentration and electrospinning voltage on the hydrophobicity of the ZENNs were studied. The increase of the zein concentration from 5 to 10 wt% resulted in an increase in the surface hydrophobicity, while its further increase from 10 to 30 wt% resulted in a decrease in the surface hydrophobicity. The increase of electrospinning voltage from 10 to 18 kV resulted in an increase in the surface hydrophobicity, while its further increase from 18 to 24 kV resulted in a decrease in the surface hydrophobicity. The difference on the surface hydrophobicity was mainly attributed to difference in surface morphology. The cell adhesion and cell growth on the ZENNs were also studied. It was observed that the cells successfully attached onto the nanofibrous network. There were more cells attached onto ZENN compared to ZCF. When the surface hydrophobicity of ZENN decreased, the amount of the cells attached on the ZENN dramatically reduced. It is demonstrated that the zein electrospun nanofibrous structure has great potential in various applications of tissue engineering.

# **Chapter 4: Formation and mechanism of super-hydrophobic/hydrophobic surfaces made from amphiphiles through droplet-mediated evaporation-induced self-assembly**

## **4.1 Introduction**

Hydrophobic surface is a kind of surface which has low wettability. Its WCA value is higher than  $90^\circ$ . It has wide applications in various areas, such as coating, textile, packaging, electronic devices, and biomedical engineering [123, 124]. When the WCA value of a hydrophobic surface is higher than  $150^\circ$ , the surface is called super-hydrophobic surface. It has self-cleaning property [126]. In order to increase the hydrophobicity of a surface, there are mainly two methods: decreasing the energy of the surface and increasing the roughness of the surface [108].

Electrospinning is one of the effective ways to make super-hydrophobic surfaces from synthetic polymers, such as polystyrene (PS) [143-145] and PLA [146]. In electrospinning, the sample solution is positively charged and pulled off to eject charged liquid jets by electronic forces. And the ejected jets are then deposited to form the highly porous network consisting of nanofibers [30]. Electrospinning could largely increase the surface hydrophobicity by increasing surface roughness and changing surface chemistry [144]. The electrospun nanofibrous mats are usually special with the additional wrinkles, grooves, or pits on individual fibers, which largely increase the surface roughness. Besides, in the process of electrospinning, the molecules of the polymers will be realigned. Cui et al. studied the effects of chemical groups on surface

wettability in electrospinning by X-ray photoelectron spectroscopy. It was observed in the study that the methylene group and the hydrophobic methyl group accumulated on the electrospun polyethylene glycol fibers and poly (D, L-lactide) fibers, respectively [147].

Zein is a primary protamine protein which is extracted from corn endosperm. It cannot be dissolved in water but can in 40~95% ethanol aqueous solution [117]. Zein is also an amphiphilic protein. More than 50% of its amino acids constituents are hydrophobic [148]. The molecular structure of zein in 70% methanol has been investigated by Argos et al. using CD spectra [5]. They proposed a structural model of a ribbon-type structure of size  $13 \times 1.2 \times 3 \text{ nm}^3$ , in which 9-10 helical segments were arranged in an antiparallel style and the segments were linked together by glutamine-rich turns. Later, Matsushima et al. examined the structure of zein in 70% ethanol solution using SAXS and a rectangular prism model, similar to the one given by Argos et al., was proposed [149]. In both arrangements, the top and bottom of the zein molecule, which are made by the glutamine-rich bridges, are hydrophilic, while the sides of the zein molecule, which are the zein  $\alpha$ -helices, are hydrophobic. Because more than 50% of its amino acids constituent is hydrophobic, zein has a great potential for hydrophobic surface formation [4, 148]. There have been many studies about the fabrication of zein nanofibers using electrospinning. Most of the studies were aiming to improve its mechanical properties to make it more suitable for clinical use, especially in tissue engineering [18, 150]. However, the research on the improvements of the surface properties, including surface hydrophobicity, of the zein electrospun film (ZEF) was

seldom done. The study on the formation of the electrospun nanofibers will not only make the control of their surface properties possible but also give a mechanism that can explain the relation between the surface hydrophobicity and the morphology.

The electrospinning of zein is a droplet-mediated, or jet-mediated evaporation-induced self-assembly process. Different from the evaporation style in the cast drying of zein solution to make zein film, during electrospinning, the zein solution is dried in the air in the shapes of droplets or jets. It was learned that the  $\alpha$ -helix to  $\beta$ -sheet transformation of zein happened during the cast drying of zein solution [148]. The  $\alpha$ -helix to  $\beta$ -sheet transformation of zein could be promoted by the increased solvent polarity [148]. During the transformation from  $\alpha$ -helix to  $\beta$ -sheet, it is the interior hydrogen bonds which connects the peptide backbones that determine peptide propensity [151]. Compared to structure of  $\alpha$ -helix, that of  $\beta$ -sheet structure was more energy favorable. Therefore, the more  $\alpha$ -helix was constrained by the hydrogen bonds, the more likely the transformation of  $\alpha$ -helix to  $\beta$ -sheet would occur [152].

The  $\alpha$ -helix to  $\beta$ -sheet transformation of zein was focused during the mechanism study of zein electrospinning, because the different behavior of the  $\alpha$ -helix to  $\beta$ -sheet transformation during zein electrospinning may result in its super-hydrophobic surface formation. The use of FTIR to determine protein secondary structures has been well applied and confirmed in scientific research [153, 154]. In FTIR spectra of zein, the peak at  $1600\text{ cm}^{-1}$  to  $1800\text{ cm}^{-1}$  is generally corresponding to the amide group, and it is also called the amide I band. In principle, the amide I band is mainly attributed to the C=O stretching and vibration [155]. Different types of secondary structures are the

results of different hydrogen bonding modes and molecular geometries, which show differences on the amide I band of the FTIR spectra [153, 155, 156]. The secondary structure of zein has been studied by Forato et al. using FTIR in 2003 [154, 156]. It was stated that the  $\alpha$ -helix structure was corresponding to a symmetric signal at about  $1656\text{cm}^{-1}$  and the  $\beta$ -sheet structure could be observed at a shoulder below the peak at about  $1620\text{cm}^{-1}$ .

In this chapter, we reported the formation the super-hydrophobic/hydrophobic surface from zein, a natural amphiphile, using electrospinning. And the formation mechanism of the super-hydrophobic/hydrophobic surface from amphiphiles during droplet-mediated evaporation-induced self-assembly, for examples electrospinning and spray drying, was proposed.

## **4.2 Materials and methods**

### ***4.2.1 Materials***

Zein was purchased from Wako Pure Chemical Industries, Ltd. (Tokyo, Japan). PEG (5,000)-b-PLA (100,000) (PEG-PLA) was obtained from Polysciences Asia Pacific, Inc. (Taipei, Taiwan). Ethanol (96% v/v) was purchased from Guangdong Guanghua Sci-Tech Co., Ltd. (Guangzhou, China).

### ***4.2.2 Sample solution preparation***

Zein solutions of two different concentrations (10 and 30 wt%) were prepared by

dissolving zein in 80% (v/v) aqueous ethanol, and followed by 10-minute sonication.

PEG-PLA solution was prepared by dissolving PEG-PLA in chloroform (5 wt%).

#### ***4.2.3 Electrospinning***

The prepared sample solutions were electrospun using a nanofiber electrospinning unit (Kato Tech Co., Ltd, Tokyo, Japan). The solution was filled in a 10 ml syringe, which was connected to a metal needle with an internal diameter of 0.9 mm [18]. The solution was delivered to the needle via the syringe pump, and the flow rate was controlled at 2.0 ml/h. The samples were collected on a rotated collector covered with an aluminum foil. The collector was placed at a distance of 15 cm from the needle tip. The applied voltage was adjusted to 18 kV. All the electrospinning processing was carried out under the ambient temperature of 25°C and 1 atm ambient pressure. The samples obtained were dried overnight before further analysis.

#### ***4.2.4 Spray drying***

The zein solution with a concentration of 10 wt% was spray dried using a SD-04 spray drier (Lab Plant, England) equipped with a 0.5 mm nozzle atomizer. Zein solution was pumped to the spray drier at a flow rate of 10 ml/min. The inlet temperature was set at 105 ° and the outlet temperature is 68 ° [157]. The dry powders were collected and stored at 4°C before analysis.

#### **4.2.5 WCA**

The hydrophobicity of the formed surface was determined by WCA value. The WCA of a hydrophobic surface is larger than 90 ° and that of a super-hydrophobic surface is larger than 150 °. A standard goniometer (Kruss GmbH DSA 100, Hamburg, Germany) was used to measure the WCA value. The water droplets were deposited on three various areas of the surface, and each area was measured for 3 times. The whole process was recorded using a camera system. The WCA value was then calculated by the computer.

#### **4.2.6 SEM**

The morphology of the ZEF and PEG-PLA electrospun film was examined using an SEM. The samples were gold coated using the Edwards S150B sputter coater, which could increase the electrical conductivity. SEM images were captured using a JEOL JSM-6490 SEM (Tokyo, Japan).

#### **4.2.7 ATR-FTIR**

ATR-FTIR spectra of ZEF, zein cast films (ZCF), and spray dried zein powder (SDZP) were measured at room temperature by a FTIR system with the ATR accessory. The spectra were collected by 16 scans and the resolution was set at 4 cm<sup>-1</sup>, from 4000 cm<sup>-1</sup> to 900 cm<sup>-1</sup>. The following data processing was conducted according to the reported method using Ominic software [154].

### 4.3 Results and discussion

#### 4.3.1 *Super-hydrophobic/hydrophobic surfaces made from amphiphiles using electrospinning*

Zein solutions of two different concentrations (10 and 30 wt%) were electrospun using a nanofiber electrospinning unit. WCA was used to characterize the surface hydrophobicity of the formed ZEFs and the results were shown in Figure 4.1. It showed that their WCAs were larger than  $130^\circ$  and they were highly hydrophobic. The one made from 10 wt% zein solution had a WCA of  $155.2^\circ$ . Moreover, as shown in Figure 4.2, the WCAs of ZCFs made from 10 wt% and 30% zein solutions were  $73.7^\circ$  and  $76.5^\circ$ , respectively. The results indicated that the hydrophobicity of the zein surface was largely improved by electrospinning. To have a better understanding of the surface of the ZEFs, their morphology was examined using SEM and the images were shown in Figure 4.3. The SEM images showed that there were two kinds of zein structures in the images: collapsed beads and smooth fibers. It is believed that the collapsed beads were formed when the zein concentration in the original solution was low while the smooth fibers were formed when the zein concentration in the original solution was high [18]. When the zein concentration was low, the viscosity of the zein solution was low, and the beads were formed instead of fibers [138]. At even lower concentration, the beads collapsed after solvent evaporation, and collapsed beads were observed instead of solid beads. The collapsed beads had rough surfaces while the fibers had smooth surfaces. So the roughness of the collapsed beads was higher than that of the smooth fibers. Therefore, at selected zein concentrations (10 and 30 wt%), the WCA of the

surface formed from the low zein concentration was higher than that ( $135.4^\circ$ ) of the surface formed from the high zein concentration.

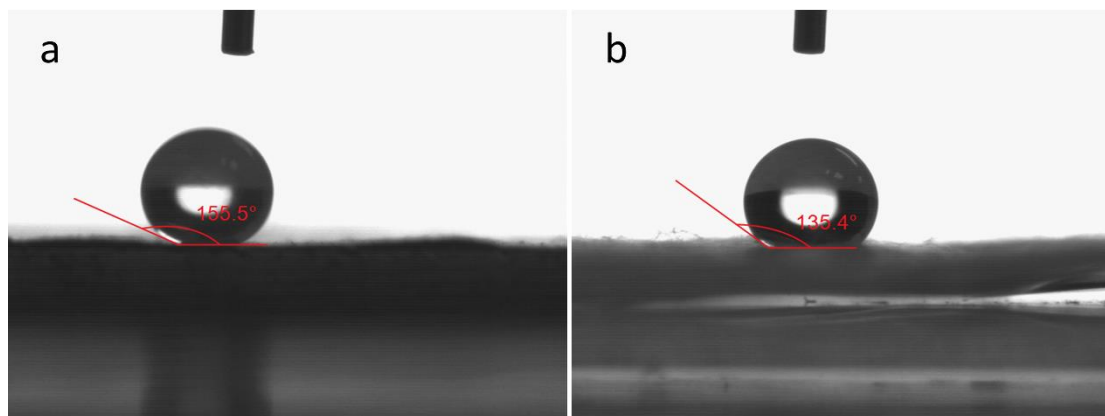


**Figure 4.1** WCA images of ZEF made from a solution containing (a) 10 and (b) 30 wt% of zein in 80% ethanol, respectively.

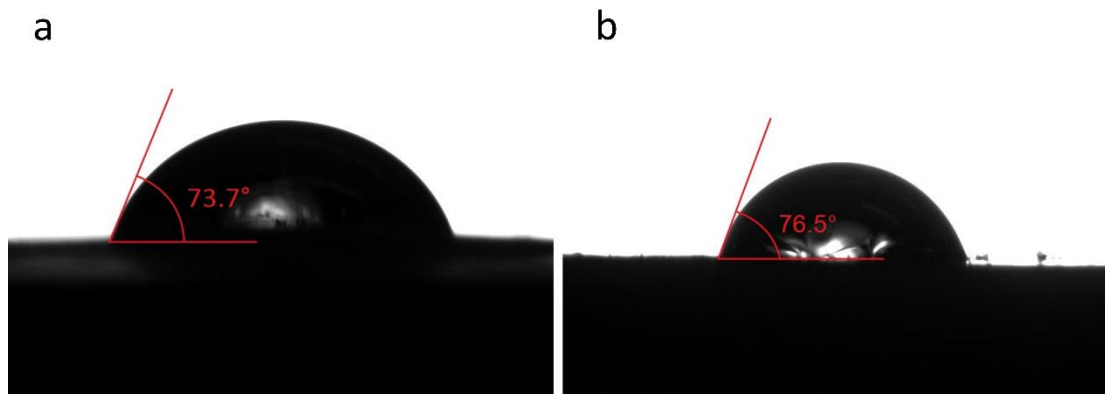


**Figure 4.2** WCA images of ZCF made from a solution containing (a) 10 and (b) 30 wt% of zein in 80% ethanol, respectively.

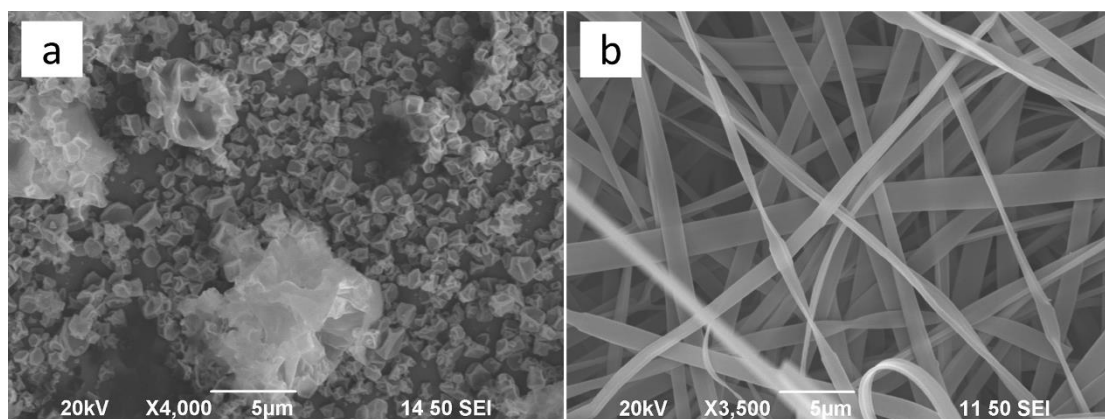


**Figure 4.3** SEM images of ZEF made from a solution containing (a) 10 and (b) 30 wt% of zein in 80% ethanol, respectively.

It is considered that the super-hydrophobic/hydrophobic surfaces can also be formed from other amphiphiles using electrospinning. A synthetic amphiphilic polymer, PEG-PLA, was selected. The PEG (5,000)-b-PLA (100,000) is amphiphilic because the PEG group is hydrophobic while the PLA group is hydrophilic. The PEG-PLA was dissolved in chloroform and the concentration was 5 wt%. After electrospinning at 18 kV and 2.0 ml/h flow rate, which were exactly the same as the electrospinning set-up for 10 wt% of zein solution, the electrospun PEG-PLA film (EPPF) formed. The hydrophobicity of the EPPF was measured using WCA. The WCA image (Figure 4.4a) of the EPPF showed that the formed surface was highly hydrophobic with a WCA of 141.4 °. A control sample was prepared by cast-drying of the PEG-PLA solution (5 wt%) (CDPP), and its WCA was measured. Compared to CDPP, which was hydrophilic and had a WCA of 88.3 ° (Figure 4.4b), the hydrophobicity of EPPF was largely improved by electrospinning, where the WCA had a dramatic increase from 88.3 ° to 141.4 °.

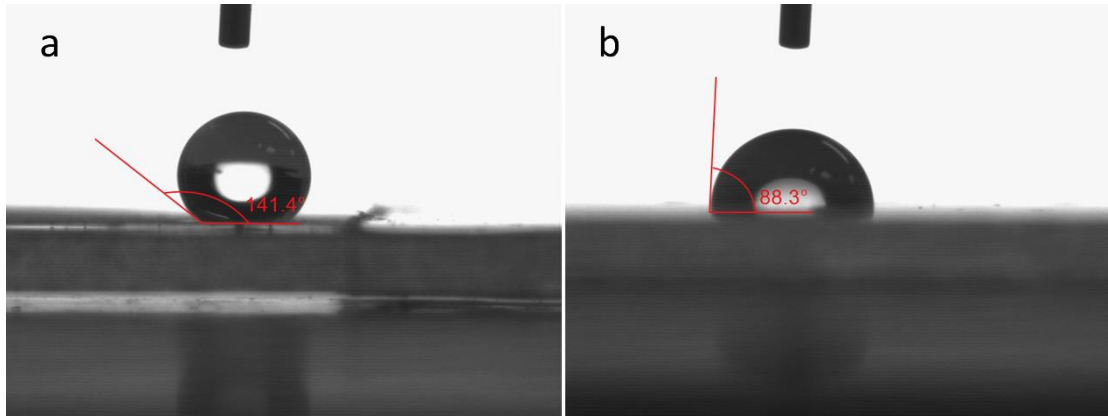


**Figure 4.4** WCA images of surface obtained from a solution containing 5 wt% of PEG-PLA in chloroform by (a) electrospinning and (b) cast drying, respectively.

### ***4.3.2 Hydrophobic surfaces made by spray drying***

After the surface hydrophobicity comparisons between ZEF and ZCF, and between EPPF and CDPP, respectively, it is obvious that, although both samples were prepared by solvent evaporation induced self-assembly, the samples made from cast drying of amphiphiles were hydrophilic and those made from electrospinning were hydrophobic/super-hydrophobic.

It is considered that the styles of the solvent evaporation, droplet-based, as in electrospinning, or surface-based, as in cast drying, during the fabrication are the key to control the surface hydrophobicity. Another fabrication method, spray drying, similar to electrospinning on the solvent evaporation style, was used to study the super-hydrophobic/hydrophobic surface formation and to explain the large improvement on the surface hydrophobicity over cast drying. Spray drying is a broadly applied way to produce dry powders. During spray drying, the solution is sprayed through a nozzle into a hot vapor stream and the liquid phase is vaporized quickly [158].

The droplet-based solvent evaporation occurring in spray drying is very similar to that in electrospinning. To further study the surface formed by spray drying, 10 wt% of zein solution was sprayed dried and the dried powder was collected. WCA was used to characterize the surface hydrophobicity of the sample while SEM was used to examine the surface morphology of the sample (Figure 4.5). The WCA of the sample surface was 125.3 °, which indicated that it was hydrophobic. And SEM showed that the formed zein particles were collapsed beads too. The SEM result indicated that the spray-dried particles were in very similar shape as the electrospun beads, which were shown in Figure 4.3a. During spray drying, the zein solution was first spread into small droplets by the atomizer. The droplets are then carried into the chamber by hot air, and the collapsed particles with wrinkled skins were formed after droplet-mediated solvent evaporation.

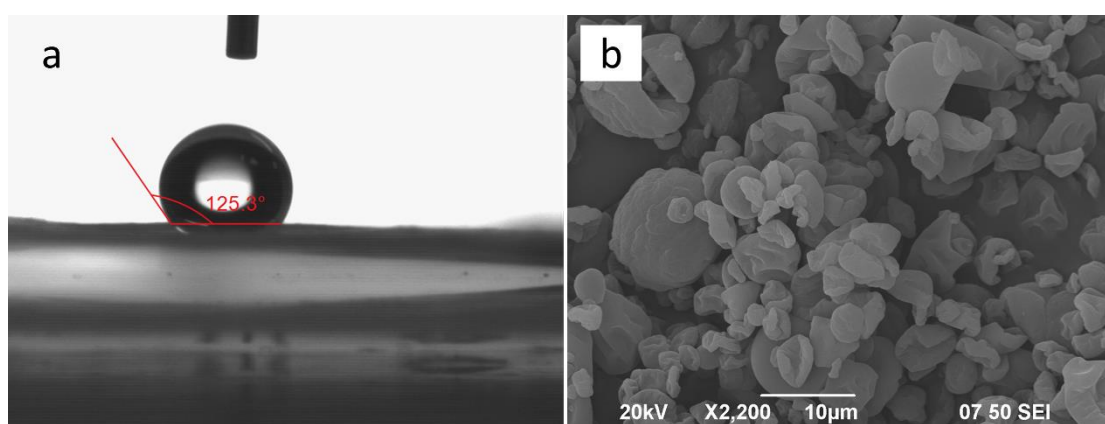


**Figure 4.5** (a) WCA and (b) SEM image of SDZP prepared from 10 wt% of zein in 80% ethanol.

### ***4.3.3 The $\alpha$ helix- $\beta$ sheet transformation during evaporation-induced self-assembly***

To further study the formation of zein super-hydrophobic surface, the ATR-FTIR spectra of the ZCF, ZEF, and SDZP were collected. The ATR-FTIR spectra (1800-1600  $\text{cm}^{-1}$ ) and their corresponding secondary derivatives of various zein solutions were presented in Figure 4.6. As shown in Figure 4.6, all the samples had the similar peak with high intensity at 1650  $\text{cm}^{-1}$ , which was attributed to the  $\alpha$ -helix structure in zein. In the secondary derivative of ZCF spectra (Figure 4.6a, red solid line), it clearly showed the presence of the  $\beta$ -sheet structure by the shoulder of the peak at 1618  $\text{cm}^{-1}$ . While, for ZEFs and the SDZPs (Figure 4.6b, Figure 4.6c, and Figure 4.6d), no peak at the shoulder of 1618  $\text{cm}^{-1}$  could be observed and identified from their secondary derivative spectra, so there is no  $\beta$ -sheet structure in the ZEF or SDZP. The result indicated that no  $\alpha$ -helix to  $\beta$ -sheet transformation occurred during electrospinning and spray drying.

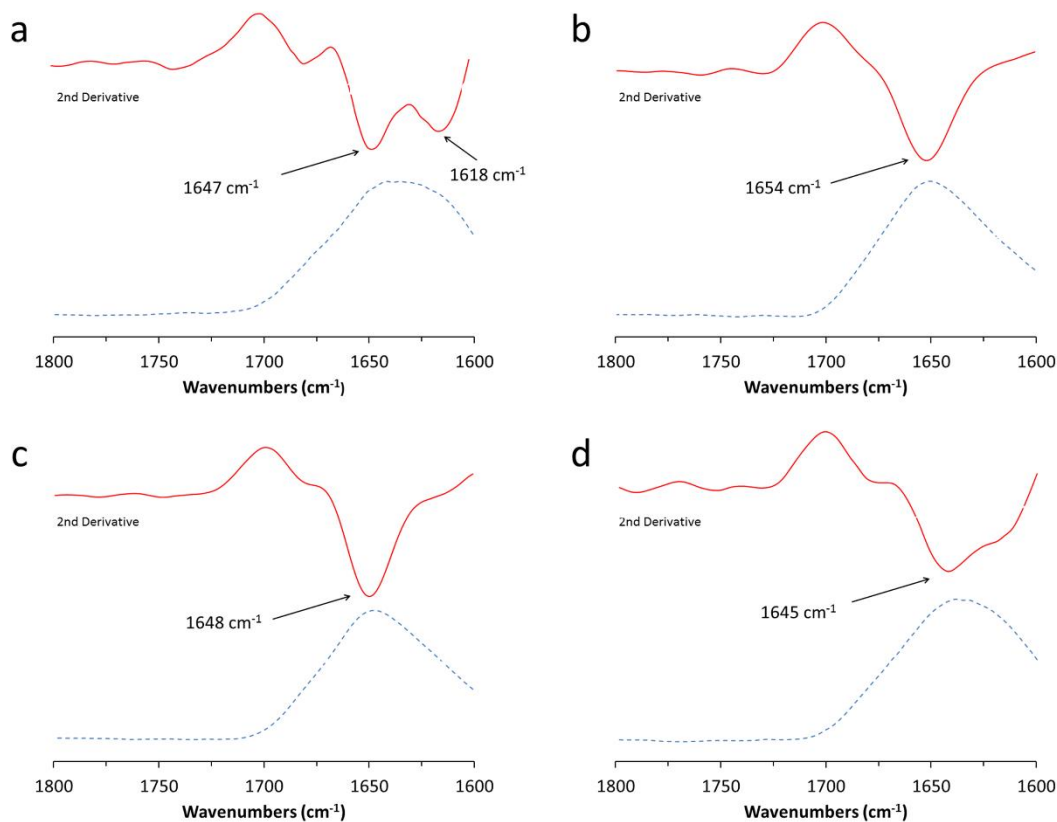


**Figure 4.6** FTIR spectra (blue dotted line) at Amide I region and the corresponding secondary derivatives (red solid line) of (a) ZCF, (b) ZEF prepared from 10 wt% zein solution, (c) ZEF prepared from 30 wt% zein solution, and (d) SDZP, respectively.

Zein has high  $\alpha$ -helix content in its original solution [159, 160]. The  $\beta$ -sheet conformation happened during the formation of ZCF could be explained by the theory of EISA. During the process of EISA, the higher evaporation rate of ethanol over water made the solvent more and more hydrophilic, which drove the conformational transitions of zein from  $\alpha$ -helix to  $\beta$ -sheet [148]. Therefore, the structure of  $\beta$ -sheet was present in the FTIR spectra of ZCF.

The differences among the secondary structures of ZCF, ZEF, and SDZP could also be explained by the differences of the styles of the solvent evaporation. The

evaporation style of the ZCF formation was surface-mediated, while the evaporation style of the ZEF and SDZP formations was droplet-mediated. The  $\alpha$ -helix to  $\beta$ -sheet structure transformation involved a process of hydrogen bond rearrangement, which needed the solvent as a medium for it to take place. Because of the loss of solvent medium in a short time during the droplet-mediated evaporation in electrospinning and spray drying, there was no occurrence of the  $\alpha$ -helix to  $\beta$ -sheet transformation. So, in the ZEFs and SDZPs, the structure was dominated by  $\alpha$ -helix while no  $\beta$ -sheet was in the structure.

#### ***4.3.4 Formation mechanism of super-hydrophobic/hydrophobic surfaces***

Based on the experimental results and related analysis, we proposed a formation mechanism of super-hydrophobic/hydrophobic surfaces made by amphiphiles through droplet-mediated evaporation-induced self-assembly, such as electrospinning and spray drying.

For both the amphiphilic molecules discussed above, zein and PEG-PLA, electrospinning improved their surface hydrophobicity over cast drying. The key difference between the two methods, cast drying and electrospinning, was the style of solvent evaporation. Cast drying is a surface-mediated solvent evaporation process, while electrospinning is a droplet-based solvent evaporation process. The droplet-mediated solvent evaporation can also be recognized by the formation of the beads with collapsed skins and the ribbon-like fibers, as shown in Figure 4.3. The formation of collapsed beads and fibers could be explained by the premature

aggregation and solidification of zein during the droplet-mediated or jet-mediated evaporation of the solvents. With low concentration solutions, the droplet-mediated or jet-mediated solvent evaporation resulted in a pressure difference between the inside and the outside of the zein aggregates, and, therefore, collapsed structures were formed [18].

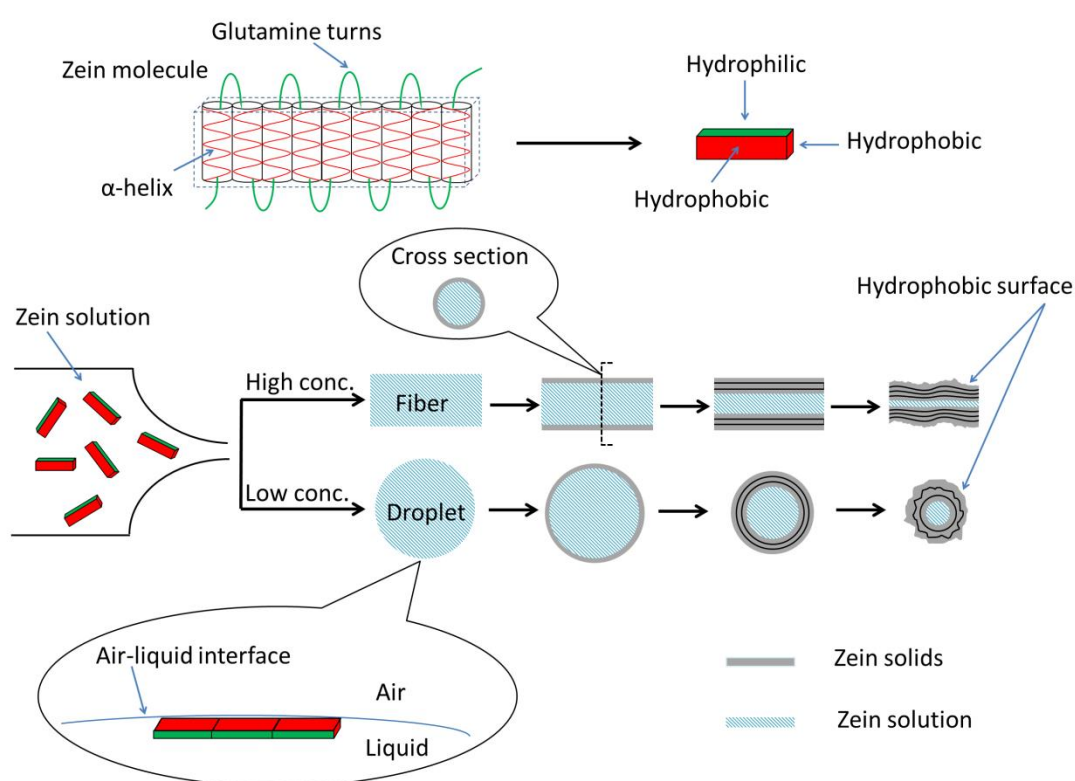


**Figure 4.7** Schematic illustration of zein super-hydrophobic/hydrophobic surface formation during electrospinning and spray drying.

It is believed that the droplet-mediated solvent evaporation contributed significantly to the orientation of zein molecules, which resulted in the formation of super-hydrophobic/hydrophobic surfaces. Figure 4.7 illustrated the mechanism of zein

super-hydrophobic/hydrophobic surface formation. During both electrospinning and spray drying, solution was ejected as liquid droplets, and the solvent was evaporated from the droplet surface in a fast speed. In an extremely brief period before the solvent completely evaporated, a radial concentration gradient of zein was generated within each droplet. The maximum of the zein concentration was at the air-liquid interface, which was moving inside towards the center of the droplet during the solvent evaporation.[161, 162] Therefore zein solidified from outside to inside “layer by layer”. At the same time, the relatively nonpolar side (air side) forced the hydrophobic compartment of zein molecules face outside. The radial concentration gradient and the presence of the liquid-air interface [163] lead to the orientation of the zein molecules as well as the growth of the dried zein, the direction of which was radially inward [164]. As a result, the surfaces of the ZEF and SDZP were super-hydrophobic or hydrophobic. Moreover, with low concentration solution, the solvent evaporation inside the droplet caused the atmospheric pressure exerted onto the prematurely solidified zein particles, and therefore collapsed structures were formed. The collapsed surface increased the roughness of surface. As a comparison to the droplet-mediated solvent evaporation of electrospinning and spray drying, the surface-mediated evaporation of cast drying had a different mechanism. During surface-mediated evaporation, the solvent evaporated from the surface of the solution and the solvent molecules moved to the solution surface. A concentration gradient was formed, as there were more solvent molecules on the surface and less solvent molecules at the bottom of the solution. The air-liquid interface would be kept on the surface of the solution. The hydrophilicity of solvent was

increasing since ethanol evaporates faster than water. Thus, the hydrophilic sides of zein molecules, which contained glutamine turns would face outside to the solvent to achieve solvent-solute stability [148]. In this way, the ZCF formed by cast drying had a hydrophilic surface.

#### **4.4 Conclusions**

ZEFs were fabricated using electrospinning, a droplet-mediated evaporation-induced self-assembly process, and their surface hydrophobicity was studied. The surfaces of the ZEFs made from both high (30 wt%) and low (10 wt%) concentrations of zein were highly hydrophobic, with WCA of 155.2° and 135.4°, respectively. Fibers were formed when the zein concentration was high while beads were formed when the zein concentration was low. Hydrophobic surfaces could also be successfully formed using the synthesized amphiphilic molecule PEG-PLA. And spray drying of zein was also tried and hydrophobic surfaces of zein have also been successfully formed. Based on all of these studies, a formation mechanism of super-hydrophobic/hydrophobic surface of amphiphiles through droplet-mediated evaporation-induced self-assembly process was proposed. It is believed that the formation of super-hydrophobic/hydrophobic surfaces from amphiphilic molecules using electrospinning and spray drying was mainly attributed to the droplet-mediated solvent evaporation style. The droplet-mediated solvent evaporation forced the hydrophobic sides of zein molecules to face outside, and made the surface hydrophobic. The chemical analysis by ATR-FTIR showed that the droplet-mediated solvent

evaporation resulted in no transformation of  $\alpha$ -helix to  $\beta$ -sheet of zein, while the transformation usually occurred during the surface-mediated evaporation-induced zein self-assembly, such as cast drying.

## **Chapter 5: Encapsulation of vitamin C using a double-layer zein/CS structure with improved stability and controlled release**

### **5.1 Introduction**

Vitamin C (ascorbic acid, VC), also called L-ascorbic acid is a kind of easily degraded and oxidized acid. It is an essential nutrient for human body which has been widely and well-studied by research groups. It is reported that functions of VC are related to many biological and physiological processes in human bodies [165, 166]. As one of the significant antioxidants in human bodies, VC has a variety of biological functions, such as immune system enhancement [167], free radical damage prevention, and oncogenic micro-organism inhabitation [168]. Moreover, it has been concluded by scientists that VC has the potential to decrease the occurrence of some cancers [165, 169]. Nevertheless, studies show that VC are not able to form inside human body because there is no L-gulonolactone oxidase which is an important enzyme for catalyzing the formation of VC [170]. Therefore, people should take certain amount of VC from outside to ensure the normal physiological processes in their bodies every day. However, there exists a big problem that VC contained in the food is not stable in the food processing and during food intake of human body. It has been reported that VC can be easily dissolved in aqueous solutions and very vulnerable to oxygen, heat, and light. Decomposition would easily occur in neutral or alkaline conditions [171]. To solve the above problems, increase its lifespan, and improve its effective absorption in human body as well, researchers have developed various methods, including

micro-encapsulation.

Micro-encapsulation is a technique used to load liquid, gaseous ingredients, or solid into capsules at micro scale. By being encapsulated by shell materials, the core ingredients inside can avoid the contact with outer environments, which can increase the stability of the core ingredients. Besides, this technique can be specifically designed to achieve desired controlled release of the medicinal ingredients in human body [172, 173]. It is reported that micro-encapsulation has been regarded as a promising technique in both pharmaceutical and food industries recently. There are lots of coating materials being studied by research groups. For example, CS, a hydrophilic polysaccharide of low toxicity, has been proved to be applied to encapsulate VC with the ton-toxic STPP as the cross-liner. Studies showed that the stability of its oral delivery was improved after VC was encapsulated by micro-structure [174]. However, fast release profile was observed from the VC-loaded CS NPs in PBS [175]. Therefore, a secondary coating of zein on CS is proposed to get a better protection of VC.

Zein, a prolamine protein stored in corn endosperm, is well applied in food and pharmaceutical industries because of its good biocompatibility and bioavailability. Zein can self-assemble to form biobased films, hydrophobic surfaces, and encapsulations, and has potential applications in food packaging, electronic devices, and for oral administration enhancement [1]. Zein is an amphiphilic and it can be easily dissolved in 75% ethanol-water mixture [135]. After solvent evaporation, it can self-assemble to form MP. Studies have proved that there was a conformational transition from  $\alpha$ -helix to  $\beta$ -sheet happening during the evaporation-induced EISA process while EISA is a

technique used to promote self-organization of nanostructures [135, 176]. EISA is a process that involves binary or tertiary solvents. During EISA the preferential evaporation of one of the solvents causes the change of the polarity of the solution. The changing polarity then serves as the force to drive the self-assembly of solutes. Because of its self-assembly ability, zein has been extensively studied to encapsulate bioactive compounds, such as essential oil [9], flax oil [177], vitamin D3 [178],  $\alpha$ -tocopherol [10], and citral and lime [179]. Compared with other wall materials, zein coating greatly improves the controlled release function of the encapsulation. For example it can delay the release of the core ingredients and protect them from gastric fluid. Nevertheless, the core ingredient selection and the size control are still primary limitations for its wide applications.

The core ingredients selected for zein encapsulations are generally hydrophobic or amphiphilic, which results from the fact that zein is more likely to aggregate around those hydrophobic or amphiphilic materials rather than hydrophilic ones. The formation of self-assembled spheres could be subsequently triggered after the aggregation of zein around the core materials. Therefore, zein is rarely used to encapsulate highly hydrophilic materials, such as heparin [180], 5-fluorouraci [13], and pDNA [14]. In spite of some reported experiments about the direct preparations of the above non-hydrophobic encapsulated zein micro/nanoparticles, the morphology of the products was not satisfactory, which inevitably affected the encapsulation efficiency and drug delivery. Moreover, in these studies of micro/nanoencapsulation, coacervation method is widely adopted to access smaller size. The micro/nanoparticles are formed

by a special method called the desolvation of zein. During the preparation procedure, a amount of aqueous solution is added into zein solution under vigorous stirring. However, the disadvantage has been pointed out that it may cause the loss of labile encapsulated ingredients in such high-energy method [10].

The objective of this work is to use CS and zein to prepare a double layer encapsulation of VC. SEM was used to characterize the morphology of the particle, and ZETASIZER was applied to measure the sizes of the formed particles and the distribution of different sizes. HPLC and electrospray ionization mass spectrometry (ESI-MS) was used to measure the VC amount in the encapsulation and investigate the stability of encapsulated VC. And *in vitro* gastrointestinal studies were conducted to study the release profile of zein-CS encapsulation of VC with a comparison of the encapsulation made by CS only.

## **5.2 Materials and methods**

### **5.2.1 Materials**

VC (99.7% purity), STPP, CS with the deacetylation degree of 80% and molecular weight of 65 kDa, pepsin (from porcine gastric mucosa) and pancreatin (from porcine pancreas) were all purchased from Sigma-Aldrich Chemical Co. Ltd. (St. Louis, MO). Zein was obtained from Wako Pure Chemical Industries, Ltd. (Tokyo, Japan). Ethanol (96% v/v) was from Anhui Bilvchun Bio-Ttch Co. Ltd (Xuzhou, China). All other reagents were of analytical grade. All chemicals were directly used as received.

### ***5.2.2 Preparation of VC-loaded CS NPs***

CS was first dissolved in 1% (w/v) acetic acid aqueous solution under continuous stirring for 20 min to get the homogeneous solution (2.0 mg/ml). VC (1.0 mg/ml) was dissolved in the deionized water and then added slowly into the acidifying CS solution under the mild stirring (1000 rpm) for 30 min. STPP (0.5 mg/ml) was dissolved in the deionized water and then dropped into the above mixture solution. The mixed solution was kept stirring (1000 rpm) for 30 min to form VC-loaded CS NP suspension [175]. The solution container was light protected to avoid the loss of VC caused by degradation. VC-loaded CS NPs were gained by ultracentrifugation ( $2.18 \times 10^4$  g) and freeze-drying.

### ***5.2.3 Preparation of VC-loaded zein/CS MPs***

To prepare VC-loaded zein/CS MPs, the solvent of VC-loaded CS NP suspension was first adjusted to 70% ethanol-water mixture by adding absolute ethanol. Then 1, 1.5, 2, 2.5, and 3 ml zein solution (10 mg/ml in 70% ethanol) were then added drop wise under continuous stirring, respectively. The mixed solutions were stirred at 1000 rpm for 30 min and poured on the evaporating dishes. The VC-loaded zein/CS MP powder was gained through EISA at room temperature (25°C). The prepared samples were stored at 4°C until further analysis.

#### ***5.2.4 Particle size evaluation and morphological observation***

The particle size of VC-loaded CS NPs was measured using Malvern ZETASIZER 3000HSA (Malvern Instrument, London, England). The particle size of VC-loaded zein/CS MPs was estimated through scanning electron microscope (SEM). ImageJ software was applied for statistical treatment for SEM images of the selected VC-loaded zein/CS MPs. The sample particles were re-suspended in deionized water and cast-dried on the foil under room temperature overnight. The foil was cut into small slices to adhere to carbon tapes. The whole tapes were then gold coated (300Å) using the Edwards S150B sputter coater, which could increase the electrical conductivity. SEM images were captured using a JEOL JSM-6490 SEM (Tokyo, Japan). The size of the MPs was determined in a random area under the microscopic field. For each sample, 5 areas were selected randomly to calculate the average size diameter. In order to analyze the morphology of VC-loaded zein/CS MPs, SEM images were also taken as above.

#### ***5.2.5 Encapsulation efficiency of VC-loaded CS NPs***

In order to calculate the encapsulation efficiency (EE) of VC-loaded CS NPs, the amount of free VC in the supernatant of the NP suspension was first measured. The NP suspension was first ultra-centrifuged and the amount of free VC can be measured by RP-HPLC analysis with the UV detection at 245nm [174]. Separation was performed on an ODS column (LiChrospher RP-18 5u, 2504.6 mm). The applied mobile phase was methanol, and the flow rate was set at 0.5 ml/min. The VC loading efficiency (LE)

was also calculated. The drug EE and LE were calculated using the following equations:

$$EE = \frac{\text{total VC} - \text{free VC}}{\text{total VC}} \times 100\%$$
$$LE = \frac{\text{mass of VC in particles (mg)}}{\text{mass of particles (g)}}$$

### **5.2.6 ESI-MS analysis**

The presence and stability of VC in zein/CS MPs were examined using ESI-MS. 1 mg VC-loaded zein/CS MPs (10 days after preparation and stored at room temperature, 25) were re-dispersed in deionized water. The dispersion was then centrifuged at 12,000 g for 20 minutes to separate MPs and free VC in the solution. The supernatant liquid was discarded to remove any residual VC on the surface of the MPs. The MPs left were then re-suspended in 200  $\mu$ L 80% methanol aqueous solution to dissolve the MPs and release the VC contained in the MPs. After that, the solution was treated with sonication for 5 min to help dissolve the MPs completely. Finally, the solution was centrifuged for 2 min to separate undissolved powder. The supernatant was measured by ESI-MS operating in a negative ionization mode [181].

### **5.2.7 Release test in simulated gastrointestinal fluids**

The release tests of VC encapsulations were carried out in simulated gastric fluid (SGF, HCl environment with digestive enzyme, pepsin) and simulated intestinal fluid (SIF, natural environment with digestive enzyme, pancreatin) with continuous stirring

at constant 37°C. 10 mg MPs were re-dispersed in 5 ml SGF and SIF, respectively. The MPs suspensions were then put into the dialysis membrane bags, the molecular weight cut-off of which was 10 kDa [10]. Afterwards, the whole dialysis membrane bags were placed into 100 ml simulated gastrointestinal fluids but no pepsin or pancreatin contained. The dialysis system was then maintained at 37°C under mild stirring. At designed time intervals, 1 ml solution sample was taken away from 100 ml simulated fluids. And to keep the dialysis system constant, 1 ml fresh solution was added to it afterwards. The collected sample solution was then filtered by a 0.45 µm Acrodisc filter. And the filtered solution was injected into HPLC analysis system to measure the VC contained in it. The HPLC conditions were the same with that described in section 5.2.5.

### **5.3 Results and discussion**

#### ***5.3.1 Particle size and morphology***

The average diameters of different particles were listed in Table 5.1, and the SEM images of selected MPs are shown in Figure 5.1. The VC-loaded CS NPs in the preparation conditions had a diameter of about 240 nm. After encapsulated by zein layer, the particle zein was further increased. It is reported that CS can interact with polyanions such as STPP, which is also called the cross linker. After a process called ionotropic gelation, CS and STPP form micro- or nanoparticles [175]. Alishsahi et al. have investigate the mechanism involved in the encapsulation of VC by CS-STPP [174]. They concluded that when dissolved in the 1% acetic acid solution, the glucosamine

groups of CS (pKa = 6.3) were converted to R-NH<sub>3</sub><sup>+</sup>. Then the protonated CS could quickly crosslink with the added STPP, which had the negative charge. After the process of intermolecular crosslinking, they together precipitated to form micro- or nanoparticles. In our work, the formation of VC-loaded zein/CS MPs was attributed to various behaviors of CS and zein when the solvent evaporated. The concentration of the ethanol aqueous solution will have significant effects on the solubility and elasticity of CS. It has been proved that, CS can hardly be dissolved in the solution with ethanol concentration higher than 50% [182]. Therefore, when the ethanol concentration was between 50-80% at the beginning of the evaporation, as the solvent evaporated, the formed VC-loaded CS NPs would maintain their elasticity in the poor soluble state while zein could precipitate around the CS NPs to form larger MPs. As a result, the CS NPs were wrapped by the zein shell before they could dissolve in the lower ethanol solution.

**Table 5.1** The average particle sizes of different particles.

Sample	VC-CS	VC-zein/CS (mas ratio 1.5)	VC-zein/CS (mass ratio 2.0)	VC-zein/CS (mass ratio 2.5)
Size (μm)	0.24±0.03	0.88±0.13	0.72±0.09	1.10±0.21

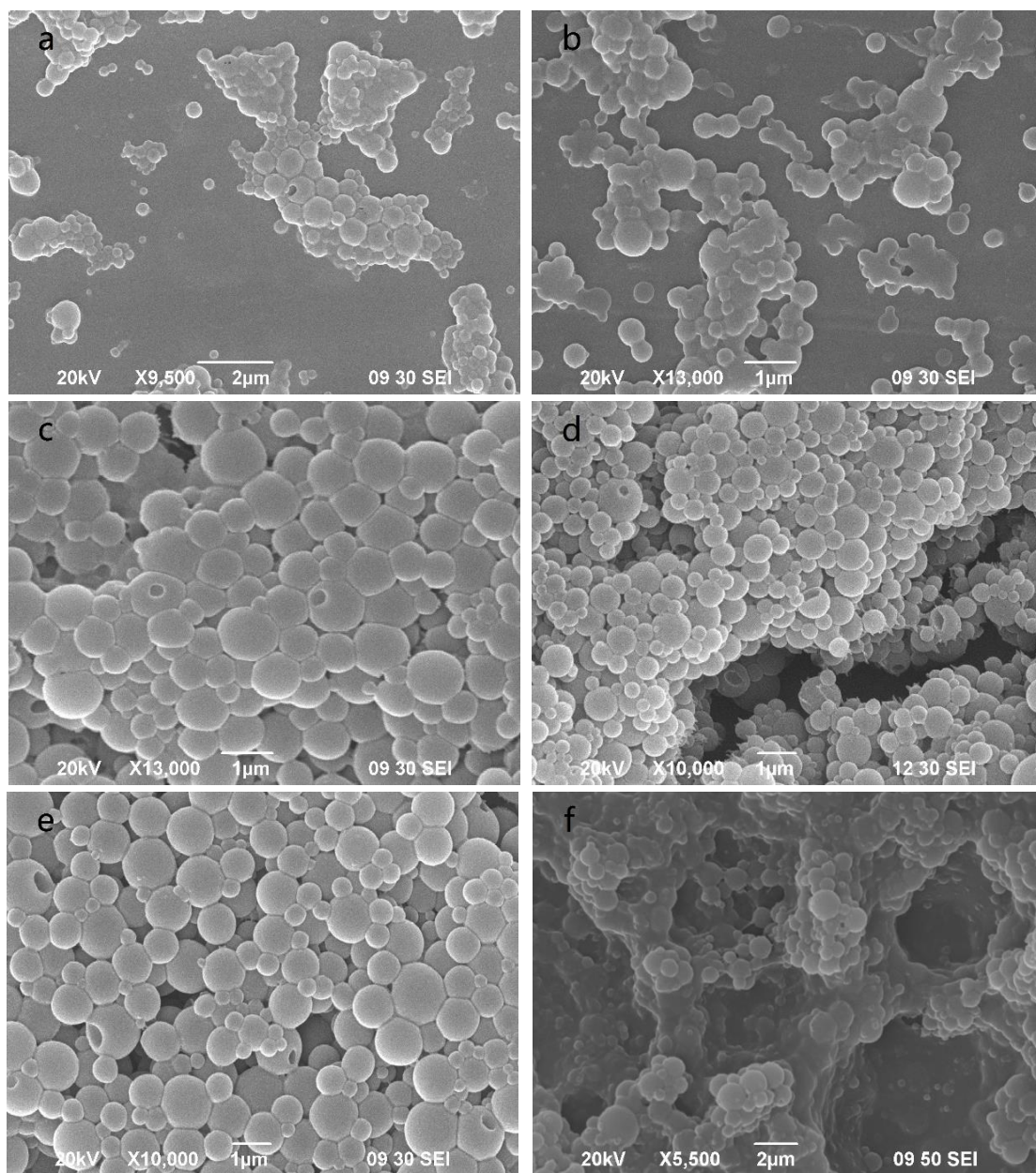


**Figure 5.1** SEM images of VC-loaded zein/CS MPs with various zein/CS mass ratio of (a) 0.5:1, (b) 1.0:1, (c) 1.5:1, (d) 2:1, (e) 2.5:1, and (f) 3.0:1.

The particle sizes of the formed zein/CS MPs were not linear with the zein concentrations. The zein/CS mass ratio of 2.0:1 produced the smallest particle size (720 nm). SEM images also showed that the MPs with zein/CS mass ratio of 1.5:1, 2.0:1 and

2.5:1 had better spherical integrity than others. At the low or high zein/CS mass ratio, the particles would deform in similar tendencies. At low zein concentration (zein/CS mass ratio < 1.5:1), larger agglomerates formed by the fusion of smaller particles. The reason for the fusion was that there was not adequate zein to fully cover CS-STPP NPs, and the partially or uncovered CS NPs would interact with each other through hydrophobic interactions with the increase of the solvent polarity, which also accounted for the wider size distribution. When zein/CS mass ratio was increased to be larger than 1.5:1, the formed particles were improved in the sphericity and the size distribution was more homogeneous. It was because enough zein was provided for the formation of the outside coating for every CS-STPP NP. However, when the zein/CS mass ratio reached 3.0:1, the threshold of film formation achieved. The dispersed sphericity was caused by the fusion of zein surrounding the CS NPs and excess zein in the solution matrix [117].

### ***5.3.2 Stability of VC-loaded in zein/CS MPs***

The sample of VC-loaded zein/CS MP (prepared with zein/CS mass ratio of 2.0:1) was examined by ESI-MS at room temperature after 10-day storage and the spectrum is shown in Figure 5.2. The ESI-MS spectrum shows a predominant peak corresponding to VC ( $m/z$  175), indicating that VC was the major chemical component of the sample. Besides the predominate peak, a small peak corresponding to dehydroascorbic acid ( $m/z$  173), which was an oxidation resultant from ascorbic acid, was also detected and the intensity of this peak was about 5% of that of the peak of VC. Then tandem mass spectrometric analysis was used to further identify the peak at  $m/z$  173 was further

(Figure 5.3). So the stability test showed that, after 10-day storage, at least 95% of the encapsulated VC were well protected from oxidation. The 5% of dehydroascorbic acid, which was the oxidative resultant of VC, was also possible to be produced during the ESI-MS test. The above results showed that our encapsulation structure performed a great protection to the VC inside.

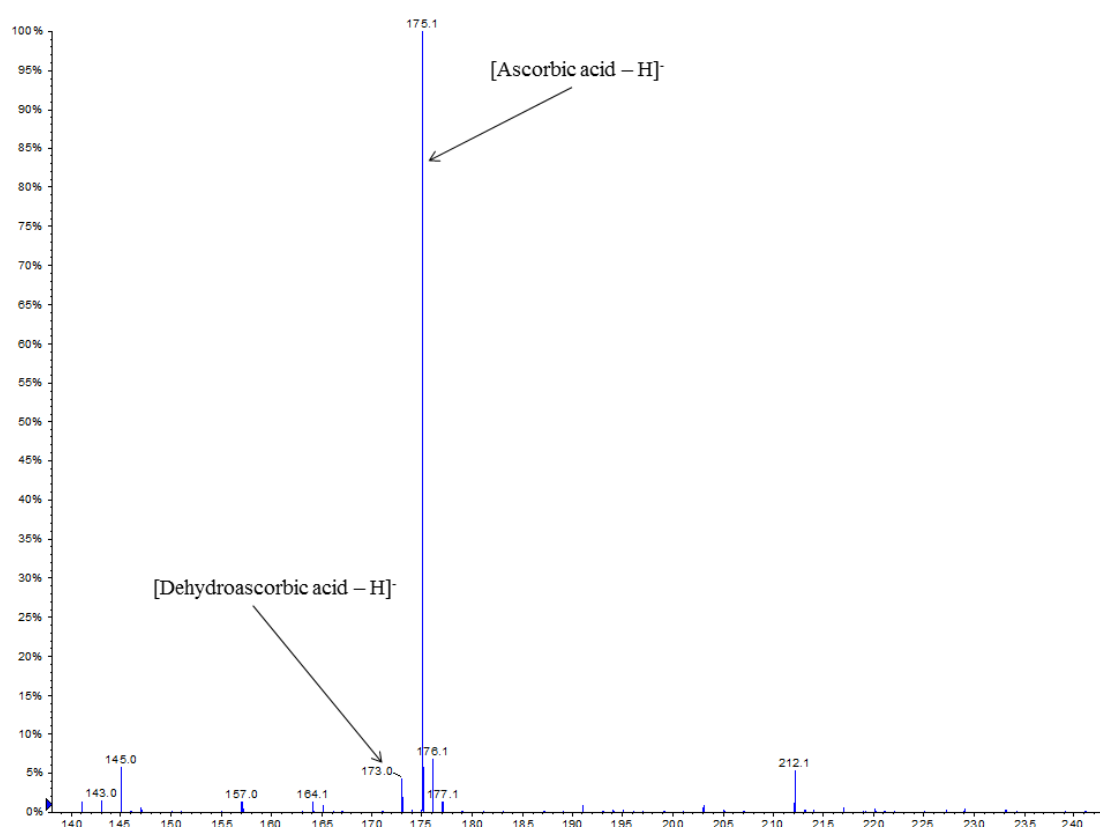


**Figure 5.2** Negative ion ESI-MS spectrum for the VC-loaded zein/CS MPs.

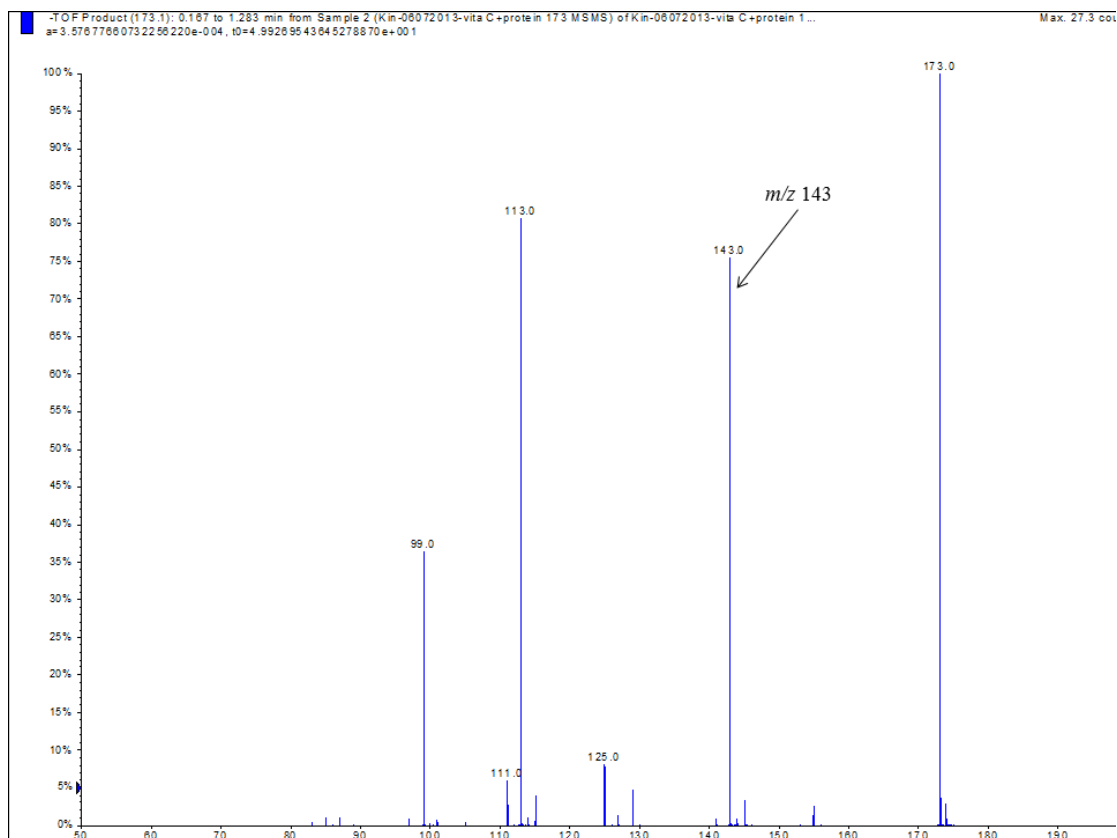


**Figure 5.3** Negative ion ESI-MS/MS spectrum for the m/z 173 ion.

### 5.3.3 Effect of different formations on *in vitro* release of VC

The release percentage of VC from the MPs was calculated as the mass ratio of the VC detected in the release medium to that of the encapsulated VC. The amount of the encapsulated VC could be calculated in the way of the amount of the added VC times EE, and EE was 51.9% (drug loading 47.6%). Figure 5.4 showed the *in vitro* release profiles of VC from CS NPs (with 0.870.12% moisture content) and zein/CS MPs (prepared with zein/CS mass ratio of 2.0:1) in SGI at 37°C for 420 min. VC was rapidly released from the formed CS NPs was during the initial 60 min, about 18% of VC being released. Then its release rate decreased to 0 and a final accumulative amount of 20% was achieved at 300 min. In comparison, the release rate was much lower for zein/CS

MPs within the first 240 min, with only about 5% VC being eluted from the MPs, and the release rate increased thereafter. In addition, the total released VC from CS NPs at 420 min was nearly 26%, more than two times of that from zein/CS MPs. The change of the release rate could be explained by the release mechanisms. The formation of VC-loaded CS NPs was driven by the ionic interactions between the anionic counterion of VC and the amino groups of CS [175]. And VC molecules distributed evenly in the formed NPs. Hence, for VC-encapsulated CS NPs, the initial rapid release was attributed to the easy diffusion of VC through the cross-linked polymer matrix to the particle surface [183]. And the gradually decreased rate in the later stage was mainly attributed to the degradation of CS, which cost more time. Furthermore, in acidic environment, the CS and STPP were strongly associated and thus prevented the matrix from degradation. On the other hand, for VC-loaded zein/CS MPs, owing to the well-sealed zein shell, the slow degradation of zein played a principal role and thus there was a very low releasing rate during initial 60 min. The later increased rate of VC releasing from zein/CS MPs could be attributed to the change of release mechanism. After 4 hours, most of zein shells were degraded which resulted in the explosion of the inner CS core. Since then, the diffusion of VC molecules began to appear, presenting a trend of increased release.

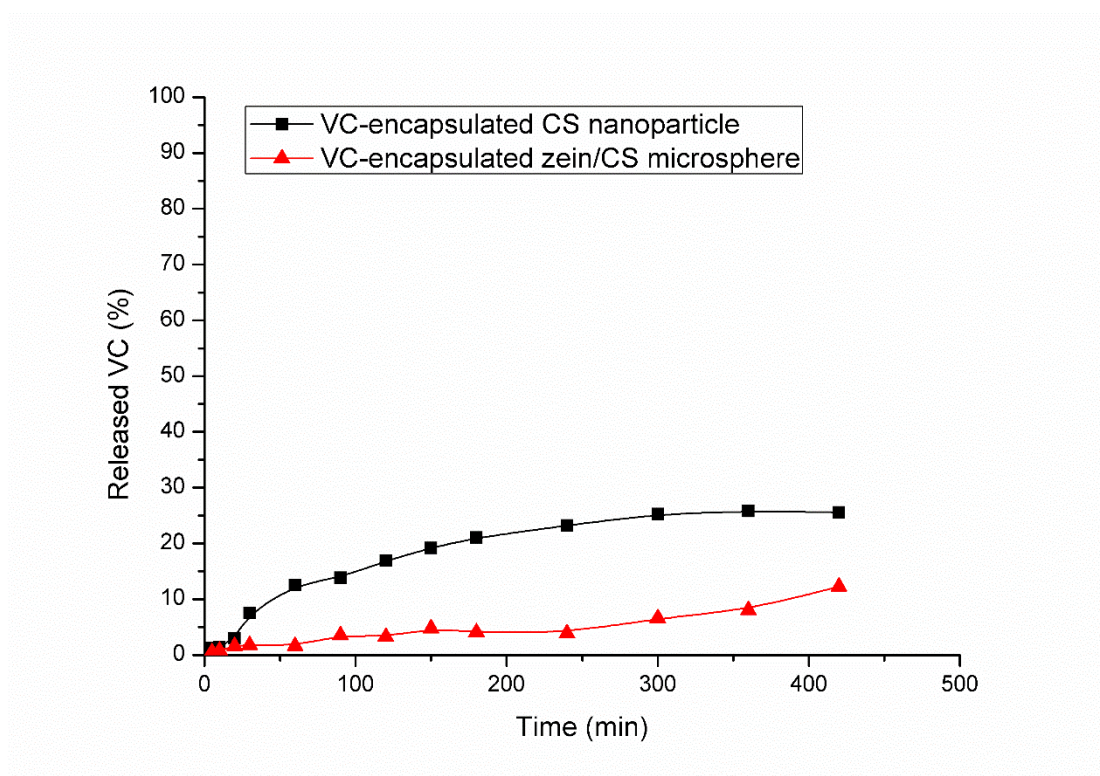


**Figure 5.4** The *in vitro* release curves of VC from VC-loaded CS NPs and VC-loaded zein/CS MPs in SGF, respectively.

#### 5.3.4 Release of VC from zein/CS MPs in different simulated fluids

The cumulative release of VC from zein/CS MPs was investigated in SGF and SIF, respectively. The release profile was showed in Figure 5.5. A burst release of VC was seen in the SIF during initial 10 min and about 20% of VC contained was released out. Afterwards, its release rate gradually decreased. And in the end approximate 66% of VC contained was released out. Compared with the total 26% of VC were released in SGF after 420 min, that in SIF was much higher. This obvious difference in release profiles between the above two was due to the effects of different digestive enzymes on zein. According to Hutrado et al. [184], pepsin in stomach solution can only degrade

$\alpha$ -zein, however, both  $\alpha$ -zein and  $\alpha$ -zein dimers can be digested by pancreatin in the intestine solution. Therefore, zein spheres can be digested at a faster rate in SIF than SGF. Figure 5.5 showed that the outer zein coating could be digested within 10 min and VC was quickly eluted from the exposed CS particle surface. However, since the limited ability of pepsin to digest zein, a relatively lower release rate was observed at the early stage in SGF.

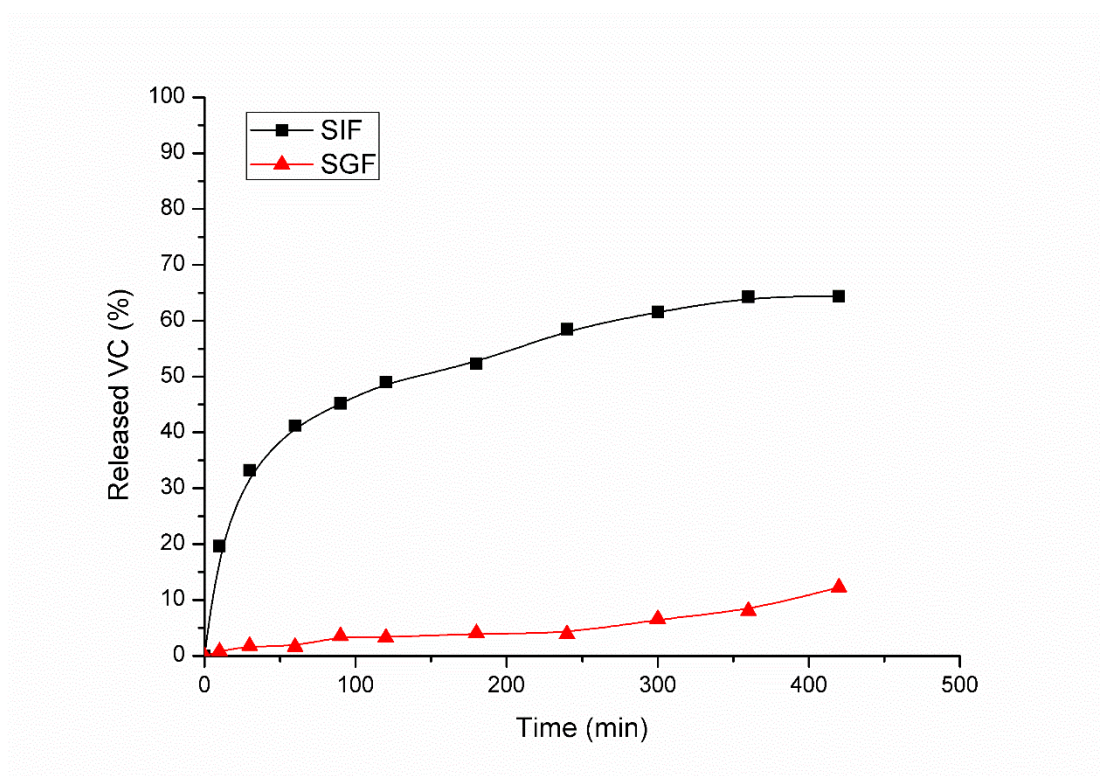


**Figure 5.5** The *in vitro* release curves of VC from VC-loaded zein/CS MPs in SGF and SIF, respectively.

#### 5.4 Conclusions

VC was encapsulated by a double-layer structure of zein and CS. The ratio

between zein and CS was studied for the formation and optimization of the double-layer encapsulation and SEM was used for the structure characterization. The ESI-MS results showed that the VC was successfully encapsulated and protected by zein and CS. The controlled release study was carried out using simulated gastrointestinal fluids. The double structure of VC-loaded CS/zein MPs protected VC from digestion, delayed the release in the stomach, and promoted the release in the intestine. The result indicated that this double-layer encapsulation is potential for the applications of encapsulations for other polar drugs to achieve controlled release.

## **Future research perspectives**

### **Zein hydrophobic surface**

The results shown the completed work imply that there are other parameters that have effects on the surface hydrophobicity of the formed zein structures, like electrospinning flow rate, tip to needle distance, temperature and solvent selection. Therefore, more parameters should be considered when fabrication zein structures by electrospinning technique. Besides the surface hydrophobicity, other properties of the formed zein structures, such as porosity and degradability will be evaluated to see the effects on cell adhesion behaviors. Also the chemical properties of the surface should be examined by techniques such as Nuclear magnetic Resonance, X-ray photoelectron spectroscopy. Moreover, chemical and physical modifications will be tried to alter the surface properties for extended application in biomedical engineering, like addition of functional molecules for special cell targeting. For the clinical application of the formed zein structures, in vivo animal models should be adopted to further access their biocompatibility and biodegradability.

### **Zein hydrophobic surface**

In the present work, VC was successfully encapsulated by a zein/CS double layer. However, the aggregation of part of the formed VC-loaded zein/CS particles was observed during the experiment, which indicated that the re-dispersion property of the formed particles is not that good. Therefore, the stability of particles in the solutions after being re-dispersed should be improved by adding some stabilizers. In the next

stage, zein will be tried to encapsulate some other anti-cancer drugs, such as doxorubicin, paclitaxel and so on. And their anti-cancer effects and cellular uptake will be evaluated in various cancer cell lines like HepG 2, MCF7 and HeLa, even some drug resistant cell lines like MCF/MDR. In addition, surface modifications of the formed zein nanoparticles will be tried to achieve targeting property and release in specific tissue sites. For example, folic acid and hyaluronic acid will be considered to be connected onto the drug-loaded zein nanoparticles. After a series of experiment conducted in cell level, *in vivo* animal model will be considered to investigate the bio-distribution and pharmacokinetic release of the nanoparticles.

## References

- [1] Shukla R, Cheryan M. Zein: the industrial protein from corn. *Industrial Crops and Products* 2001;13:171-92.
- [2] Danzer LA, Rees ED. Purification of Zein on a Laboratory Scale by Charcoal or Gel Filtration. *Cereal Chem* 1971;48:118-&.
- [3] Clegg GA, Dole M. Molecular Beams of Macroions .3. Zein and Polyvinylpyrrolidone. *Biopolymers* 1971;10:821-&.
- [4] Mark HF, Bikales NM. *Encyclopedia of polymer science and technology : plastics, resins, rubbers, fibers : supplement*. New York: Interscience Publishers; 1976.
- [5] Argos P, Pedersen K, Marks MD, Larkins BA. A Structural Model for Maize Zein Proteins. *J Biol Chem* 1982;257:9984-90.
- [6] Matsushima N, Danno G, Takezawa H, Izumi Y. Three-dimensional structure of maize alpha-zein proteins studied by small-angle X-ray scattering. *Biochim Biophys Acta* 1997;1339:14-22.
- [7] Wang Q, Wang JF, Geil PH, Padua GW. Zein adsorption to hydrophilic and hydrophobic surfaces investigated by surface plasmon resonance. *Biomacromolecules* 2004;5:1356-61.
- [8] Grason GM. The packing of soft materials: Molecular asymmetry, geometric frustration and optimal lattices in block copolymer melts. *Phys Rep* 2006;433:1-64.
- [9] Parris N, Cooke PH, Hicks KB. Encapsulation of Essential Oils in Zein Nanospherical Particles. *Journal of Agricultural and Food Chemistry* 2005;53:4788-92.
- [10] Luo Y, Teng Z, Wang Q. Development of Zein Nanoparticles Coated with

Carboxymethyl Chitosan for Encapsulation and Controlled Release of Vitamin D3.

Journal of Agricultural and Food Chemistry 2011;60:836-43.

[11] Wang Y, Su CP, Schulmerich M, Padua GW. Characterization of core-shell structures formed by zein. Food Hydrocolloid 2013;30:487-94.

[12] Zhong Q, Jin M. Zein nanoparticles produced by liquid-liquid dispersion. Food Hydrocolloid 2009;23:2380-7.

[13] Lai LF, Guo HX. Preparation of new 5-fluorouracil-loaded zein nanoparticles for liver targeting. International Journal of Pharmaceutics 2011;404:317-23.

[14] Regier MC, Taylor JD, Boreyk T, Yang YQ, Pannier AK. Fabrication and characterization of DNA-loaded zein nanospheres. J Nanobiotechnol 2012;10.

[15] Croston CB, Evans CD, Smith A. Zein fibers: Preparation by wet spinning. Industrial Engineering Chemistry 1945;42:482-5.

[16] Uy WC. Dry spinning process for zein fibers. US Patent 1998;5:064.

[17] Pelosi LF. Crosslinking processes/agents for zein. US Patent 1997;5:080.

[18] Torres-Giner S, Gimenez E, Lagarona JM. Characterization of the morphology and thermal properties of zein prolamine nanostructures obtained by electrospinning. Food Hydrocolloid 2008;22:601-14.

[19] Sharfrin E, Zisman WA. Constitutive relations in the wetting of low energy surfaces and the theory of the retraction method of preparing monolayers. The Journal of Physical Chemistry 1960;64:519-24.

[20] Furstner R, Barthlott W, Neinhuis C, Walzel P. Wetting and self-cleaning properties of artificial superhydrophobic surfaces. Langmuir 2005;21:956-61.

- [21] Qian BT, Shen ZQ. Fabrication of superhydrophobic surfaces by dislocation-selective chemical etching on aluminum, copper, and zinc substrates. *Langmuir* 2005;21:9007-9.
- [22] Zhai L, Cebeci FC, Cohen RE, Rubner MF. Stable superhydrophobic coatings from polyelectrolyte multilayers. *Nano Letters* 2004;4:1349-53.
- [23] Daoud WA, Xin JH, Tao XM. Superhydrophobic silica nanocomposite coating by a low-temperature process. *Journal of the American Ceramic Society* 2004;87:1782-4.
- [24] Michaelides A, Morgenstern K. Ice nanoclusters at hydrophobic metal surfaces. *Nature Materials* 2007;6:597-601.
- [25] Vilcnik A, Jerman I, Vuk AS, Kozelj M, Orel B, Tomsic B, et al. Structural Properties and Antibacterial Effects of Hydrophobic and Oleophobic Sol-Gel Coatings for Cotton Fabrics. *Langmuir* 2009;25:5869-80.
- [26] Fahmy TM, Samstein RM, Harness CC, Saltzman WM. Surface modification of biodegradable polyesters with fatty acid conjugates for improved drug targeting. *Biomaterials* 2005;26:5727-36.
- [27] Wikipedia. [http://en.wikipedia.org/wiki/Tissue\\_engineering](http://en.wikipedia.org/wiki/Tissue_engineering).
- [28] Stevens MM, George JH. Exploring and engineering the cell surface interface. *Science* 2005;310:1135-8.
- [29] Langer R, Vacanti JP. Tissue Engineering. *Science* 1993;260:920-6.
- [30] Sill TJ, von Recum HA. Electro spinning: Applications in drug delivery and tissue engineering. *Biomaterials* 2008;29:1989-2006.
- [31] Venkatraman S, Boey F, Lao LL. Implanted cardiovascular polymers: Natural,

- synthetic and bio-inspired. *Prog Polym Sci* 2008;33:853-74.
- [32] Hersel U, Dahmen C, Kessler H. RGD modified polymers: biomaterials for stimulated cell adhesion and beyond. *Biomaterials* 2003;24:4385-415.
- [33] Grafahrend D, Heffels KH, Beer MV, Gasteier P, Moller M, Boehm G, et al. Degradable polyester scaffolds with controlled surface chemistry combining minimal protein adsorption with specific bioactivation. *Nature Materials* 2011;10:67-73.
- [34] Manning CN, Schwartz AG, Liu W, Xie J, Havlioglu N, Sakiyama-Elbert SE, et al. Controlled delivery of mesenchymal stem cells and growth factors using a nanofiber scaffold for tendon repair. *Acta Biomater* 2013;9:6905-14.
- [35] Li MY, Mondrinos MJ, Gandhi MR, Ko FK, Weiss AS, Lelkes PI. Electrospun protein fibers as matrices for tissue engineering. *Biomaterials* 2005;26:5999-6008.
- [36] Mano JF, Silva GA, Azevedo HS, Malafaya PB, Sousa RA, Silva SS, et al. Natural origin biodegradable systems in tissue engineering and regenerative medicine: present status and some moving trends. *J R Soc Interface* 2007;4:999-1030.
- [37] Resende RR, Fonseca EA, Tonelli FMP, Sousa BR, Santos AK, Gomes KN, et al. Scale/Topography of Substrates Surface Resembling Extracellular Matrix for Tissue Engineering. *Journal of Biomedical Nanotechnology* 2014;10:1157-93.
- [38] Matthews JA, Wnek GE, Simpson DG, Bowlin GL. Electrospinning of collagen nanofibers. *Biomacromolecules* 2002;3:232-8.
- [39] Boland ED, Matthews JA, Pawlowski KJ, Simpson DG, Wnek GE, Bowlin GL. Electrospinning collagen and elastin: Preliminary vascular tissue engineering. *Front Biosci* 2004;9:1422-32.

- [40] Balu B, Breedveld V, Hess DW. Fabrication of "roll-off" and "sticky" superhydrophobic cellulose surfaces via plasma processing. *Langmuir* 2008;24:4785-90.
- [41] Li SH, Zhang SB, Wang XH. Fabrication of superhydrophobic cellulose-based materials through a solution-immersion process. *Langmuir* 2008;24:5585-90.
- [42] Li SH, Xie HB, Zhang SB, Wang XH. Facile transformation of hydrophilic cellulose into superhydrophobic cellulose. *Chem Commun* 2007:4857-9.
- [43] Cunha AG, Gandini A. Turning polysaccharides into hydrophobic materials: a critical review. Part 1. Cellulose. *Cellulose* 2010;17:875-89.
- [44] Cunha AG, Gandini A. Turning polysaccharides into hydrophobic materials: a critical review. Part 2. Hemicelluloses, chitin/chitosan, starch, pectin and alginates. *Cellulose* 2010;17:1045-65.
- [45] Haaparanta AM, Jarvinen E, Cengiz IF, Ella V, Kokkonen HT, Kiviranta I, et al. Preparation and characterization of collagen/PLA, chitosan/PLA, and collagen/chitosan/PLA hybrid scaffolds for cartilage tissue engineering. *J Mater Sci-Mater M* 2014;25:1129-36.
- [46] Lou T, Leung M, Wang XJ, Chang JYF, Tsao CT, Sham JGC, et al. Bi-Layer Scaffold of Chitosan/PCL-Nanofibrous Mat and PLLA-Microporous Disc for Skin Tissue Engineering. *Journal of Biomedical Nanotechnology* 2014;10:1105-13.
- [47] Holmes DR, Hirshfeld J, Faxon D, Vlietstra RE, Jacobs A, King SB. ACC expert consensus document on coronary artery stents. *J Am Coll Cardiol* 1998;32:1471-82.
- [48] Hanawa T. Materials for metallic stents. *J Artif Organs* 2009;12:73-9.

- [49] Fischman DL, Leon MB, Baim DS, Schatz RA, Savage MP, Penn I, et al. A Randomized Comparison of Coronary-Stent Placement and Balloon Angioplasty in the Treatment of Coronary-Artery Disease. *New Engl J Med* 1994;331:496-501.
- [50] Grabow N, Martin DP, Schmitz KP, Sternberg K. Absorbable polymer stent technologies for vascular regeneration. *J Chem Technol Biot* 2010;85:744-51.
- [51] Kraitzer A, Kloog Y, Zilberman M. Approaches for prevention of restenosis. *J Biomed Mater Res B* 2008;85B:583-603.
- [52] Virmani R, Guagliumi G, Farb A, Musumeci G, Grieco N, Motta T, et al. Localized hypersensitivity and late coronary thrombosis secondary to a sirolimus-eluting stent should we be cautious? *Circulation* 2004;109:701-5.
- [53] Joner M, Finn AV, Farb A, Mont EK, Kolodgie FD, Ladich E, et al. Pathology of drug-eluting stents in humans - Delayed healing and late thrombotic risk. *J Am Coll Cardiol* 2006;48:193-202.
- [54] Lanzer P, Sternberg K, Schmitz KP, Kolodgie F, Nakazawa G, Virmani R. Drug-eluting coronary stent very late thrombosis revisited. *Herz* 2008;33:334-42.
- [55] FreijLarsson C, Nylander T, Jannasch P, Wesslen B. Adsorption behaviour of amphiphilic polymers at hydrophobic surfaces: Effects on protein adsorption. *Biomaterials* 1996;17:2199-207.
- [56] Pulverer B, Anson L, Surridge C, Allen L. *Cancer. Nature* 2001;411:335-.
- [57] Farokhzad OC, Langer R. Impact of Nanotechnology on Drug Delivery. *Acs Nano* 2009;3:16-20.
- [58] Silva GA. Nanotechnology applications and approaches for neuroregeneration and

- drug delivery to the central nervous system. *Ann Ny Acad Sci* 2010;1199:221-30.
- [59] Youan BBC. Impact of nanoscience and nanotechnology on controlled drug delivery. *Nanomedicine-Uk* 2008;3:401-6.
- [60] Jin S, Ye KM. Nanoparticle-mediated drug delivery and gene therapy. *Biotechnology Progress* 2007;23:32-41.
- [61] Dianzani C, Minelli R, Mesturini R, Chiocchetti A, Barrera G, Boscolo S, et al. B7h Triggering Inhibits Umbilical Vascular Endothelial Cell Adhesiveness to Tumor Cell Lines and Polymorphonuclear Cells. *J Immunol* 2010;185:3970-9.
- [62] Sharma A, Sharma US. Liposomes in drug delivery: Progress and limitations. *International Journal of Pharmaceutics* 1997;154:123-40.
- [63] Li WJ, Das S, Ng KY, Heng PWS. Formulation, Biological and Pharmacokinetic Studies of Sucrose Ester-Stabilized Nanosuspensions of Oleanolic Acid. *Pharm Res-Dordr* 2011;28:2020-33.
- [64] Gao DW, Tang SN, Tong Q. Oleanolic acid liposomes with polyethylene glycol modification: promising antitumor drug delivery. *Int J Nanomed* 2012;7:3517-26.
- [65] Vyas D, Castro P, Saadeh Y, Vyas A. The Role of Nanotechnology in Gastrointestinal Cancer. *Journal of Biomedical Nanotechnology* 2014;10:3204-18.
- [66] Xing H, Tang L, Yang XJ, Hwang K, Wang WD, Yin Q, et al. Selective delivery of an anticancer drug with aptamer-functionalized liposomes to breast cancer cells in vitro and in vivo. *Journal of Materials Chemistry B* 2013;1:5288-97.
- [67] Ma XP, Zhou ZX, Jin EL, Sun QH, Zhang B, Tang JB, et al. Facile Synthesis of Polyester Dendrimers as Drug Delivery Carriers. *Macromolecules* 2013;46:37-42.

- [68] Zhou ZX, Ma XP, Jin EL, Tang JB, Sui MH, Shen YQ, et al. Linear-dendritic drug conjugates forming long-circulating nanorods for cancer-drug delivery. *Biomaterials* 2013;34:5722-35.
- [69] Huang C, Neoh KG, Xu LQ, Kang ET, Chiong E. Polymeric Nanoparticles with Encapsulated Superparamagnetic Iron Oxide and Conjugated Cisplatin for Potential Bladder Cancer Therapy. *Biomacromolecules* 2012;13:2513-20.
- [70] Bian T, Shang L, Yu HJ, Perez MT, Wu LZ, Tung CH, et al. Spontaneous Organization of Inorganic Nanoparticles into Nanovesicles Triggered by UV Light. *Advanced Materials* 2014;26:5613-+.
- [71] Yin Q, Tong R, Yin LC, Fan TM, Cheng JJ. Anticancer camptothecin-N-poly(lactic acid) nanoconjugates with facile hydrolysable linker. *Polym Chem* 2014;5:1581-5.
- [72] Tang L, Cheng JJ. Nonporous silica nanoparticles for nanomedicine application. *Nano Today* 2013;8:290-312.
- [73] Langer R. Drug delivery and targeting. *Nature* 1998;392:5-10.
- [74] Li LL, Yin Q, Cheng JJ, Lu Y. Polyvalent Mesoporous Silica Nanoparticle-Aptamer Bioconjugates Target Breast Cancer Cells. *Advanced Healthcare Materials* 2012;1:567-72.
- [75] Iversen TG, Skotland T, Sandvig K. Endocytosis and intracellular transport of nanoparticles: Present knowledge and need for future studies. *Nano Today* 2011;6:176-85.
- [76] Sorkin A. Cargo recognition during clathrin-mediated endocytosis: a team effort.

Curr Opin Cell Biol 2004;16:392-9.

[77] Schmid EM, McMahon HT. Integrating molecular and network biology to decode endocytosis. *Nature* 2007;448:883-8.

[78] dos Santos T, Varela J, Lynch I, Salvati A, Dawson KA. Effects of Transport Inhibitors on the Cellular Uptake of Carboxylated Polystyrene Nanoparticles in Different Cell Lines. *Plos One* 2011;6.

[79] Olton DYE, Close JM, Sfeir CS, Kumta PN. Intracellular trafficking pathways involved in the gene transfer of nano-structured calcium phosphate-DNA particles. *Biomaterials* 2011;32:7662-70.

[80] Fernando LP, Kandel PK, Yu JB, McNeill J, Ackroyd PC, Christensen KA. Mechanism of Cellular Uptake of Highly Fluorescent Conjugated Polymer Nanoparticles. *Biomacromolecules* 2010;11:2675-82.

[81] Sahay G, Querbes W, Alabi C, Eltoukhy A, Sarkar S, Zurenko C, et al. Efficiency of siRNA delivery by lipid nanoparticles is limited by endocytic recycling. *Nat Biotechnol* 2013;31:653-U119.

[82] Nam HY, Kwon SM, Chung H, Lee SY, Kwon SH, Jeon H, et al. Cellular uptake mechanism and intracellular fate of hydrophobically modified glycol chitosan nanoparticles. *J Control Release* 2009;135:259-67.

[83] Yamany AS, Mehlhorn H, Adham FK. Yolk protein uptake in the oocyte of the Asian tiger mosquito *Aedes albopictus* (Skuse) (Diptera: Culicidae). *Parasitol Res* 2012;111:1315-24.

[84] Rothberg KG, Heuser JE, Donzell WC, Ying YS, Glenney JR, Anderson RGW.

- Caveolin, a Protein-Component of Caveolae Membrane Coats. *Cell* 1992;68:673-82.
- [85] Mayor S, Pagano RE. Pathways of clathrin-independent endocytosis. *Nat Rev Mol Cell Bio* 2007;8:603-12.
- [86] Kirkham M, Parton RG. Clathrin-independent endocytosis: New insights into caveolae and non-caveolar lipid raft carriers (vol 1744, pg 273, 2005). *Bba-Mol Cell Res* 2005;1746:349-63.
- [87] Frick M, Bright NA, Riento K, Bray A, Merrified C, Nichols BJ. Coassembly of flotillins induces formation of membrane microdomains, membrane curvature, and vesicle budding. *Curr Biol* 2007;17:1151-6.
- [88] Shao YF, Akmentin W, Toledo-Aral JJ, Rosenbaum J, Valdez G, Cabot JB, et al. Pincher, a pinocytic chaperone for nerve growth factor/TrkA signaling endosomes. *J Cell Biol* 2002;157:679-91.
- [89] Orth JD, McNiven MA. Get off my back! Rapid receptor internalization through circular dorsal ruffles. *Cancer Res* 2006;66:11094-6.
- [90] Overholtzer M, Mailleux AA, Mouneimne G, Normand G, Schnitt SJ, King RW, et al. A nonapoptotic cell death process, entosis, that occurs by cell-in-cell invasion. *Cell* 2007;131:966-79.
- [91] Sandvig K, Torgersen ML, Raa HA, Van Deurs B. Clathrin-independent endocytosis: from nonexisting to an extreme degree of complexity. *Histochem Cell Biol* 2008;129:267-76.
- [92] Doherty GJ, McMahon HT. Mechanisms of Endocytosis. *Annu Rev Biochem* 2009;78:857-902.

- [93] Grimmer S, van Deurs B, Sandvig K. Membrane ruffling and macropinocytosis in A431 cells require cholesterol. *J Cell Sci* 2002;115:2953-62.
- [94] van Kerkhof P, Sachse M, Klumperman J, Strous GJ. Growth hormone receptor ubiquitination coincides with recruitment to clathrin-coated membrane domains. *J Biol Chem* 2001;276:3778-84.
- [95] Larkin JM, Brown MS, Goldstein JL, Anderson RGW. Depletion of Intracellular Potassium Arrests Coated Pit Formation and Receptor-Mediated Endocytosis in Fibroblasts. *Cell* 1983;33:273-85.
- [96] Damke H, Baba T, Vanderblik AM, Schmid SL. Clathrin-Independent Pinocytosis Is Induced in Cells Overexpressing a Temperature-Sensitive Mutant of Dynamin. *J Cell Biol* 1995;131:69-80.
- [97] Lajoie P, Nabi IR. Lipid Rafts, Caveolae, and Their Endocytosis. *Int Rev Cel Mol Bio* 2010;282:135-63.
- [98] He B, Lin P, Jia ZR, Du WW, Qu W, Yuan L, et al. The transport mechanisms of polymer nanoparticles in Caco-2 epithelial cells. *Biomaterials* 2013;34:6082-98.
- [99] Steinman RM, Mellman IS, Muller WA, Cohn ZA. Endocytosis and the Recycling of Plasma-Membrane. *J Cell Biol* 1983;96:1-27.
- [100] Bareford LA, Swaan PW. Endocytic mechanisms for targeted drug delivery. *Adv Drug Deliver Rev* 2007;59:748-58.
- [101] Theti DS, Bavetsias V, Skelton LA, Titley J, Gibbs D, Jansen G, et al. Selective delivery of CB300638, a cyclopenta[g]quinazoline-based thymidylate synthase inhibitor into human tumor cell lines overexpressing the alpha-isoform of the folate

receptor. *Cancer Res* 2003;63:3612-8.

[102] Holladay SR, Yang ZF, Kennedy MD, Leamon CP, Lee RJ, Jayamani M, et al. Riboflavin-mediated delivery of a macromolecule into cultured human cells. *Bba-Gen Subjects* 1999;1426:195-204.

[103] Quick G, van Zyl J, Hawtrey A, Ariatti M. Effect of nicotinic acid conjugated to DNA-transfecting complexes targeted at the transferrin receptor of HeLa cells. *Drug Deliv* 2000;7:231-6.

[104] Artus GRJ, Jung S, Zimmermann J, Gautschi HP, Marquardt K, Seeger S. Silicone nanofilaments and their application as superhydrophobic coating. *Advanced Materials* 2006;18:2758-+.

[105] Wu LB, Zhang H, Zhang JC, Ding JD. Fabrication of three-dimensional porous scaffolds of complicated shape for tissue engineering. I. Compression molding based on flexible-rigid combined mold. *Tissue engineering* 2005;11:1105-14.

[106] Zhang X, Shi F, Niu J, Jiang YG, Wang ZQ. Superhydrophobic surfaces: from structural control to functional application. *J Mater Chem* 2008;18:621-33.

[107] Accardo A, Gentile F, Mecarini F, De Angelis F, Bughammer M, Di Fabrizio E, et al. In Situ X-ray Scattering Studies of Protein Solution Droplets Drying on Micro- and Nanopatterned Superhydrophobic PMMA Surfaces. *Langmuir* 2010;26:15057-64.

[108] Sun TL, Feng L, Gao XF, Jiang L. Bioinspired surfaces with special wettability. *Accounts of Chemical Research* 2005;38:644-52.

[109] [https://en.wikipedia.org/wiki/Surface\\_roughness](https://en.wikipedia.org/wiki/Surface_roughness).

[110] Roach P, Shirtcliffe NJ, Newton MI. Progress in superhydrophobic surface

development. *Soft Matter* 2008;4:224-40.

[111] Guo ZG, Liu WM, Su BL. Superhydrophobic surfaces: From natural to biomimetic to functional. *J Colloid Interf Sci* 2011;353:335-55.

[112] Xu LG, He JH. Fabrication of Highly Transparent Superhydrophobic Coatings from Hollow Silica Nanoparticles. *Langmuir* 2012;28:7512-8.

[113] Li XM, Reinhoudt D, Crego-Calama M. What do we need for a superhydrophobic surface? A review on the recent progress in the preparation of superhydrophobic surfaces. *Chemical Society Reviews* 2007;36:1350-68.

[114] Ke QP, Fu WQ, Wang S, Tang TD, Zhang JF. Facile Preparation of Superhydrophobic Biomimetic Surface Based on Octadecyltrichlorosilane and Silica Nanoparticles. *ACS Applied Materials & Interfaces* 2010;2:2393-8.

[115] Wang CF, Wang YT, Tung PH, Kuo SW, Lin CH, Sheen YC, et al. Stable superhydrophobic polybenzoxazine surfaces over a wide pH range. *Langmuir* 2006;22:8289-92.

[116] Love JC, Estroff LA, Kriebel JK, Nuzzo RG, Whitesides GM. Self-assembled monolayers of thiolates on metals as a form of nanotechnology. *Chemical Reviews* 2005;105:1103-69.

[117] Wang Y, Padua GW. Formation of Zein Microphases in Ethanol-Water. *Langmuir* 2010;26:12897-901.

[118] Wang Y, Padua GW. Formation of zein spheres by evaporation-induced self-assembly. *Colloid and Polymer Science* 2012;290:1593-8.

[119] Lai HM, Padua GW, Wei LS. Properties and microstructure of zein sheets

- plasticized with palmitic and stearic acids. *Cereal Chem* 1997;74:83-90.
- [120] Shukla R, Cheryan M, DeVor RE. Solvent extraction of zein from dry-milled corn. *Cereal Chem* 2000;77:724-30.
- [121] Yoshimitsu Z, Nakajima A, Watanabe T, Hashimoto K. Effects of surface structure on the hydrophobicity and sliding behavior of water droplets. *Langmuir* 2002;18:5818-22.
- [122] Carrasco J, Hodgson A, Michaelides A. A molecular perspective of water at metal interfaces. *Nat Mater* 2012;11:667-74.
- [123] Fahmy TM, Samstein RM, Harness CC, Mark Saltzman W. Surface modification of biodegradable polyesters with fatty acid conjugates for improved drug targeting. *Biomaterials* 2005;26:5727-36.
- [124] Vilčnik A, Jerman I, Šurca Vuk A, Koželj M, Orel B, Tomšič B, et al. Structural Properties and Antibacterial Effects of Hydrophobic and Oleophobic Sol–Gel Coatings for Cotton Fabrics. *Langmuir* 2009;25:5869-80.
- [125] Saito H, Takai K, Takazawa H, Yamauchi G. A study on snow sticking weight to water-repellent coatings. *Mater Sci Res Int* 1997;3:216-9.
- [126] Fürstner R, Barthlott W, Neinhuis C, Walzel P. Wetting and Self-Cleaning Properties of Artificial Superhydrophobic Surfaces. *Langmuir* 2005;21:956-61.
- [127] Degasne I, Basle MF, Demais V, Hure G, Lesourd M, Grolleau B, et al. Effects of roughness, fibronectin and vitronectin on attachment, spreading, and proliferation of human osteoblast-like cells (Saos-2) on titanium surfaces. *Calcified Tissue Int* 1999;64:499-507.

- [128] Valamehr B, Jonas SJ, Polleux J, Qiao R, Guo SL, Gschweng EH, et al. Hydrophobic surfaces for enhanced differentiation of embryonic stem cell-derived embryoid bodies. *P Natl Acad Sci USA* 2008;105:14459-64.
- [129] Sun T, Feng L, Gao X, Jiang L. Bioinspired Surfaces with Special Wettability. *Accounts of Chemical Research* 2005;38:644-52.
- [130] Ailan QU XW, Pihui PI, Jiang CHENG, Zhuoru YANG. Morphologies and Superhydrophobicity of Hybrid Film Surfaces Based on Silica and Fluoropolymer. *J Mater Sci Technol* 2008;24:693-9.
- [131] Wu L, Zhang H, Zhang J, Ding J. Fabrication of three-dimensional porous scaffolds of complicated shape for tissue engineering. I. Compression molding based on flexible-rigid combined mold. *Tissue engineering* 2005;11:1105-14.
- [132] Artus GRJ, Jung S, Zimmermann J, Gautschi HP, Marquardt K, Seeger S. Silicone Nanofilaments and Their Application as Superhydrophobic Coatings. *Advanced Materials* 2006;18:2758-62.
- [133] Liu J. Oleanolic acid and ursolic acid: research perspectives. *J Ethnopharmacol* 2005;100:92-4.
- [134] Cunha A, Gandini A. Turning polysaccharides into hydrophobic materials: a critical review. Part 1. Cellulose. *Cellulose* 2010;17:875-89.
- [135] Wang Y, Padua GW. Formation of Zein Microphases in Ethanol–Water. *Langmuir* 2010;26:12897-901.
- [136] Perakslis ED, Gardner SD, Pittman CU. Surface composition of carbon fibers subjected to oxidation in nitric acid followed by oxygen plasma. *J Adhes Sci Technol*

1997;11:531-51.

[137] Lindstrom ES, Stadler P, Weisse T. Live sorting and survival of unstained and DAPI-stained ciliates by flow cytometry. *Arch Hydrobiol* 2003;157:173-84.

[138] Fong H, Chun I, Reneker DH. Beaded nanofibers formed during electrospinning. *Polymer* 1999;40:4585-92.

[139] Theron SA, Zussman E, Yarin AL. Experimental investigation of the governing parameters in the electrospinning of polymer solutions. *Polymer* 2004;45:2017-30.

[140] Chen M, Patra PK, Lovett ML, Kaplan DL, Bhowmick S. Role of electrospun fibre diameter and corresponding specific surface area (SSA) on cell attachment. *Journal of Tissue Engineering and Regenerative Medicine* 2009;3:269-79.

[141] Parizek M, Kasalkova N, Bacakova L, Slepicka P, Lisa V, Blazkova M, et al. Improved Adhesion, Growth and Maturation of Vascular Smooth Muscle Cells on Polyethylene Grafted with Bioactive Molecules and Carbon Particles. *Int J Mol Sci* 2009;10:4352-74.

[142] Bacakova L, Filova E, Parizek M, Ruml T, Svorcik V. Modulation of cell adhesion, proliferation and differentiation on materials designed for body implants. *Biotechnol Adv* 2011;29:739-67.

[143] Zheng J, He A, Li J, Xu J, Han CC. Studies on the controlled morphology and wettability of polystyrene surfaces by electrospinning or electrospraying. *Polymer* 2006;47:7095-102.

[144] Kang M, Jung R, Kim HS, Jin HJ. Preparation of superhydrophobic polystyrene membranes by electrospinning. *Colloid Surface A* 2008;313:411-4.

- [145] Menini R, Farzaneh M. Production of superhydrophobic polymer fibers with embedded particles using the electrospinning technique. *Polym Int* 2008;57:77-84.
- [146] Buruaga L, Gonzalez A, Irusta L, Iruin JJ. Production of Hydrophobic Surfaces in Biodegradable and Biocompatible Polymers Using Polymer Solution Electrospinning. *J Appl Polym Sci* 2011;120:1520-4.
- [147] Cui WG, Li XH, Zhou SB, Weng J. Degradation patterns and surface wettability of electrospun fibrous mats. *Polym Degrad Stabil* 2008;93:731-8.
- [148] Wang Y, Padua GW. Nanoscale Characterization of Zein Self-Assembly. *Langmuir* 2012;28:2429-35.
- [149] Matsushima N, Danno G-i, Takezawa H, Izumi Y. Three-dimensional structure of maize  $\alpha$ -zein proteins studied by small-angle X-ray scattering. *Biochimica et Biophysica Acta (BBA) - Protein Structure and Molecular Enzymology* 1997;1339:14-22.
- [150] Torres-Giner S, Martinez-Abad A, Gimeno-Alcaniz JV, Ocio MJ, Lagaron JM. Controlled Delivery of Gentamicin Antibiotic from Bioactive Electrospun Polylactide-Based Ultrathin Fibers. *Adv Eng Mater* 2012;14:B112-B22.
- [151] Cerpa R, Cohen FE, Kuntz ID. Conformational switching in designed peptides: the helix/sheet transition. *Folding and Design* 1996;1:91-101.
- [152] Ding F, Borreguero JM, Buldyrey SV, Stanley HE, Dokholyan NV. Mechanism for the  $\alpha$ -helix to  $\beta$ -hairpin transition. *Proteins: Structure, Function, and Bioinformatics* 2003;53:220-8.
- [153] Forato LA, Bernardes R, Colnago LA. Protein structure in KBr pellets by infrared

- spectroscopy. *Anal Biochem* 1998;259:136-41.
- [154] Forato LA, Bicudo TDC, Colnago LA. Conformation of  $\alpha$  zeins in solid state by Fourier transform IR. *Biopolymers* 2003;72:421-6.
- [155] Forato LA, Doriguetto AC, Fischer H, Mascarenhas YP, Craievich AF, Colnago LA. Conformation of the Z19 prolamin by FTIR, NMR, and SAXS. *Journal of Agricultural and Food Chemistry* 2004;52:2382-5.
- [156] Forato LA, Bicudo TC, Colnago LA. Conformation of alpha Zeins in solid state by Fourier transform IR. *Biopolymers* 2003;72:421-6.
- [157] Chen HQ, Zhong QX. Processes improving the dispersibility of spray-dried zein nanoparticles using sodium caseinate. *Food Hydrocolloid* 2014;35:358-66.
- [158] Krishnaiah D, Nithyanandam R, Sarbatly R. A Critical Review on the Spray Drying of Fruit Extract: Effect of Additives on Physicochemical Properties. *Crit Rev Food Sci* 2014;54:449-73.
- [159] Wang Y, Chen L. Electrospinning of Prolamin Proteins in Acetic Acid: The Effects of Protein Conformation and Aggregation in Solution. *Macromolecular Materials and Engineering* 2012;297:902-13.
- [160] Wang YX, Chen LY. Electrospinning of Prolamin Proteins in Acetic Acid: The Effects of Protein Conformation and Aggregation in Solution. *Macromolecular Materials and Engineering* 2012;297:902-13.
- [161] Jayanthi GV, Zhang SC, Messing GL. Modeling of Solid Particle Formation during Solution Aerosol Thermolysis - the Evaporation Stage. *Aerosol Sci Tech* 1993;19:478-90.

- [162] Brinker CJ, Lu YF, Sellinger A, Fan HY. Evaporation-induced self-assembly: Nanostructures made easy. *Advanced Materials* 1999;11:579-+.
- [163] Yang H, Coombs N, Sokolov I, Ozin GA. Free-standing and oriented mesoporous silica films grown at the air-water interface. *Nature* 1996;381:589-92.
- [164] Yang H, Coombs N, Ozin GA. Morphogenesis of shapes and surface patterns in mesoporous silica. *Nature* 1997;386:692-5.
- [165] Esposito E, Cervellati F, Menegatti E, Nastruzzi C, Cortesi R. Spray dried Eudragit microparticles as encapsulation devices for vitamin C. *International Journal of Pharmaceutics* 2002;242:329-34.
- [166] Shiau SYaTSH. Stability of Ascorbic-Acid in Shrimp Feed during Analysis. *Nippon Suisan Gakkaishi* 1993;59.
- [167] Vohra K, Khan AJ, Telang V, Rosenfeld W, Evans HE. Improvement of neutrophil migration by systemic vitamin C in neonates 1990.
- [168] Jacobs EJ, Henion AK, Briggs PJ, Connell CJ, McCullough ML, Jonas CR, et al. Vitamin C and Vitamin E Supplement Use and Bladder Cancer Mortality in a Large Cohort of US Men and Women. *American Journal of Epidemiology* 2002;156:1002-10.
- [169] Bozkır A, Şimşek B, Güngör A, Torun M. Ascorbic acid and uric acid levels in lung cancer patients. *Journal of Clinical Pharmacy and Therapeutics* 1999;24:43-7.
- [170] Burr M, Appleby P, Key T, Thorogood M. Plasma ascorbic acid and risk of heart disease and cancer. *The Lancet* 2001;357:2135-6.
- [171] Handbook of Vitamins (4th Edition). Boca Raton, FL, USA: CRC Press; 2007.
- [172] Bhardwaj V, Hariharan S, Bala I, Lamprecht A, Kumar N, Panchagnula R, et al.

Pharmaceutical Aspects of Polymeric Nanoparticles for Oral Drug Delivery. *Journal of Biomedical Nanotechnology* 2005;1:235-58.

[173] Sahana DK, Mittal G, Bhardwaj V, Kumar MNVR. PLGA nanoparticles for oral delivery of hydrophobic drugs: Influence of organic solvent on nanoparticle formation and release behavior In Vitro and In Vivo using estradiol as a model drug. *Journal of Pharmaceutical Sciences* 2008;97:1530-42.

[174] Alishahi A, Mirvaghefi A, Tehrani MR, Farahmand H, Shojaosadati SA, Dorkoosh FA, et al. Shelf life and delivery enhancement of vitamin C using chitosan nanoparticles. *Food Chemistry* 2011;126:935-40.

[175] Desai KGH, Park HJ. Encapsulation of vitamin C in tripolyphosphate cross-linked chitosan microspheres by spray drying. *J Microencapsul* 2005;22:179-92.

[176] Wang Q, Yin L, Padua G. Effect of Hydrophilic and Lipophilic Compounds on Zein Microstructures. *Food Biophysics* 2008;3:174-81.

[177] Quispe-Condori S, Saldana MDA, Temelli F. Microencapsulation of flax oil with zein using spray and freeze drying. *Lwt-Food Sci Technol* 2011;44:1880-7.

[178] Luo XY, Yang MH, Wu FX, Wu LJ, Chen L, Tang Z, et al. Vitamin D receptor gene BsmI polymorphism B allele, but not BB genotype, is associated with systemic lupus erythematosus in a Han Chinese population. *Lupus* 2012;21:53-9.

[179] Wang Y, Pi SF, Zhou JH, Gao HL, Li JL, Sun HZ. One-step Synthesis of Lemonile from Citral by Liquid Phase Catalytic Ammoxidation. *Adv Mater Res-Switz* 2013;641-642:959-61.

[180] Wang HJ, Lin ZX, Liu XM, Sheng SY, Wang JY. Heparin-loaded zein

- microsphere film and hemocompatibility. *J Control Release* 2005;105:120-31.
- [181] Song L, Choi KS, Park YM, Kazim AL, Marlar K, Kong ES, et al. Capillary-LC-mu ESI-MS/MS and nano-LC-nano ESI-MS/MS analysis using a single binary pump capillary LC system: Applications in proteomics. *J Liq Chromatogr R T* 2005;28:1271-89.
- [182] Sano M, Hosoya O, Taoka S, Seki T, Kawaguchi T, Sugibayashi K, et al. Relationship between Solubility of Chitosan in Alcoholic Solution and Its Gelation. *CHEMICAL & PHARMACEUTICAL BULLETIN* 1999;47:1044-6.
- [183] Zhou S, Deng X, Li X. Investigation on a novel core-coated microspheres protein delivery system. *J Control Release* 2001;75:27-36.
- [184] Hurtado-López P, Murdan S. Zein microspheres as drug/antigen carriers: A study of their degradation and erosion, in the presence and absence of enzymes. *J Microencapsul* 2006;23:303-14.